Design and Experimental Evaluations of a

Pump-Controlled Hydraulic Circuit

by

Ehsan Jalayeri

A Thesis submitted to the Faculty of Graduate Studies at
The University of Manitoba
in partial fulfilment of the requirements of the degree of

Doctor of Philosophy

Department of Mechanical Engineering
University of Manitoba
Winnipeg, Manitoba, Canada

TABLE OF CONTENTS

TABLE OF FIGURES

LIST OF TABLES

ABSTRACT

This thesis presents a novel, low cost, high precision , and efficient design for an electro-hydrostatic circuit for single rod hydraulic cylinders. The design is the main contribution of candidate to fulfill the regiments of PhD degree. The challenge of existing deigns of electro-hydrostatic circuits for single-rod cylinders is using one pump to control the cylinder under switching (resistive-assistive) loads. The proposed circuit utilizes off-the-shelf industrial elements. It uses two counterbalance valves to manage switching loads and one on/off solenoid valve to redirect the differential flow of the single rod cylinder to tank. A set of simulation studies is conducted using Simhydraulic tools of Matlab in order to study performances of the proposed circuit and compare it with existing designs. Pump-controlled hydraulic circuit for double rod cylinders was developed and is widely used by industry. It is used as the benchmark for simulation studies. As well, the proposed circuit and two major existing pump-controlled circuits for single rod cylinders are compared to the benchmark circuit. Evaluations are conducted by comparing chamber pressure responses as well as pressure *vs* position of the cylinder end-effector for each individual circuit. Results indicate that the proposed circuit performed as well as the benchmark circuit by controlling pressures to both sides of the cylinder at the same time. Moreover, the load in the proposed circuit is more controllable compared to the benchmark circuit. Experimental results, obtained from the developed test rig, validate accuracy of the simulation model. Maximum steady state position error of 0.06 mm applications is experimentally observed when the test rig is tested under different loading conditions with various amplitudes and frequencies. The circuit consumes up to 20% of the energy that is required by a valve controlled circuit given the same sinusoidal tracking signal. The relative efficiency of the proposed circuit over a valve

controlled circuit depends on the pattern and frequency of the tracking signal. In all the experiments, a simple proportional controller, which uses readings of a linear position transducer, is employed. The use of the proportional controller makes the proposed circuit easy to implement and shows it is good candidate for industrial applications. The accuracy of the position response of the proposed circuit indicates, it is a good candidate for robotic applications too.

CHAPTER 1

INTRODUCTION

1.1. Statement of the problem

Single rod hydraulic cylinders are commonly used in different fields of industry, spanning aviation to construction, and mining to load handling. The efficiency of the operation of such industrial machines is an important parameter that is directly connected to the cost of energy usage and the environmental impact of the operation. For example, a typical excavator machine is energized by a 147 hp (110 KW) diesel engine and consumes 33 liters of diesel fuel per hour; however, only 30% of this energy is used for digging and lifting [1, 2]. The rest of the consumed energy is dissipated in mechanical and hydraulic elements. About 35% of the delivered energy to the hydraulic system is consumed in metering valves which only heat up the hydraulic oil [1, 2]. Conversely, the oil cooler of the machine consumes energy to dissipate the excessive heat produced by metering valves. A centralized hydraulic power unit delivers the pressurized hydraulic fluid to the ports of metering valves, and each valve controls one cylinder. Centralized hydraulic systems are not only large, heavy, and noisy [1, 3, 4], they are also costly and energy inefficient. Furthermore, the

amount of pollutants emitted by the machine in the form of carbon monoxide, nitrogen dioxide, and nitrogen monoxide is considerable [1]. Any improvement made in the energy efficiency of hydraulic systems reduces the environmental impact of industrial activities and saves energy.

One solution to improve the efficiency of industrial machines is to use a system in which no metering element is employed. Such systems are recognized as pump-controlled or electro-hydrostatic systems. When a hydraulic cylinder is controlled with a variable displacement pump and the prime mover is a fixed speed motor, the circuit is called pump-controlled. When the pump is a fixed displacement pump and the prime mover is a variable speed electric motor, the cylinder is named a variable speed pump-controlled, or an electro-hydrostatic, actuator (EHA) [5, 6]. Pump-controlled hydraulic actuators are also known as throttle-less hydraulic actuators [7]. These systems do not need a central hydraulic power unit, and each cylinder is controlled by its own individual pump. Due to this pairing, when energy is required, the pump supplies the fluid to the cylinder directly. Two types of hydraulic cylinders (actuators) are used in industry: double rod or symmetric and single rod or asymmetric. Double rod hydraulic cylinders are larger than single rod ones, therefore, they need more space for installation and operation. Pump-controlled hydraulic circuits for double rod hydraulic cylinders have been well developed and used in industry [8]. The challenge of using a pump-controlled single rod hydraulic cylinder is dealing with different flows at the opposite ports of the cylinder. This challenge can be offset by using a pump to maintain the performance of the operation [1]. Up until this point, two methods have been used for pump control of single rod hydraulic cylinders: using asymmetric axial piston pumps and conventional pumps [9]. In a comparison with conventional pumps, asymmetric axial piston pumps are new,

expensive, and high-maintenance [9, 10]. Two major methods have been employed to control flows of a single rod hydraulic cylinder by using conventional pumps: using two pumps or using one pump. In the case of two-pump systems, each pump controls the flow of a separate side of the single rod cylinder. Using two pumps for controlling each cylinder of an industrial machine makes the machine expensive and heavy [9]. Moreover, synchronizing displacements of two pumps and keeping their flows at the same flow rate of the cylinder in real time is challenging [11].

Many pump-controlled hydraulic circuits using one pump to control a single rod hydraulic cylinder have been designed and tested [2, 7, 12, 13, 14, 15, 16]. However, none of these designs have been widely used in the market. This indicates that there has not yet been an ideal model produced for pump-controlled single rod hydraulic cylinders [17]. The common challenge of these circuits is attempting to control the flow of an asymmetric hydraulic cylinder using a symmetric hydraulic pump. In these existing designs, one chamber of the single rod cylinder must be directly connected to the low-pressure side of the hydraulic circuit which makes it uncontrollable under some load conditions. Researchers have used different methods to overcome existing concerns [1, 7, 17, 18]. Nevertheless, existing solutions are either complicated by using more sensors and extra feedback loops, or pose some limitations which include the bad handling switching load [17]. When the load is against the cylinder end effector force the load is resistive and when the load force is in the same direction of the cylinder end effector force, the load recognized as assistive load. If the load force direction is changing from assistive to resistive it is switching. Simplicity, reliability, efficiency and low-cost are important factors belonging to an ideal industrial hydraulic circuit.

1.2.Objective of this research

This thesis introduces the design and evaluation of a simple, low-cost, efficient, and easy to control single pump pump-controlled hydraulic circuit which uses two counterbalance valves and one on/off valve. The designed circuit positions a single rod hydraulic cylinder for all four load quadrants (two assistive and two resistive quadrants). The effect of pilot ratio and the setting of counterbalance valves on the load handlings of the proposed circuit need to be studied. The behavior of the proposed circuit needs to be studied and compared to major existing pump-controlled circuits. The simulation tool and the proposed circuit need to be evaluated with experimental tests. An experimental test rig needs to be designed and manufactured by using off-the-shelf industrial parts which comprises of an on/off valve and two counterbalance valves. Also, a switching load setup needs to be designed and prototyped to create a controllable and adjustable switching load. Next, the variation of the proposed circuit needs to be studied for non-switching loads. A variable weight load setup needs to be designed, and manufactured to simulate lifting loads in order to evaluate the modified proposed circuit (with a removed counterbalance valve). Finally, the performance of the proposed circuit on test rig needs to be studied under different fluctuations of load and patterns of motion.

1.3.Methodology

Existing pump-controlled hydraulic circuits and the proposed circuit will be simulated under a unique switching load. Two major pressure plots including cylinder port pressures versus its end-effector position and, port A pressure versus port B pressure of the cylinder will be presented and compared to the simulation results of the well accepted pump-controlled circuit for double rod cylinders as the benchmark.

Next, designing and manufacturing of a test rig will provide a medium to create experimental evaluations. The test rig will be manufactured using off-the-shelf and low-cost industrial parts in order to ensure that the performance of the proposed circuit is only the result of its design. This makes the design appealing for day to day industrial applications. To evaluate the accuracy of the simulations, a desired position signal will be applied to both the simulation setup of the proposed circuit and the test rig, comparing their respective responses. To study the effect of pilot ratio and pressure setting of counterbalance valves to the energy efficiency of the proposed circuit, a simulation will be performed for different pilot ratios and different pressure settings. Furthermore, some tests are designed to study the steady state error of the proposed circuit and the position tracking of the circuit needs to be investigated. Finally, the energy efficiency of the circuit will be recorded and compared to the energy consumption of a valve controlled circuit to perform the same pattern of load motion. To make the transition from an experimental object to an industrial machine, the sensitivity of the test rig responses, including its energy efficiency to the pattern of motion need to be studied.

1.4. Thesis outline

Chapter 2 includes the literature review of the thesis. Chapter 3 introduces the proposed circuit and its variation for non-switching loads. Chapter 4 presents the simulation study results on the existing and proposed circuits as well as their comparisons. Chapter 5 presents the design and technical information of the test rig, which includes a switching and a non-switching load. The accuracy of the simulations will be validated by comparing the results obtained from the simulation of the test rig with experimental results. Also included in Chapter 5 is a description of the

performance of the proposed circuit. Chapter 6 contains a brief study of the performance of the test rig; it will include a review of the sensitivity, energy efficiency, and average position response of the proposed circuit in relation to the pattern and frequency of the motion of the load. Chapter 7 includes the conclusion which is followed by the Appendix that represents the governing formulas of the Simhydraulic blocks of Matlab used for simulations.

CHAPTER 2

LITERATURE REVIEW

2.1. Background

Douglas DC-3 was the first airliner equipped with hydraulically-actuated flight control surfaces, but the hydraulic system was heavy, inefficient, and unreliable [19]. Failing the central hydraulic power unit or breaking a hydraulic line resulted in the loss of control of the airplane [19, 20]. The use of electric actuators over hydraulic actuators greatly improves performance of avionic hydraulic systems in two ways: (i) electric energy sources have less harmful environmental impact as they do not need a heavy central hydraulic power unit and are not susceptible to oil leaks; (ii) electric wires are more flexible and lighter than hydraulic lines, thereby increasing the fuel efficiency of the aircraft. Conversely, the hydraulic cylinders are lighter, low-maintenance, and perform better than electric actuators under heavy loads [19, 21, 22, 23]. When a double rod hydraulic cylinder—with the servomotor as the prime mover, a fixed displacement hydraulic pump (gear pump), and electronic drivers/boards—is compacted in a case and energized with an electric cable, the package is known as an

actuator powered by wire [24]. These power-by-wire hydraulic double rod cylinders were developed for aviation industry [19, 25]. In valve-controlled hydraulic systems, hydraulic fluid circulates continuously through a cycle including the tank, pump, accumulator tanks, valve, and actuators, respectively. In circuits, such as Figure 2-1, the hydraulic fluid does not leave the loop of the pump/actuator; therefore, it is known as a hydrostatic circuit. Figure 2-1 shows the fluid flows when the end-effector acts in different directions against a load. When the prime mover is a variable speed electric motor (servomotor or DC motor), coupled to a fixed displacement pump (see Figure 2-1), the actuator is recognized as *Electro-hydrostatic Actuator* (EHA). The areas on the two sides of the piston for a single rod cylinder are different. Therefore, the circuit of the pump-controlled hydraulic double rod cylinder is not applicable to the case of a single rod cylinder. EHA actuators are popular in aviation and marine industries. When a variable displacement pump controls the flow of a hydraulic actuator, the circuit is called a pump-controlled circuit. When there is no throttling hydraulic servo valve present, it is known as a throttle-less circuit. Aside from aviation, hydrostatic hydraulic actuators are developed as hydrostatic transmission for heavy-duty mobile machines [26].

As compared to the double rod hydraulic cylinder, single rod cylinders need less space for operation and therefore are more popular in industry [27]. Researchers and engineers have introduced different pump-controlled designs for circuits with single rod hydraulic cylinder [28, 29, 27, 26, 30, 31].
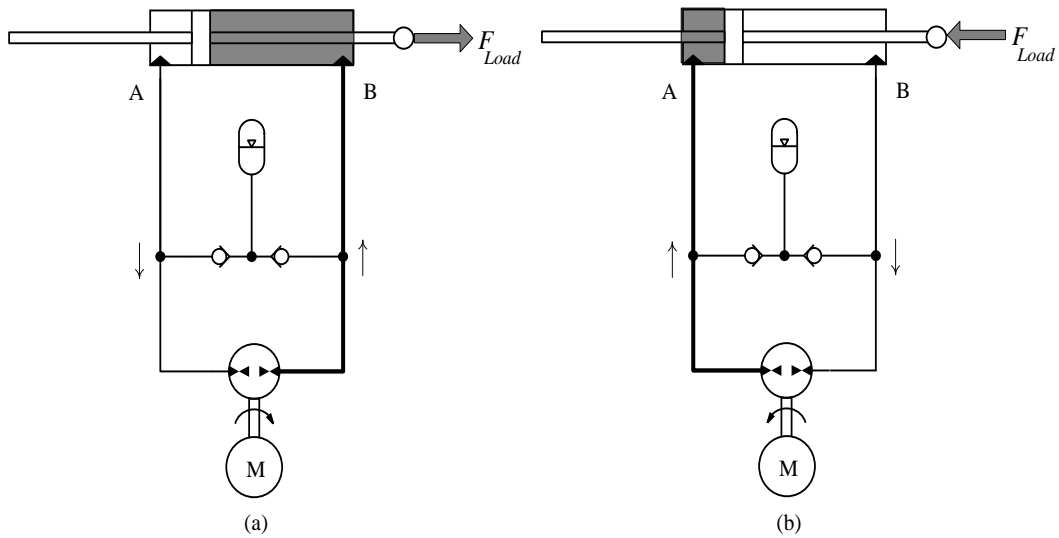
Figure 2-1: Electro-hydrostatic actuator for a double rod cylinder, (a) and (b) show fluid flows in the circuit when the end-effector of cylinder works against a load.

2.2. Circuits with more than one pump

J. Lodewyks [32] applied the concept of the hydraulic transformer to compensate for the differential flow rates of a single rod cylinder (Figure 2-2). In Figure 2-2 (a) when pump I feeds fluid to port A of cylinder, hydro motor HM of the hydraulic transformer rotates and pump HM pumps the required differential fluid to port A. In Figure 2-2 (b) shows the circulation of the fluid in the circuit when the cylinder retracts. Pump I feeds the fluid to port B, return fluid from port A rotate motor HM in reverse direction and pump HP returns the differential fluid to tank.   As illustrated in Figure 2-2, the hydraulic transformer ratio (flow ratio) needs to match the ratio of the hydraulic cylinder [33]. Nowadays in the market, hydraulic transformers are available in certain ratios [34, 35], while hydraulic cylinders are available in a wide variety of ratios. When the load helps the end-effector in motion the pump I in Figure 2-2 needs less torque from prime mover M to feed the oil to the circuit, in the extreme case of assistive load hydraulic machine I can work as a hydraulic motor by changing the torque on its shaft from positive to negative. In this case if the prime mover can save

energy like charging a battery bank the system can recycle some energy. Hydraulic machine I in this circuit operate in four hydraulic quadrants. Figure 2-3 defines the four operation quadrants of a hydraulic machine (pump/motor). As observed in Figure 2-3, when *PA* (pressure at port A) > *PB* (pressure at port B) and oil flows from port B to port A (*Q*>0), the hydraulic machine receives energy from the prime mover (positive torque, positive direction of rotation for the shaft) and delivers it to the hydraulic circuit. This scenario is an example of the pumping mode in the first quadrant. When *PA* < *PB*, and oil still flows from port B to port A (*Q*>0) of the hydraulic machine, the scenario is an example of the motoring mode in the second quadrant. In this case, the pump receives energy from the hydraulic circuit and delivers it to the prime.
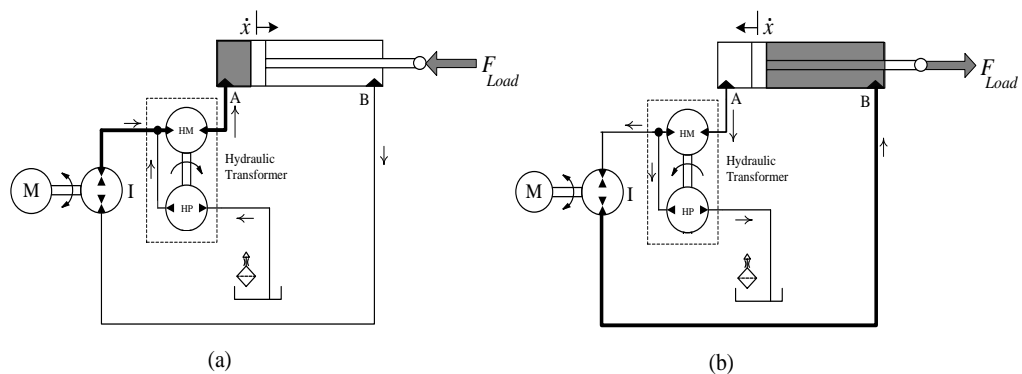
Figure 2-2: Hydraulic transformer compensates the differential flow rates of a single rod cylinder, (a) hydraulic transformer suck the oil from the tank, adds it to the main stream to the cylinder port, (b) hydraulic transformer suck the fluid from the cylinder port, return the differential fluid of cylinder to tank and the rest of it feeds to the pump port.

Also in the circuit showed in Figure 2-2, hydraulic pump and hydraulic transformer controls the pressure at opposite sides of the cylinder which makes the circuit controllable in the case of switching loads. Figure 2-4briefly represents the concept of resistive and assistive loads for a single rod cylinder. In one stroke of the cylinder, when the direction of the load force changes from assistive to resistive or vice versa,

the load is switching. $\ddot{x}$ is the acceleration of the end effector of the cylinder, and load force against the rod end effector is presented by F_{Load} (see Figure 2-4). To handle a resistive load the hydraulic machine works in pumping mood and in the case of assistive loads the hydraulic cylinder feeds hydraulic energy to hydraulic circuit.
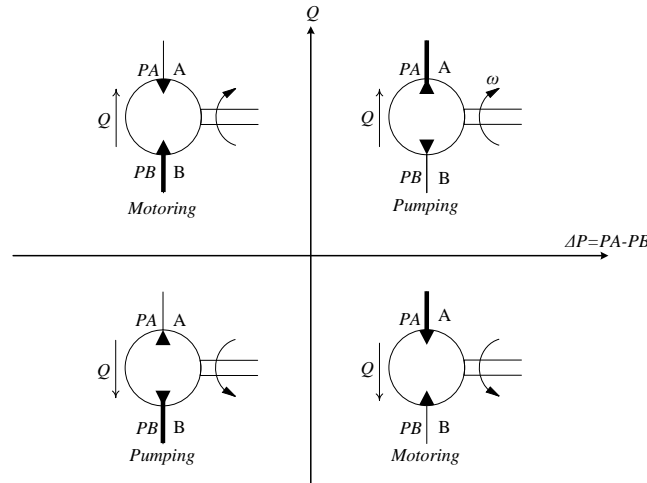
Figure 2-3: Four operational quadrants of a hydraulic machine in steady state condition.
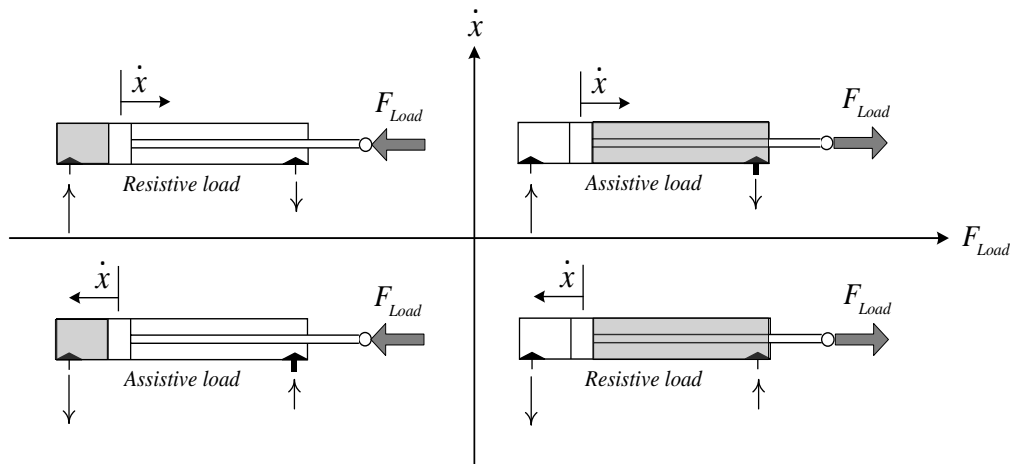
Figure 2-4: Load force at the end-effector, acceleration vector, direction of fluid flow to cylinder in two resistive and two assistive load cases in steady state condition.

In general an assistive load can shift the hydraulic machine from pumping mood to motoring mood. Resistive loads require pumping mood from the hydraulic machine.

11

Ceasby and Plummer [22] designed and prototyped a pump-controlled hydraulic circuit using special single rod hydraulic cylinders having ratio 1:2 for a hydraulic flight simulator. Each cylinder was connected to a pair of identical fixed displacement gear pumps acting as a tandem pump which was coupled to an electric servomotor. As seen in Figure 2-5, accumulator tank AC compensate the weight of the load, support the differential flow from two sides of the cylinder, recover some energy, and improve the energy efficiency of the whole hydraulic machine. The home position of the hydraulic cylinder was located at its mid stroke [22]. Figure 2-5(a) and (b) presents the fluid flow in hydraulic circuit and pumps I and II are tandem pumps. Draw backs act as disadvantages when it comes to this circuit's cost and simplicity. First, the presences of a wide variety of cylinder ratios which are not 1:2 are greatly available in market. This poses a challenge in the growing popularity of this circuit which needs cylinder ratios of 1:2. Second, the circuit's demand for two pumps per cylinder makes the industrial machine heavy, complicated and expensive.

There are some different configurations of using multi hydraulic pumps to control a general single rod cylinder [11]. Figure 2-6 shows three of these configurations under resistive load and in retraction and extraction. The ratio and size of cylinders and the availability of off-the-shelf hydraulic pumps in the market are parameters to consider when choosing the proper configuration of a two-pump circuit [11]. In Figure 2-6 in details the fluid flows in each hydraulic circuit when the load is resistive. Pressures two sides of the cylinder control by at least one pump for two-pump configurations and it shows these circuits has potential of recycling some energy when the load is assistive.

12
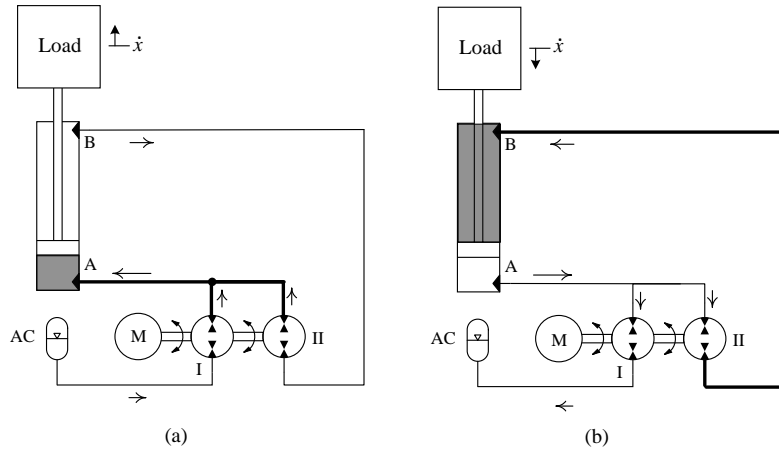
Figure 2-5:Two identical gear pumps control a cylinder with the ratio of 1:2, (a) pumps feed the fluid to bigger chamber of cylinder and load moves upward, (b) right pump feeds the fluid to smaller chamber of the cylinder.
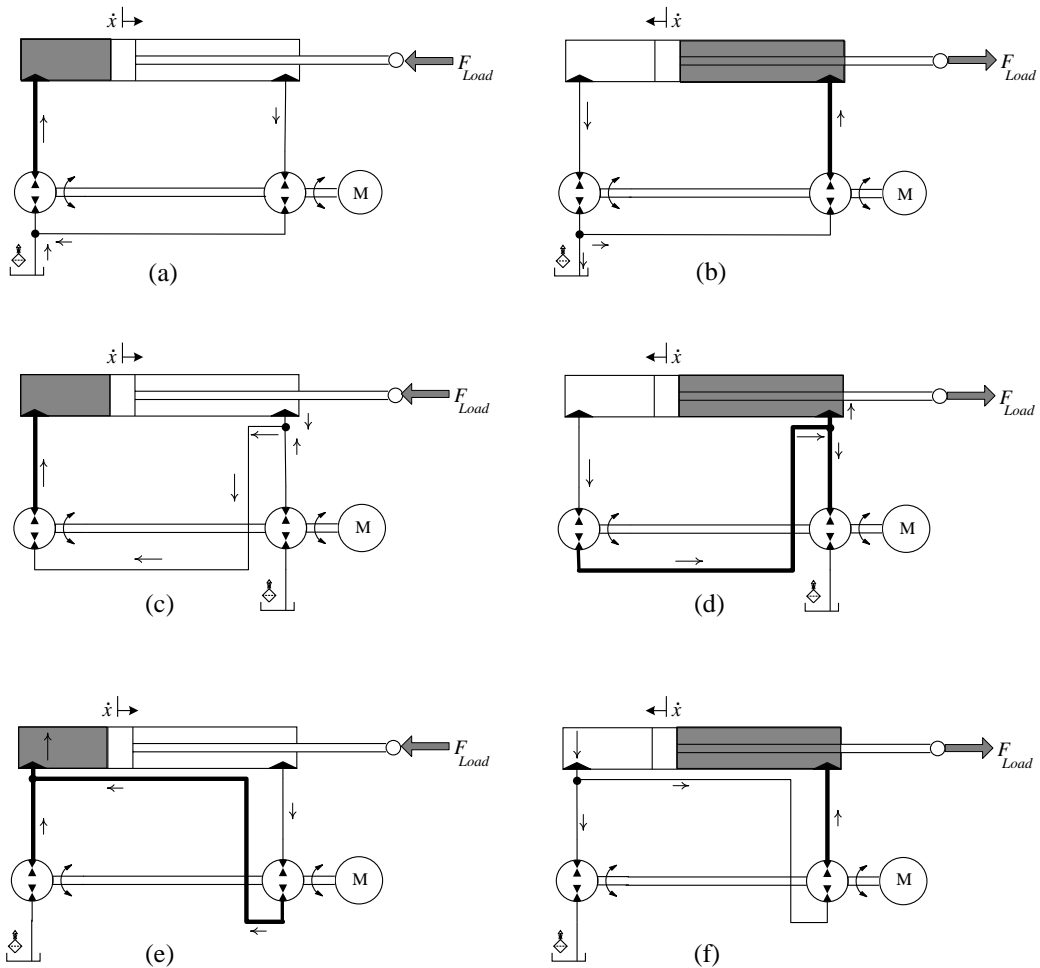
Figure 2-6:Two-pump configurations in extraction and retraction, (a) and (b) show fluid flows in circuit for the first type of two-pump configuration in retraction and extraction, (c) and (d) show fluid flows in circuit for the second type of two-pump configuration, (e) and (f) show the third type of two pump configuration under resistive load.

13

Lin *et al.* applied the concept of a two-pump circuit to the boom cylinder (a general ratio cylinder) of an excavator [36]. They coupled one variable displacement pump to a fixed speed prime mover, and a hydraulic motor to an electric generator to recover some potential energy when the boom was lowered. They showed that the positioning was not accurate and the speed of the boom was not stable [36]. In general, using two pumps to control a single rod hydraulic cylinder makes the industrial machine complex, high-maintenance, heavy and expensive.

2.3.Circuits using one pump

A. J. Hewett [37] was the first researcher who documented and patented a throttle-less hydraulic circuit using one pump to actuate a single rod hydraulic cylinder. He used a solenoid three-port two-position valve to redirect differential flow of a single rod hydraulic cylinder. The solenoid valve (see Figure 2-7) directs the differential flow from both sides of the cylinder to the tank. Two check valves protect the pump against cavitation. As it is shown in Figure 2-7 (a) when the load is resistive and pump I feeds the fluid to port B of cylinder, lower check valve (see Figure 2-7 a) and the solenoid valve blocks the hydraulic line from pump I to tank, rod-end-effector retracts, pump sucks oil from port A of cylinder, solenoid valve redirects the differential fluid of cylinder from port A to tank.

In this case pump absorbs mechanical energy from prime mover M and works in pumping mode. In the case of sudden load force changes from resistive to assistive. Load force helps to pump to retraction of end-effector and load experience an uncontrollable motion. As long as the solenoid valve does not change the position load will fall off uncontrollably. From the time that the solenoid valve changes the

position, the pump works as hydraulic motor and feeds mechanical energy to prime mover M.
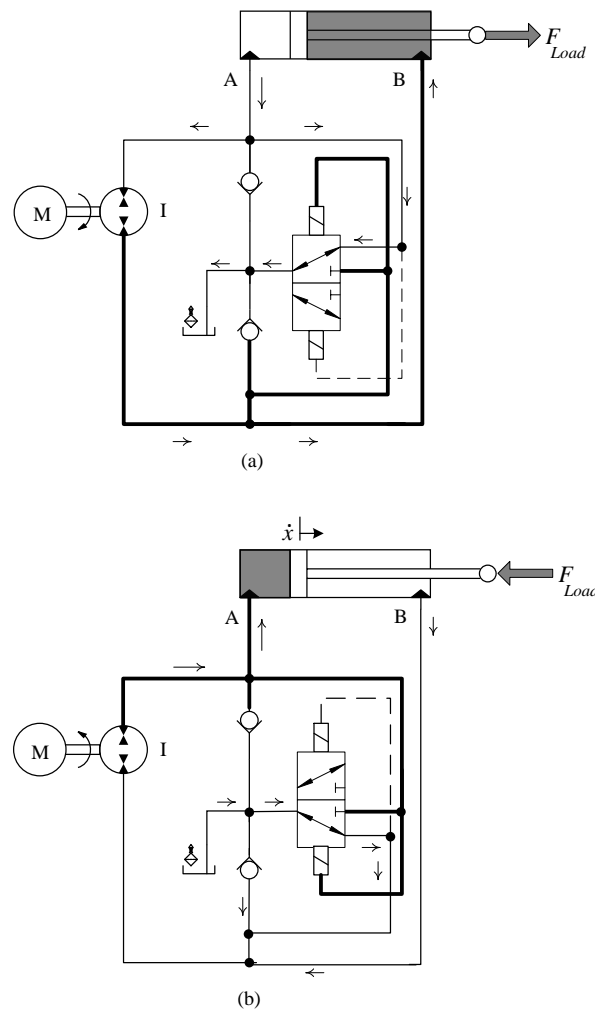
Figure 2-7: Circuit using a three-port two-position valve to redirect the differential flow of a single rod cylinder, (a) and (b) shows the circuit in pumping mood and resistive load.

The hydraulic pump in this circuit operates in four hydraulic quadrants and it can recycle some energy when the load is assistive. The circuit was applied to some forestry machines, and the results showed evidence of uncontrollable load vibrations [17, 38]. Since one side of the cylinder is always connected to the low-pressure side of the hydraulic circuit through the solenoid valve (Figure 2-7 tank pressure), the circuit is uncontrollable in sudden switching load conditions [17].

Rahmfeld and Ivantysynova [29] used a similar idea [37] when they replaced the solenoid valve with two pilot check valves [39] and [29] (see Figure 2-8). As it is shown in Figure 2-8 (a) when the load is resistive, pump feeds the port B of cylinder and retraces the end-effector of the cylinder. High pressure at port B of cylinder keeps the pilot check valve PCVb closed and pilot check valve PCVa remains open under effect of its pilot pressure. Pump I sucks oil from port A of the cylinder, differential fluid from port A of cylinder to pump I is directed to tank by open port of pilot check valve PCVa, pump I works in pumping mode. In the case of sudden load force changes from resistive to assistive, load helps to speeds up the end-effector motion uncontrollably in retraction motion until the pressure at port B of cylinder drops and pilot check valve PCVa closes the port, end-effector experience a sudden stop motion. Under effect of the assistive load pressure at port A of cylinder raises, pilot check valve PCVb open its port by effect of the pilot pressure and end-effector starts to retract. From this moment pump I works as a hydraulic motor. This scenario shows pump I in this configuration also operates in four quadrants. Zimmerman *et al.* [2] and Grabbel and Ivantysynova [13] applied the circuit to a concrete pump truck, a loader, and a multi joint manipulator. Later on, Williamson and Ivantysynova showed that in some load conditions, two pilot check valves and swash plate of the piston pump vibrate [18]. Williamson *et al.* [29] clearly reviewed the undesirable oscillations of the hydraulic cylinder and the pump when the circuit is handling a switching load (from assistive to resistive). They overcame some of the vibration issues. The solution was complicated and involved extra pressure readings and extra control loops therefore; the hydraulic circuit has not been wildly used in industry [17].

Wang *et al.* theoretically showed that the circuit illustrated in Figure 2-8, operates unstably under some load conditions [17]. They showed that when one side of the

cylinder is connected to the low pressure side of a hydraulic circuit, the hydraulic

cylinder in general is uncontrollable.

(a)

(b)
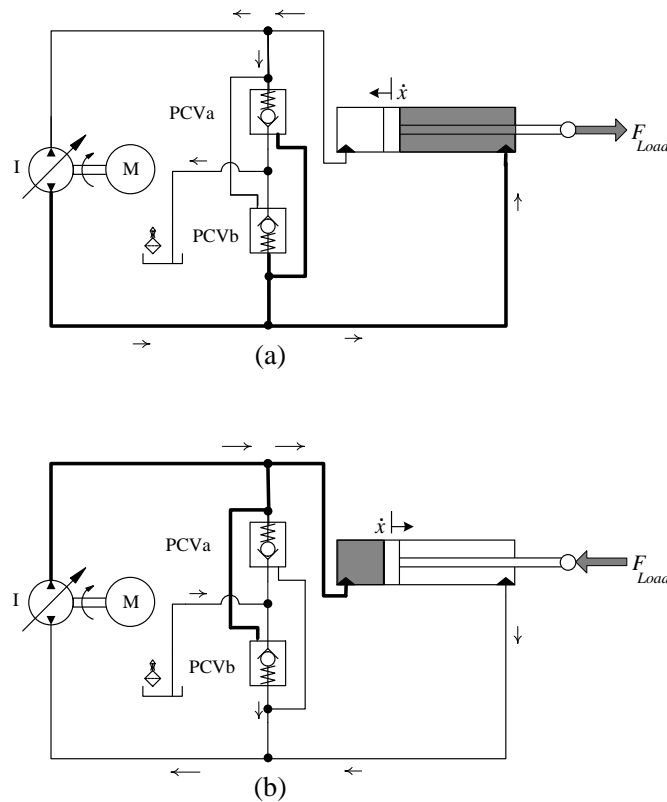
Figure 2-8:Circuit using two pilot check valves to redirect the differential flow
of a single rod cylinder, (a) and (b) show fluid flows and action of the circuit
under resistive load and in pumping mood.

They replaced the two pilot check valves with a shuttle valve as a pilot operated

logic valve, added two pressure sensors and two on/off solenoid valves in order to

bleed and dampen the pressures' oscillations in extreme load conditions (see Figure

2-9). The control loop which involves an extra internal loop requires real time

pressure readings and cylinder end-effector position monitoring to stabilize the circuit

[17]. This made the solution complicated. Figure 2-9 (a) and (b) show the fluid flow

direction in the circuit when the load is resistive and the end effector of the cylinder is

retracting and extracting.

17
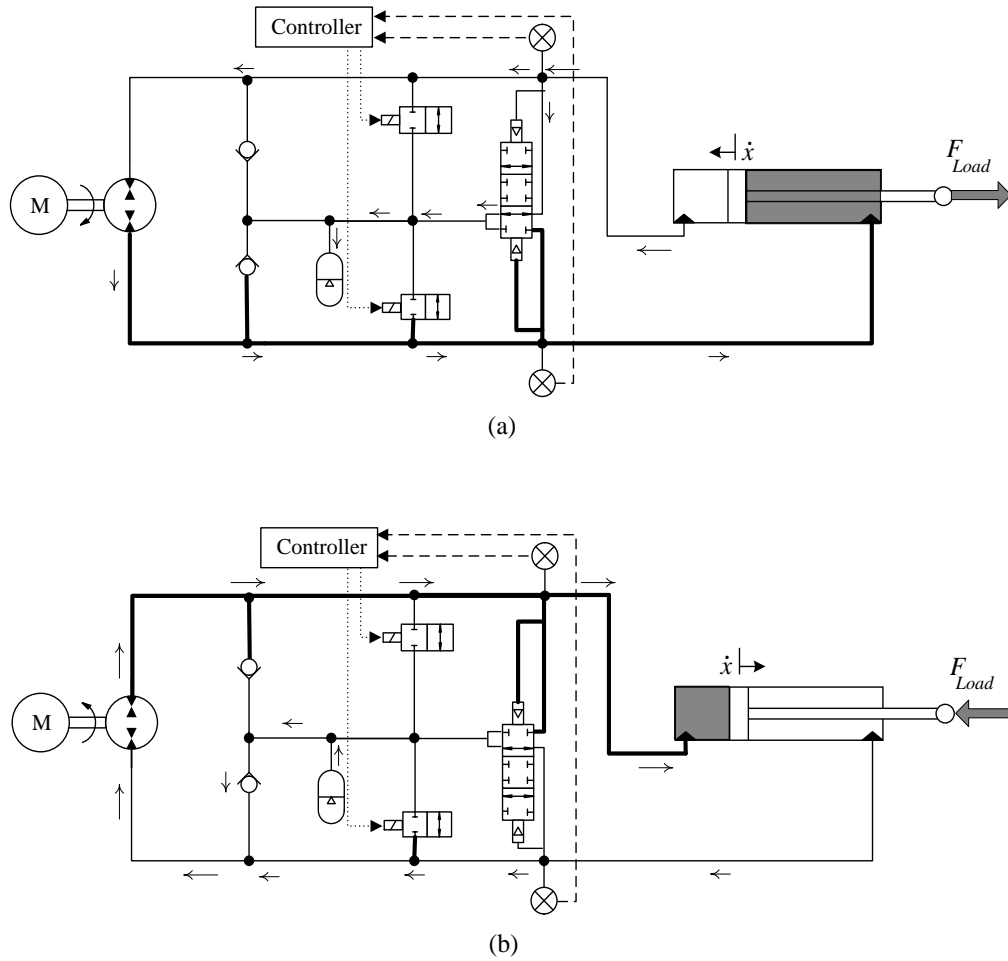
Figure 2-9: Circuit using a pilot operated logic valve to redirect the differential flow of a single rod cylinder and an internal control loop that reads pressures two sides of cylinder and damping pressure transients by fast opening and closing of two solenoid valves, (a) and (b) shows the fluid directions in the hydraulic circuit when the load is resistive and in the case of extraction and retraction of the cylinder rod.

In previous addressed circuits by using one pump to control flows of an asymmetric hydraulic cylinder always one side of the cylinder is connected to low pressure side of the hydraulic circuit. In the case of load switching some transients on pressures creates undesirable vibrations on end-effector of the cylinder. For the case of small resistive loads they are couple of designs that will be covered in next few pages.

A pump-controlled circuit design by Festo automation for fraction of horse power resistive load applications is presented in Figure 2-10 [40] . As it is seen in this figure,

a DC electric motor is coupled to a fixed displacement bidirectional hydraulic pump. Adjustable check valves CV1 and CV2 are improving the stiffness of the cylinder against small assistive loads by raising the low pressure. Set of two pilot to open check valves PCV1 and PCV2 lock the end-effector of the cylinder at its position when the circuit is in rest. Set of pilot to close check valves PCV3 and PCV4 redirects the differential flows of the single rod cylinder to the tank. The circuit is highly inefficient due to use two adjustable check valves CV1 and CV2 to improve the response of the end-effector to resistive loads.

(a)

(b)
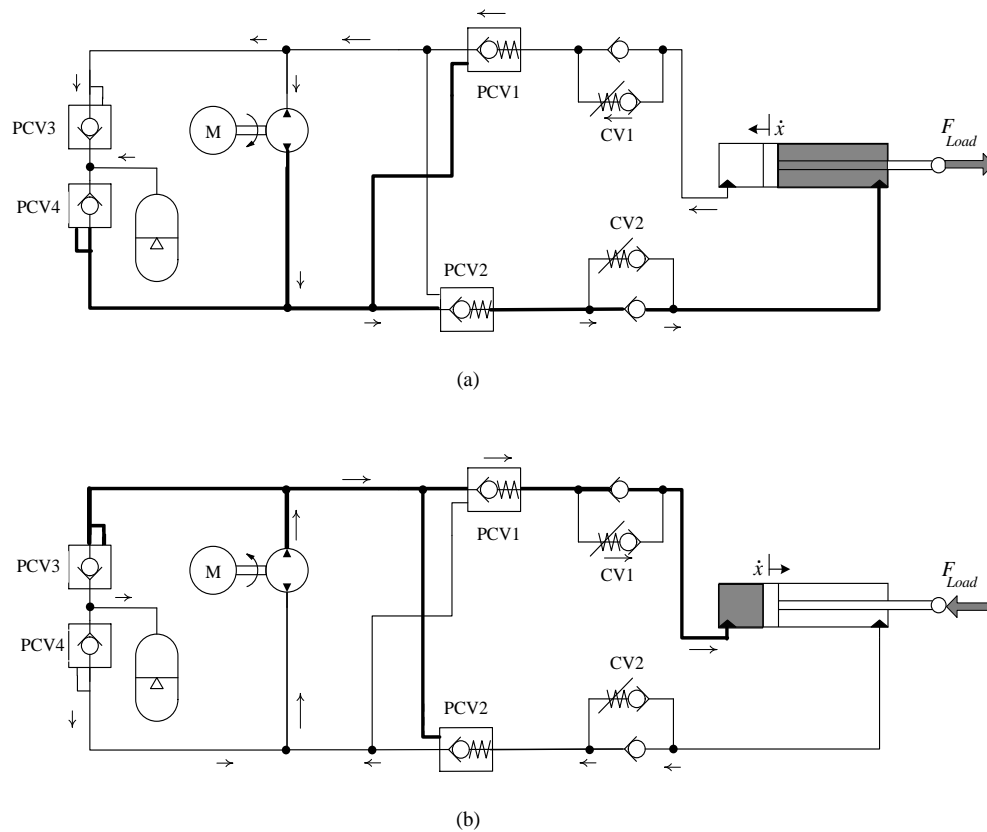
Figure 2-10: The circuit using two pilot check valves and two adjustable check valves to eliminate vibrations when the load changes its mode, this circuit works for resistive loads (patented by Festo [40], (a) and (b) show the flows of the circuit for retraction and extraction of end-effector.

Parker commercialized a low power (fraction of horse power) pump-controlled hydraulic circuit for resistive load applications (pallet jacks, truck tailgate locks,

19

scissor tables) (see Figure 2-11) [41]. When the electromotor-pump in Figure 2-11 is not energized, pilot check valves PCV1 and PCV2 isolate the hydraulic cylinder from the rest of the circuit to keep the load at its position (cylinder will not retract under the load). When the cylinder retracts, an extra volume of fluid creates an excessive pressure buildup inside the bigger chamber side of the circuit. Backpressure relief valves (BPV) sense the extra pressure and redirect extra fluid to the tank. The circuit is highly inefficient.

(a)

(b)
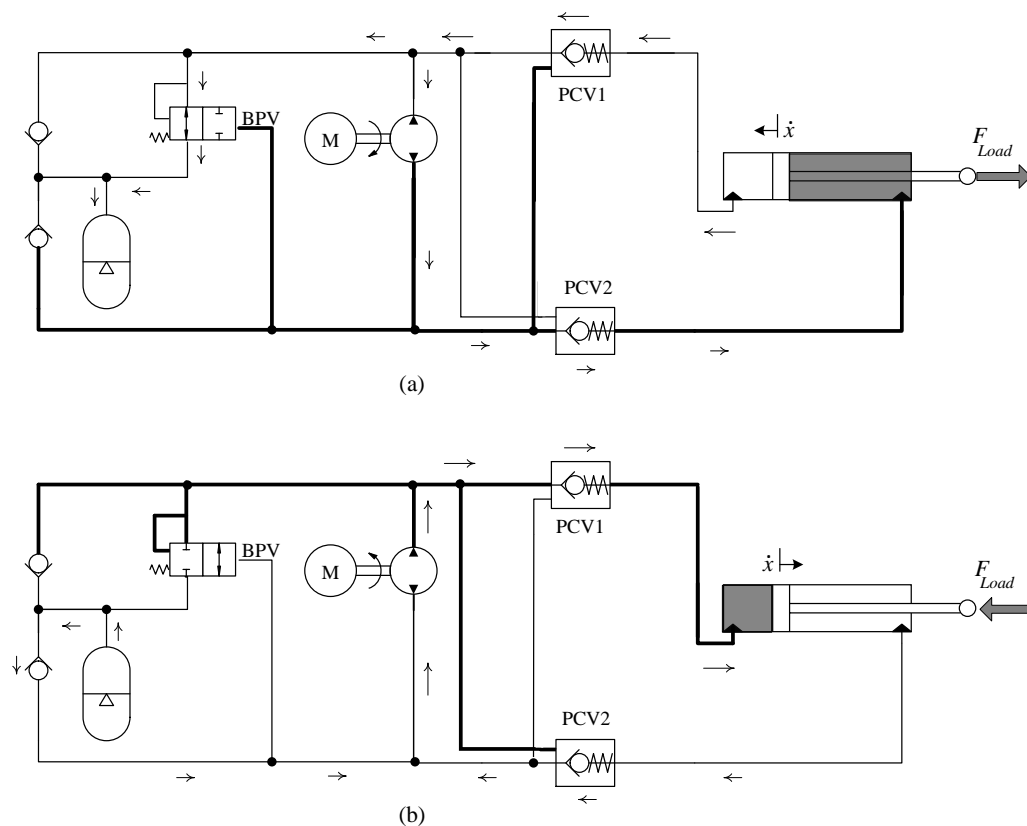
Figure 2-11: Friction of horse power electro-hydrostatic actuation system by Parker [41], (a) and (b) show how hydraulic fluid flows in circuit when the cylinder retracts and extracts.

2.4. Summary

This chapter reviewed the concept of pumping and motoring operation modes of a hydraulic machine. In addition, concepts of resistive, assistive, and switching loads were briefly studied. A brief history of pump-controlled hydraulic circuits and

existing designs for these circuits was discussed. The pros and cons of each circuit were highlighted. The main concern of existing pump-controlled circuits was determined to be the sensitivity of the position response of these circuits to switching loads. One side of the cylinder always connects to the low pressure side of the hydraulic circuit, and when the load switches suddenly, both sides of the cylinder connect to the low pressure side of the circuit and make the circuit uncontrollable.

CHAPTER 3

THE PROPOSED CIRCUIT

3.1. Design of the proposed circuit

In this chapter, a novel, simple, controllable, and efficient pump-controlled hydraulic circuit is introduced for switching load applications [42]. The proposed circuit is shown in Figure 3-1. Pump I is a fixed displacement gear pump, and prime mover M is a variable speed bidirectional electromotor. The differential flow rate exchange from the two sides of the cylinder is controlled by an on/off valve SV and two check valves, CVa and CVb. The open circuit section of valve SV is a check valve that protects pump I against cavitation in extreme load conditions. The pump feeds the ports of the cylinder through two counterbalance valves: CBV1 and CBV2. Counterbalance valves are normally used as safety valves for systems working with assistive or suspended loads [43]. A counterbalance valve incorporates a check valve for free flow in one direction and an adjustable pressure controlled valve to control the flow in reverse direction (see Figure 3-2).
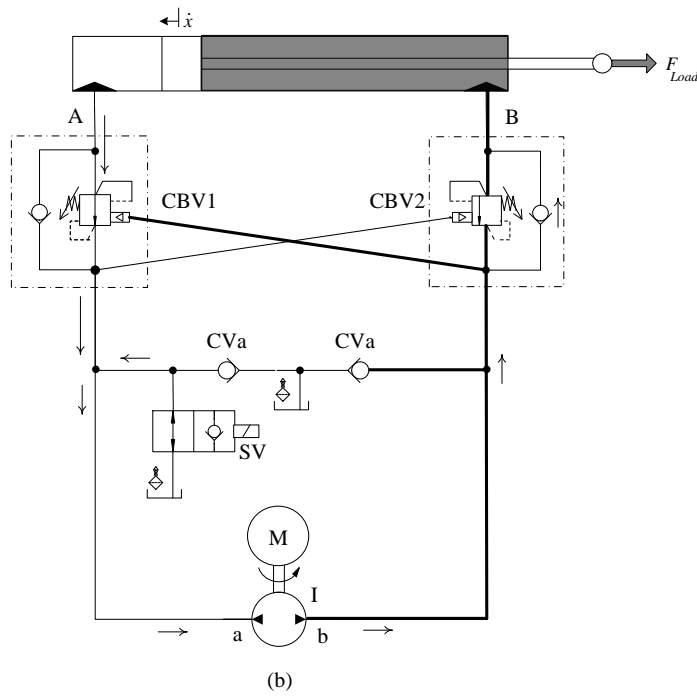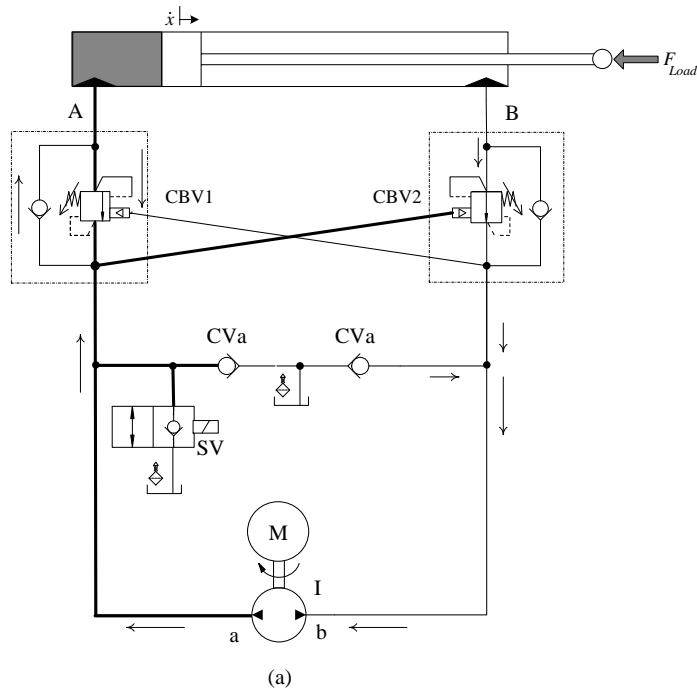
Figure 3-1: Schematic of the proposed circuit acting against resistive load and flow directions in extraction and (b) retraction of end-effector.
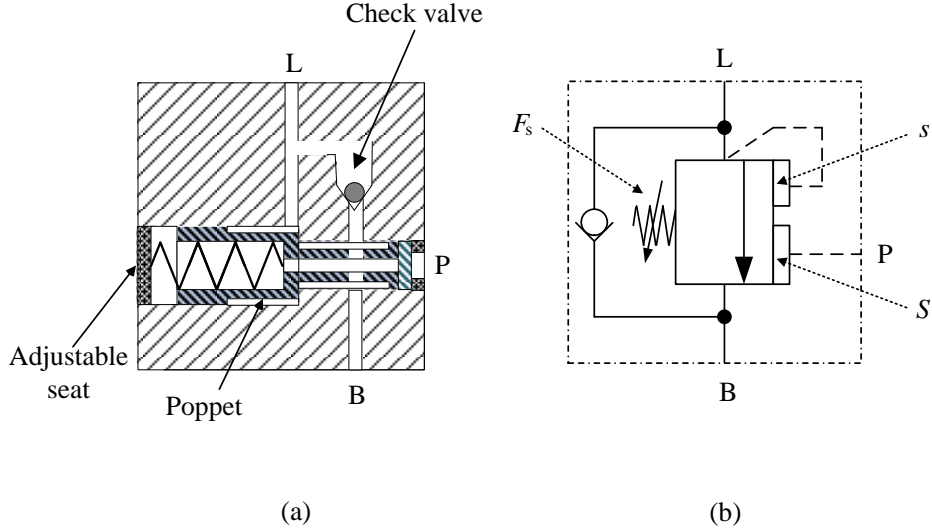
Figure 3-2: (a) Schematic of a typical counterbalance valve, (b) symbol of a counterbalance valve.

The force balance equation of a counterbalance valve is described as [44, 45]:

$$F_s + sx = P_{pilot}S + sP_{load} \tag{1}$$

where, F_s is the force of the pre-charged spring and is equal to (sp_s), where p_s is the valve setting value when the valve acts as a pure pressure relief valve and where s is the stiffness of the spring. The valve poppet displacement is x. P_{pilot} and P_{load} represent the pilot pressure (pressure at port P) and load pressure (pressure at port L) respectively. The poppet effective area at the pilot port is S and the poppet effective area at port L is s respectively. When P_{pilot} is less than the pre-set pressure, port L is blocked, and the load is hydraulically locked (see Figure 3-2a). When P_{pilot} reaches the pre-set pressure, the poppet moves in order to connect port B to port L which allows the end-effector to move. Pilot ratio of a counterbalance valve is defined as the ratio of the pilot port effective area to the load port effective area $(\alpha = {}^S\!/_{s})$ and it is higher than one. Valve setting is $(P_s = F_s/S)$, P_s is the pressure induced by applying the highest possible load at the load port of the counterbalance valve and F_s is the

24

force of the valve spring necessary to have the poppet closed and keep the load in position. In the case of assistive load (negative force), when the cylinder is extracting and the counterbalance CBV2 is governing the load motion, the force balance equations will be:

$$\begin{cases} SPA + sPB = F_s \\ A_APA - A_BPB = -F \end{cases}$$
(2.a)

and when the load is resistive (positive force):

$$\begin{cases} SPA + sPB = F_s \\ A_APA - A_BPB = F \end{cases}$$
(2.b)

To simplify equations:

$$\alpha = \frac{S}{s}; \beta = A_A + \alpha A_B$$
(3)

and by solving equations (2.a and 2.b) for the cylinder chambers pressures:

$$\begin{cases} PA = (-sF + A_AF_s)/_{s\beta} \\ \\ PB = (A_AF_s - FS)/_{s\beta} \end{cases}$$
(4.a)

$$\begin{cases} PA = (sF + A_AF_s)/_{s\beta} \\ \\ PB = (A_AF_s + FS)/_{s\beta} \end{cases}$$
(4.b)

Set of equation 4 (4.a 4.b) is valid for steady state conditions when the load force and end-effector velocity are constant. Figure 3-3 shows the counterbalance valve operation plot. By rearranging Eq. (4) we get:

$$\begin{cases} PA = (-1/_\beta)F + (^{A_BF_s}/_{s\beta}) \\ \\ PB = (-\alpha/_\beta)F + (^{A_AF_s}/_{s\beta}) \end{cases}$$
(5.a)

$$\begin{cases} PA = (^1/_\beta)F + (^{A_B F_s}/_{s\beta}) \\ PB = (^\alpha/_\beta)F + (^{A_A F_s}/_{s\beta}) \end{cases}$$

(5.b)

By changing the ratio of the counterbalance valves, the slopes of the pressure lines in Figure 3-3 change and by changing the setting of counterbalance valves' pressure lines in Figure 3-3 are shifting up and down. High pilot ratio allows end-effector motion with reduced pilot pressure for a faster operation and better energy efficiency [46]. However, the low pilot ratio provides more accurate and smoother motion [47]. As long as the pump builds up pressure and feeds the flow, P_{pilot} keeps the counterbalance valve fully open and the end-effector moves smoothly.
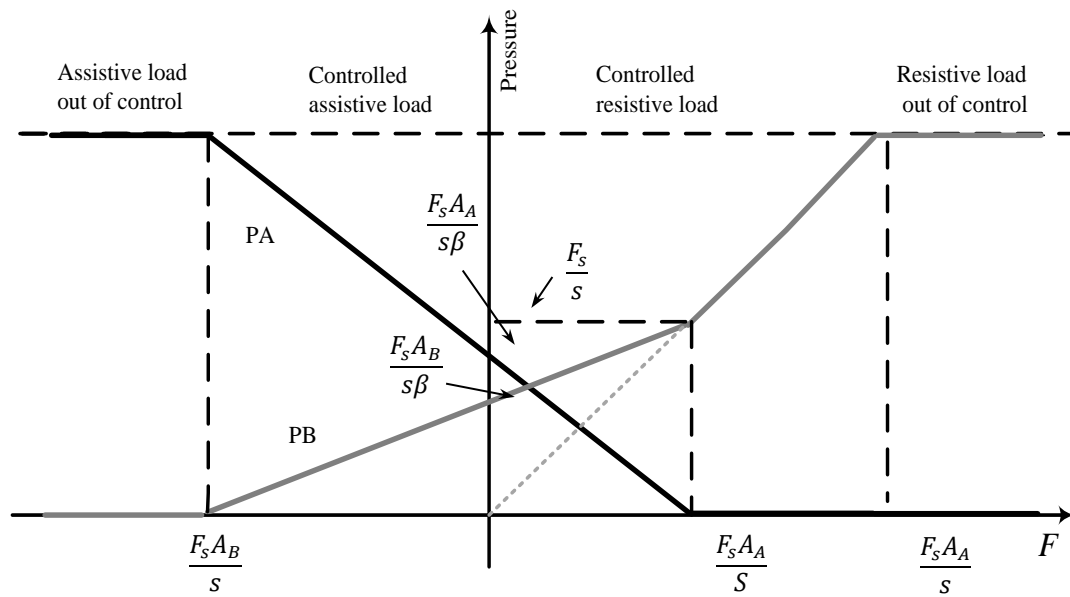
Figure 3-3: Counterbalance valve operation plot.

Suction pressure of the pump in the proposed circuit showed in Figure 3-1 is the tank pressure when the cylinder is extracting:

$$P = (Pa - Pb) > 0 \quad \text{when} \quad Q>0$$

(6)

Pump I operates in the pumping mode (see Figure 2-3). The counterbalance valve does not allow the circuit to work in the motoring mode and therefore, the circuit

26

cannot recycle energy.

In the retracting motion of the end-effector in Figure 2-3, the pump differential pressure and flow of the pump are represented by:

$$P = (Pa - Pb) > 0 \quad \text{when} \quad Q > 0 \tag{7}$$

The pump works in pumping mode (3rd quadrant in Figure 2-3) in this retraction motion and therefore the circuit does not recycle energy. When the pump does not rotate, the set of two counterbalance valves keep the end-effector in its position. Two counterbalance valves keep the cylinder port's pressures higher than the tank pressure while check valves CVa and CVb maintain the pressure of the pump ports equal or greater to the tank pressure [46]. Counterbalance valves make the hydraulic cylinder controllable in the case of switching loads [46]. Pressures at ports A and B of the cylinder depend on pilot ratios, setting of counterbalance valves, and load dynamics [45, 48]. When the pump supplies pressure at port a, port b sucks oil from the tank through check valve CVb, and the valve SV remains closed. Pressure builds up at port A of the cylinder through check valve CBV1, and pressure increases at port B (see Figure 3-1a). Counterbalance valve CBV2 keeps the line closed until its pilot pressure reaches its setting pressure. Once the CBV2 opens, the end-effector pushes the right spring. When the pump feeds oil trough port b, valve SV opens, the pump sucks oil from tank trough valves SV and check valve CVb while check valve CBV2 opens the pressure to port B of the cylinder, and pressure builds up at port A of the cylinder. Counterbalance valve CBV1 remains closed until pilot pressure from port b reaches the setting pressure. When CBV1 opens, the rod retracts and the end-effector pushes against the left spring. Valve SV returns the differential flow of the cylinder to the tank (see Figure 3-1b). Counterbalance valves prevent the circuit from working in motoring mode and recycling energy. Systems with counterbalance valves work with

27

higher pressures and consume more energy from the pump. When the load is not switching (pure assistive and pure resistive) like industrial lifters or elevators, using just one counterbalance valve on the load side of the cylinder has some advantages. The next section will introduce a pump-controlled circuit for industrial lifters using one counterbalance valve.

3.2. Proposed circuit for non-switching loads

Figure 3-4 shows the schematic of the simplified proposed circuit for industrial lifters like tote dumper [49]. The actuator is a single rod hydraulic cylinder.

When the circuit shown in Figure 3-4 is at rest, the prime mover is off and the load stops at its position. Also, both the internal check valve of solenoid valve SV and check valve CVa keep pump ports almost at tank pressure. Meanwhile, the counterbalance valve CBV2 remains off and blocks the hydraulic line and check valve CVb keeps pressure at port b of pump I approximately equal to the tank pressure. Afterwards, mass load builds pressure at port B of cylinder and stands at its position without the effort of the prime mover. When motion is needed, pump I will start from a condition where the pressure at the two ports equals tank pressure.

To perform the lowering motion, pump I feeds the hydraulic fluid to port A of the cylinder (Figure 3-4) causing the buildup of pressure at that port. . The check valve CVb opens the tank to port b of the pump. The pressure at port b will approximately equal the tank pressure. Once the pilot pressure of the counterbalance valve reaches the cracking pressure, the line from port B of the cylinder is opened to port b of the pump. In this case, the on/off solenoid valve SV will stay off and the pump provide the hydraulic oil to port A of the cylinder directly. The tank provides the pump with the differential flow rate from both sides of the cylinder. The pump

works in pumping mode (1st quadrant in Fig.1).

To raise the load, the pump supplies the hydraulic fluid from port b to the hydraulic circuit (Figure 3-4). The port a of the pump acts as a suction port, and valve SV is switched on. Valve SV opens port A of the pump and port A of the cylinder to the tank. Extra fluid from port A is diverted to the tank through valve SV. The hydraulic fluid from the pump port b passes through check valve CBV2, and builds up pressure at port B of the cylinder. Check valve CVb will stay closed under pressure in this case, pump I works in the pumping mode (3rd quadrant in Figure 2-3) therefore, the circuit does not recycle energy. Prime mover M is a variable speed electric motor. Next section reviews the simulation results of some important existing pump-controlled circuits and the simulation results of the proposed circuit (Figure 3-4) under a switching load.
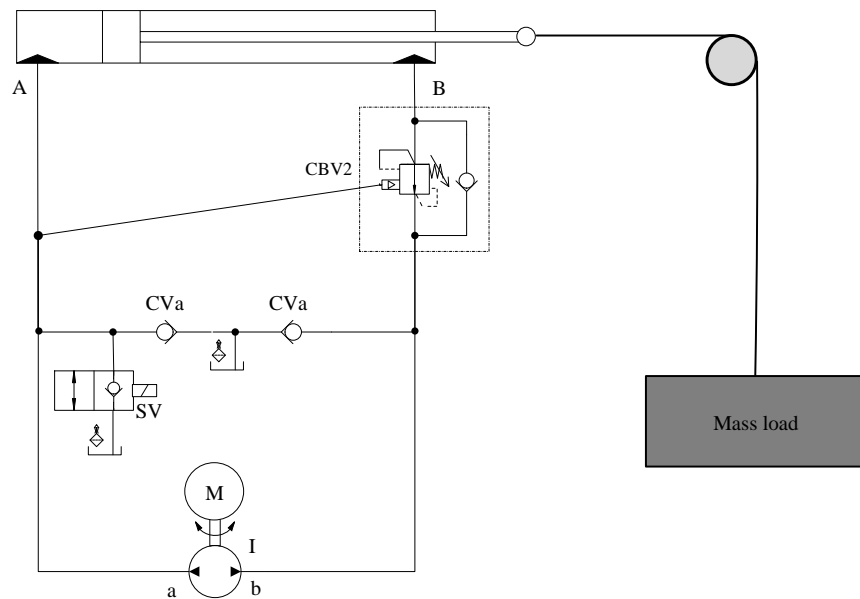
Figure 3-4: Schematic of the proposed circuit for resistive loads.

3.3. Summary

A novel and easy to control design for pump-controlled hydraulic actuator using two counterbalance valves and one on/off valve was introduced. The performance of a counterbalance valve was reviewed, and its governing formulas were introduced. The proposed circuit was able to handle switching loads. When one counterbalance valve is removed, the simplified proposed circuit for lifting applications can also control non-switching loads (lifting applications).

CHAPTER 4

EXPERIMENTAL TEST RIG

To control the end-effector of a hydraulic cylinder, pressures at both sides of the cylinder need to be controlled. The literature review showed that the pressures at both sides of the cylinder are controllable in two-pump pump-controlled hydraulic circuits and the proposed circuit. The cost, weight, noise, maintenance, and complexity of control make two-pump pump-controlled circuits less attractive for industrial applications. Counterbalance valves prevent the proposed circuit from recycling energy. Moreover, due to the fact that counterbalance valves keep extra pressure at both sides of the cylinder, the proposed circuit has a high probability of consuming more power to run as compared to a pump-controlled circuit without counterbalance valves. Therefore, counterbalance valves make the circuit controllable and at the same time increase the energy consumption of the circuit. To evaluate the performance of the proposed circuit, an experimental setup is needed. The structure of such a solid, compact, and low-cost test rig is introduced by using off-the-shelf industrial elements. Also, by employing two identical compression springs, a switching load is developed. To test the performance of the proposed circuit under non-switching resistive and assistive loads, a weight load setup is designed and manufactured.

4.1. Design of the test rig

A typical pump-controlled hydraulic cylinder might include the following five major units:

- A single rod hydraulic cylinder to handle the load,
- A pump-prime mover unit to energize the hydraulic cylinder,
- A set of valves to manage the flow of the single rod cylinder and prevent the circuit from over pressure, and
- A controller and sensors to record and screen the experimental results.

An ideal test rig should be able to connect to any single rod hydraulic cylinder of an industrial hydraulic machine. It is difficult to pressurize a wide variety of single rod hydraulic cylinders in industry using just one test rig. Common hydraulic pumps in industry are piston pumps and gear pumps. Piston pumps are pricy and more sophisticated in compare to gear pumps and they need a charge pump to work but, their responses are faster. To evaluate the proposed circuit in a lab environment under switching and non-switching loads, a small pump-controlled hydraulic test rig using the most economic and off-the-shelf parts is designed and prototyped. The compact test rig is prototyped using off-the-shelf industrial parts for smaller cylinders and loads which need less than 5 hp power. The prime mover is a brakeless; three phase industrial induction electric motor, controlled by a Variable Frequency Drive (VFD). Variable frequency drives are most economic and common speed controllers in the market and they are widely used in industry. A compact reservoir tank is designed and prototyped in a way that the pump, check valves, and pressure relief valves are submerged into the hydraulic oil to protect the pump against cavitation at the suction port. Figure 4-1(a) shows the prototyped compact test rig. Figure 4-1(b) illustrates the two pressure relief valves that protect the whole circuit against over pressure and the

two check valves connect the ports of the pump to tank. Two manifolds with extra ports provide a configurability feature for the test rig. The submerged part of the compact unit is shown in Figure 4-1 (b). Parameters of the manufactured test rig and spring loads are summarized in Table 4-1.

Table 4-1: Test rig parts technical information.

Part	Value/Specification
Cylinder	Parker HMD series, ratio 1:1.8, 11.40 cm^2, 6.33 cm^2 , stroke 71.12 cm
Pump	Parker PGM 511 series, type (0100), gear motor displacement 10 cm^3/Rev
Counterbalance valve	Sun Hydraulics CBCA, 3:1 ratio, Series 3, 40 L/min
Check valve	Sun Hydraulics CXFA, 160 L/min
Pressure relief valve	Sun Hydraulics RDHA, 380 L/min, 3000 psi
On/Off Solenoid valve	Parker DSL series ,101 NRT, 60 L/min
Electromotor	Leeson AC Motor, Model 184THTS8058BS, 5 HP Vector duty, 3 phase, 460 V, 6.7 A
Variable frequency drive (VFD)	Leeson AC adjustable drive, SM2 Series, Model 174625
Pressure transducer	Ashcroft K1 (0-2000 psi, 0-10 V), %1 of 2000 psi accurate
Sensitivity of linear position transducer	1 μm
Data acquisition board	Quanser, Q8, PCI, Using Quarc 2.4
Operation system	Windows 7
Spring load	Compression, 16700 N/m

Figure 4-2 shows the control structure of the test rig; a Q8 Quanser DAQ board interfaces the test rig to a desktop computer. For interfacing Quarc 2.4 Matlab Simulink blocks are used. Control loop is closed on readings of a linear position transducer with sensitivity of 1μm.
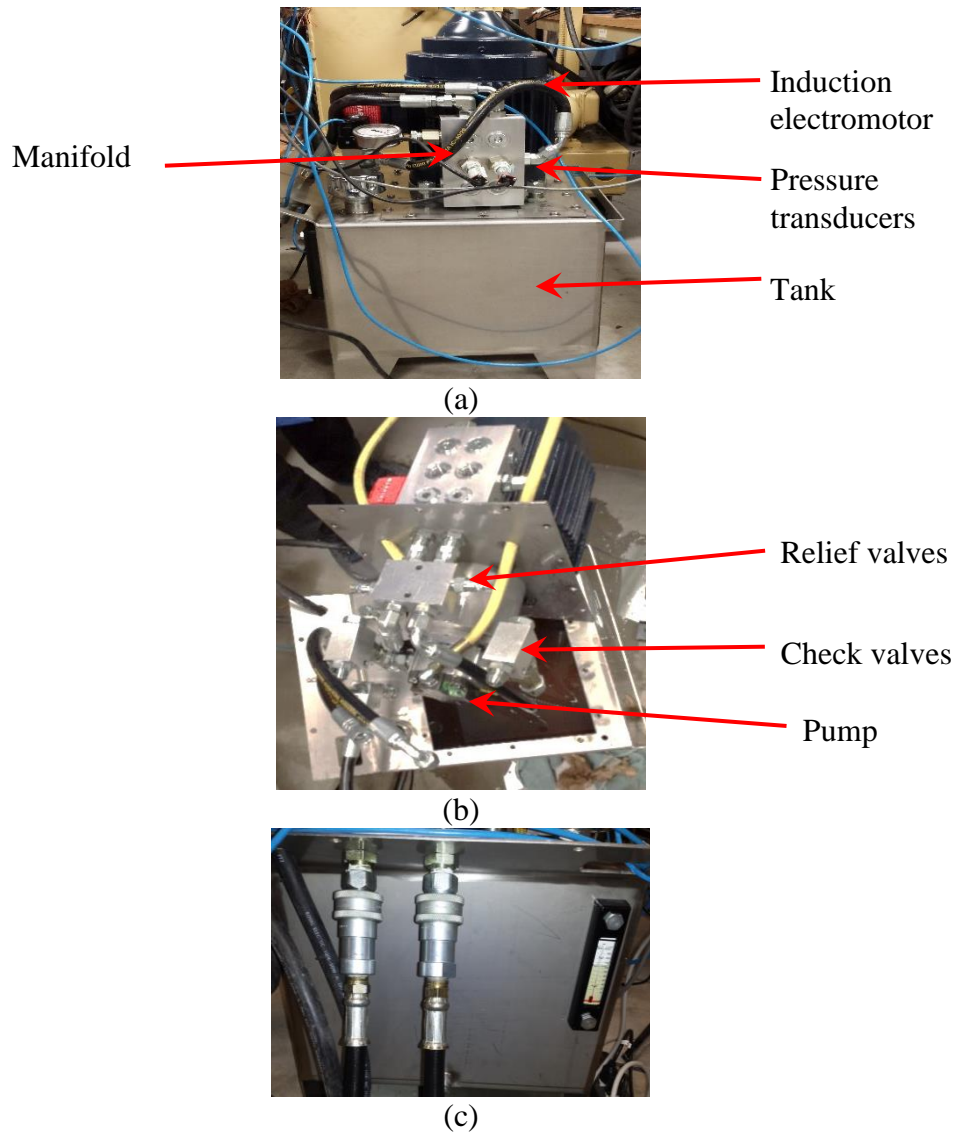
Figure 4-1: (a) Assembled compact test rig, (b) submerged components, (c) ports of the compact test rig.
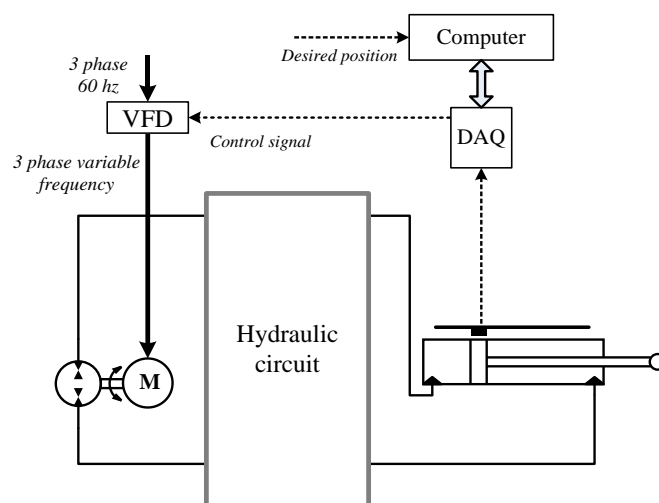
Figure 4-2: Control structure of test rig.

4.2. Design of load setup

To validate the proposed circuit under a switching load, a load setup using two identical springs was designed and manufactured. Figure 4-3 shows the design of the switching load setup, from top to bottom in Figure 4-3 cylinder extracts and retracts. The first two top drawing show how two springs create assistive and resistive forces against rod-end effector. The third and fourth drawings demonstrate assistive and resistive action of springs when the rod-end effector retracts. In one cycle of motion the rod-end effector experience two assistive and two resistive load forces. Installing two counterbalance valves on ports of cylinder keep the pressure inside the cylinder chambers and in rest position the rest of the hydraulic circuit experience tank pressure. Figure 4-4(a) shows the cylinder, counterbalance valves and hydraulic-quick-couplings. Figure 4-4(b) shows the manufactured switching load setup using two identical compression springs with stiffness of 16700 N/m.
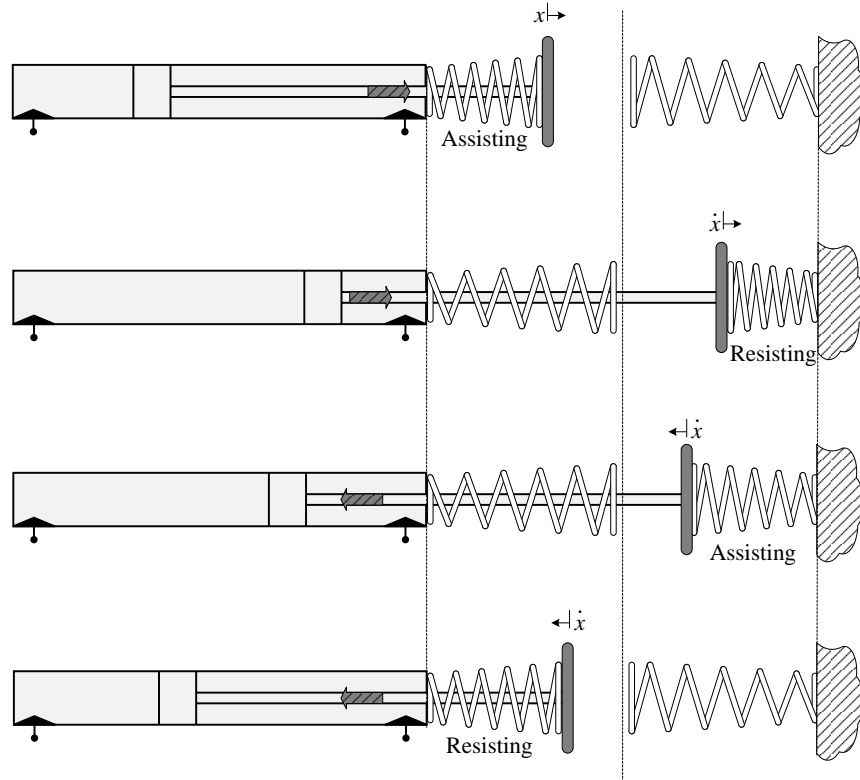
Figure 4-3: Design of switching load setup using two identical compression springs.

To experimentally validate the proposed circuit under non-switching resistive and assistive loads, the weight load setup shown in Figure 4-5 is designed. In the case of lowering load the weight of load helps to pump and the load acts as an assistive load. In the case of raising the mass load it works as resistive load. the load setup with a maximum load of 136 kg shown in Figure 4-6 is developed and be able to replace by spring switching loads connected to end-effector of the cylinder. In the case of weight load the counterbalance valve from port A of the cylinder is removed to improve the efficiency of the system and the counterbalance valve at port B of the cylinder is set to keep the load in its position when no movement of load was required. At resting condition, the load stands still spending no energy from the pump and prime mover to keep it at position.

(a)

(b)
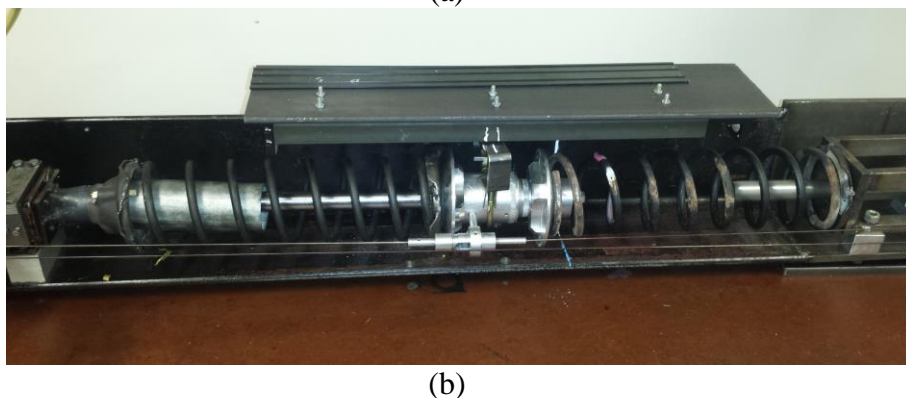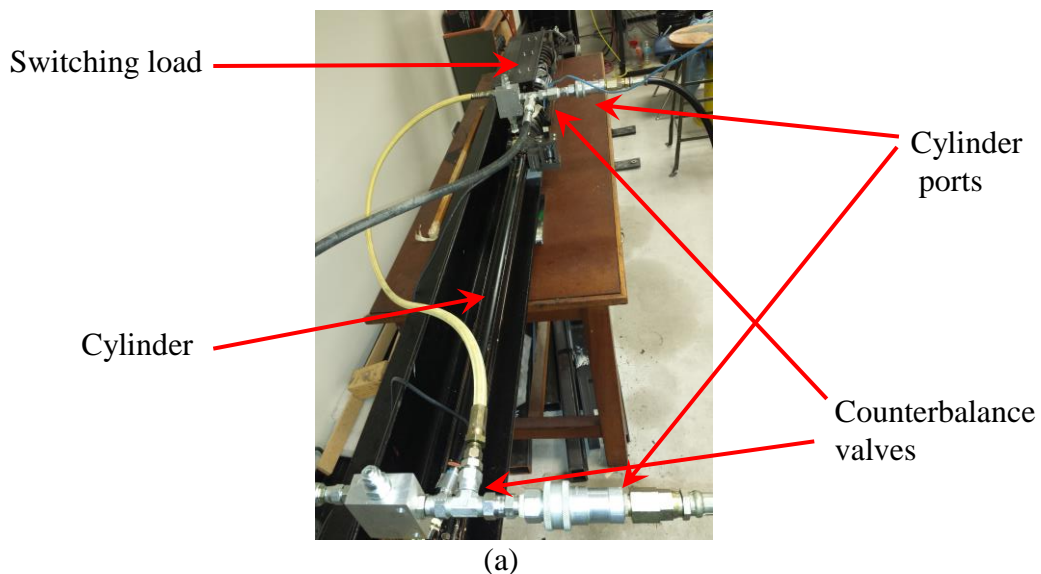
Figure 4-4: (a) Cylinder load setup, (b) switching load.
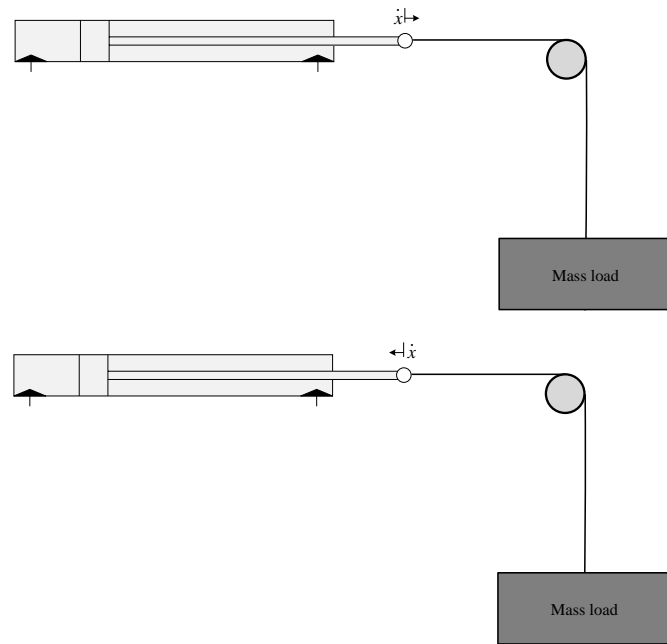
Figure 4-5: Weight load design for non-switching loads.
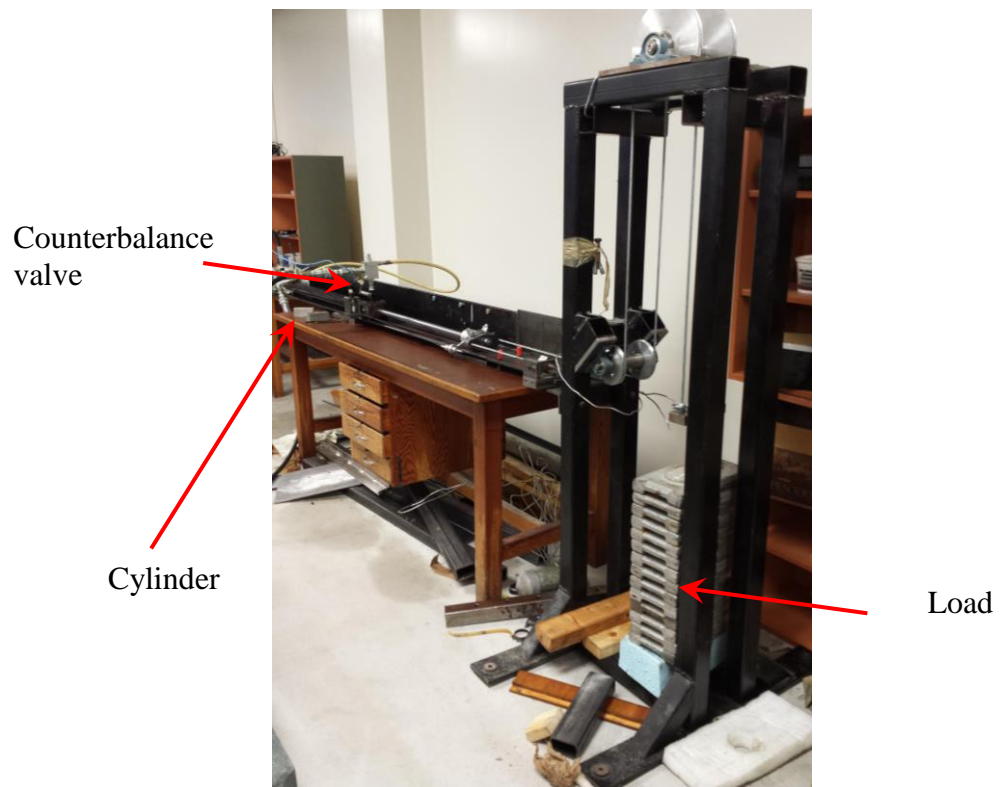
Figure 4-6: Load setup for validation of the proposed circuit under non-switching load.

4.3. Summary

This chapter presented the design and manufacturing of a test rig using off-the-shelf industrial parts for the evaluation of the proposed circuit. The setup comprised four main units: (i) a single rod hydraulic cylinder to handle the load, (ii) a pump-prime mover unit to energize the hydraulic cylinder, (iii) a set of valves to manage the flow of the single rod cylinder and prevent the circuit from over pressure, and (iv) a controller and sensors to record and screen the experimental results. Moreover, two load setups for switching and non-switching loads were designed and introduced.

.

CHAPTER 5

SIMULATION STUDIES

This chapter presents a simulation study of three major pump-controlled single rod cylinder circuits using one pump (see Chapter 2). Simulation results of a pump-controlled hydraulic circuit for a double rod cylinder, as a sample of a well behaved and industrially accepted circuit, are considered as the benchmark for further comparisons. The other three circuits are: (i) the pump-controlled circuit using a three-port two-position valve, (ii) a pump-controlled circuit using two pilot check valves, and (iii) the proposed circuit using two counterbalance valves and one on/off solenoid valve. Simhydraulic tools of Matlab Simulink software [43] are used to perform simulation study. Mathematical modeling for each hydraulic element, used for simulations, is presented in Appendix A. To evaluate the accuracy of Simhydraulic tools and simulation setup, as the first step, the test rig is simulated. The same tracking signal is applied to both simulation setup and test rig when the end-effector interacts with a switching load. A comparison of the results verifies the accuracy of Simhydraulic tools and simulation setups. In the next step, the effect of

pilot ratio and pressure setting of counterbalance valves on energy consumption and pressure responses is studied. The simulation runs for three different pilot ratios and three different pressure settings of counterbalance valves. The pump delivered hydraulic power is calculated and compared to required hydraulic power by a valve controlled circuit to perform the same tracking response when the pump is pressure compensated. Finally, the pressure settings of counterbalance valves are set to optimum settings that are explored by the last simulation study, and the performance of the proposed circuit is compared to the designs of three major throttles-less circuits.

To make the results comparable, a unique size of a hydraulic cylinder and hydraulic pump are used. The control loops of these four circuits are closed on readings of end-effector position sensor of cylinder with a proportional gain. The desired position signal has a magnitude of 40 cm (20 com of extraction and 20 cm of retraction) that lasts for 10 seconds at a constant speed, i.e., 4 seconds extraction, 4 seconds retraction, and 2+2 seconds of rest at the beginning and at the end of test. The signal is shown in Figure 5-1(a).

For tuning proportional gains, a constant 13500 N load force (see Figure 5-1b) is applied to the end-effector in each test such that the position error of the tracking signal is less than 0.5 cm. The force load against end-effector is constant and resistive for the first half of the test, and assistive for the second half of the motion. After tuning gain of the circuits control loops, two different switching load forces are applied to the end- effectors. To compare the position responses of four circuits, when the load is fast switching, a square load signal with amplitude of 13500 N and frequency of 0.25 Hz applies to simulation setups (see Figure 5-1c). To compare the responses, when the load is smooth switching, a sinusoidal load signal, shown in Figure 5-1(d), applies to those four designs. By applying the square and sinusoidal

40

switching loads tracking responses and position errors of circuits and pressure behavior of cylinders will be studied and compared to the results of double rod cylinder circuit as the benchmark.
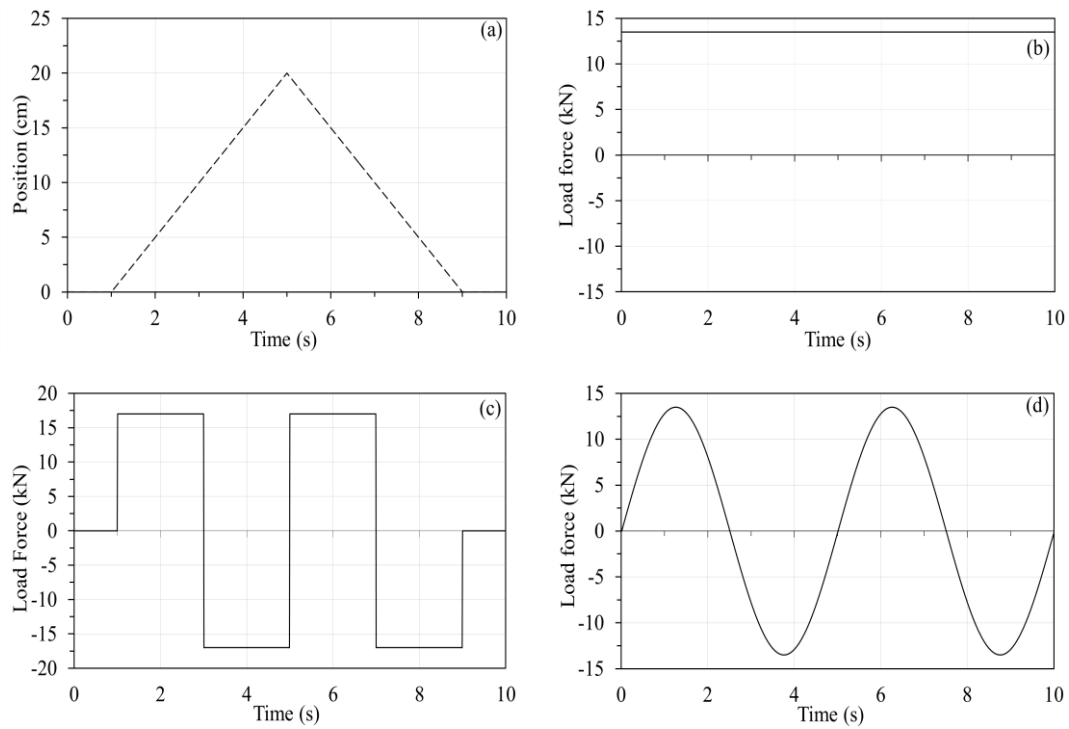
Figure 5-1: (a) Desired position signal, (b) constant load force, (c) square switching load and (d) sinusoidal switching load against end-effector of cylinders.

5.1. Evaluation of simulation tools with experimental results of the test rig

At the first step to evaluate the accuracy of the simulation tools, the test rig is going to be simulated with Simhydraulic tools of Matlab. Figure 5-2(a) presents the drawing of the test rig and Figure 5-2(b) shows the Simhydraulic simulation setup of the test rig and its switching spring load. Governing equations of Simhydraulic block parameters used in the simulation setup are presented in Appendix A. To evaluate the accuracy of the simulation method and assess the tracking performance of the proposed circuit, a square signal shown Figure 5-3(a) is applied to variable frequency drive of the test rig and angular velocity source of simulation setup. Table 5-1

41

presents the drawings blocks borrowed from Microsoft Visio 2010 software to draft the test rig lay out along with Simhydraulic blocks used to create the simulation setup of test rig shown in Figure 5-2(b) represents the technical data of hydraulic elements used in test rig.

To evaluate the accuracy of simulation tools a square signal shown in Figure 5-3(a) is created and applied to the variable frequency drive of the test rig and the ideal angular velocity source of the simulation setup. Comparing position response of the simulation setup shown in Figure 5-3(b) and actual position readings of end-effector of cylinder shown in Figure 5-3(c) shows the accuracy of simulation position tracking except when the rod-end of cylinder starts its motion. Figure 5-3(d) and Figure 5-3(f) are pressure responses of simulation setup at the cylinder ports versus time and end-effector position and Figure 5-3(e) and (g) present the pressure readings at the cylinder ports of test rig versus time and end-effector position. Comparison of pressure simulation results and experimental data show identical trends in all moments except at following moments: t=2s to 2.9 s, 8s to 8.5 s, 16s to 16.7s and 26s to 26.5s. Test rig and simulation position responses are the same. At those moments, in the case of test rig, the inertia of rotating parts of the electromotor/pump unit, the response delay of the VFD (variable frequency drive), friction of the cylinder, undissolved air in hydraulic fluid, flexibility and length of hydraulic lines in the test rig are responsible for the difference of simulation and experimental results. The valve pressure settings of the counterbalance valves for simulation and test rig are set to 500 psi for the valve on port A and 800 psi for the valve on port B of the cylinder. In the simulation setup, in order to speed up the simulation process, a few assumptions were made.

Figure 5-2: (a) Schematic of the test rig, (b) simulation setup of test rig using Simhdraulic simulation blocks.

First, the hydraulic fittings were assumed to be ideal and not create any drops in pressure and second, lengths of hydraulic lines are assumed to be zero with pressure drop. For the test rig, the cylinder was connected to the pump unit by a pair of 4.5

meter, flexible 0.25 inch diameter hydraulic lines. The flexible hose damps some pressure ripples which results in smoother pressure plots in the experimental results.

Table 5-1: Drawing and Simhydraulic block symbols
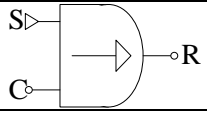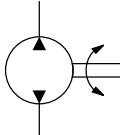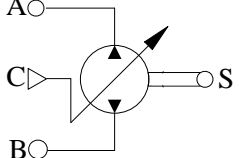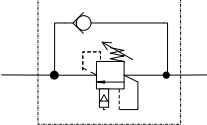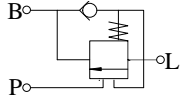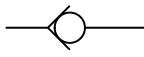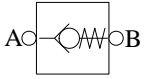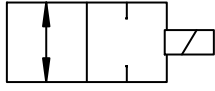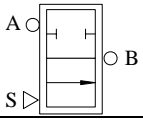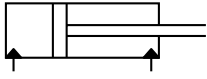
Block name	Microsoft Visio 2010 block (see Figure 5-7 a)	Simhydraulic symbol (see Figure 5-7 b)
Variable speed electromotor		
Fixed displacement bidirectional hydraulic pump		
Counterbalance valve		
Check valve		
Solenoid valve		
Single rod cylinder		
Compression spring		

Table 5-2: Simhydraulic simulation blocks parameters and symbols
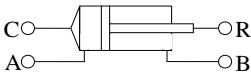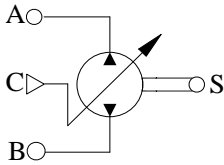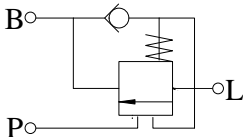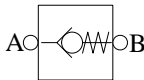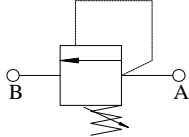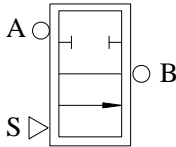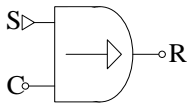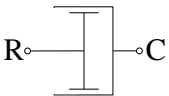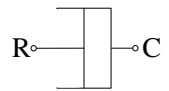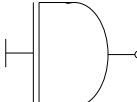
Block	Symbol	Value/Specification
Cylinder		A_A;11.40 cm^2, A_B; 6.33 cm^2 , stroke; 71.00 cm, dead volumes; 6.5 cm^3 each
Pump		Maximum displacement 10 cm^3/Rev, maximum stroke 2.5 cm, nominal pressure 2500, Max RPM 1800, volumetric efficiency proportionality coefficient 0.05, volumetric efficiency pressure coefficient 0.65, volumetric efficiency angular velocity coefficient 0.2, volumetric efficiency displacement coefficient 0.8, mechanical efficiency proportionality coefficient 0.06, mechanical efficiency pressure coefficient 0.65
Counterbalance valve		Valve spring stiffness 5×10^9, Pilot Ratio 3, back pressure ration 4, time constant 0.06 s, leakage area 5×10^{-9} m^2, By Max opening, Max orifice area 0.5 cm^2, orifice discharge coefficient 0.7, orifice critical Reynolds number 12, check valve maximum passage area 3.5 cm^2, check valve cracking pressure 2 psi, check valve maximum opening pressure 5 psi, check valve flow discharge coefficient 0.7
Check valve		Maximum passage area 3.5 cm^2, Cracking pressure 5 psi, Maximum opening pressure 15 psi, Flow discharge coefficient 0.7, Critical Reynolds number 12, Leakage area 10^{-55} cm^2
Pressure relief valve		Maximum passage area 1.55 cm^2, valve pressure setting 3000 psi, valve regulation range 150 psi, flow discharge coefficient 0.7, critical Reynolds number 12, leakage area 10^{-55} cm2
On/Off Solenoid valve		Model works by maximum area and opening, valve passage maximum area 3.5 cm^2, valve maximum opening 2.5 cm^2, flow discharge coefficient 0.7, initial opening 0 cm, critical Reynolds number 12, leakage area 10^{-55} cm2
Ideal angular velocity source		S port for control signal, C and R are mechanical ports
Rotyational spring		Spring rate 10^{12} N.m/rad

Table 5-2 (contd.): Simhydraulic simulation blocks parameters and symbols

Rotational damper	R○──┤├──○C	Damping coefficient 0.05 N.m/(rad/s)
Translational spring	R○──/\/\/\──○C	16700 N/m
Translational damper	R○──┤├──○C	Damping coefficient 300 N/(m/s)
Inertia	┤│D──○	$1 \ kg.m^2$
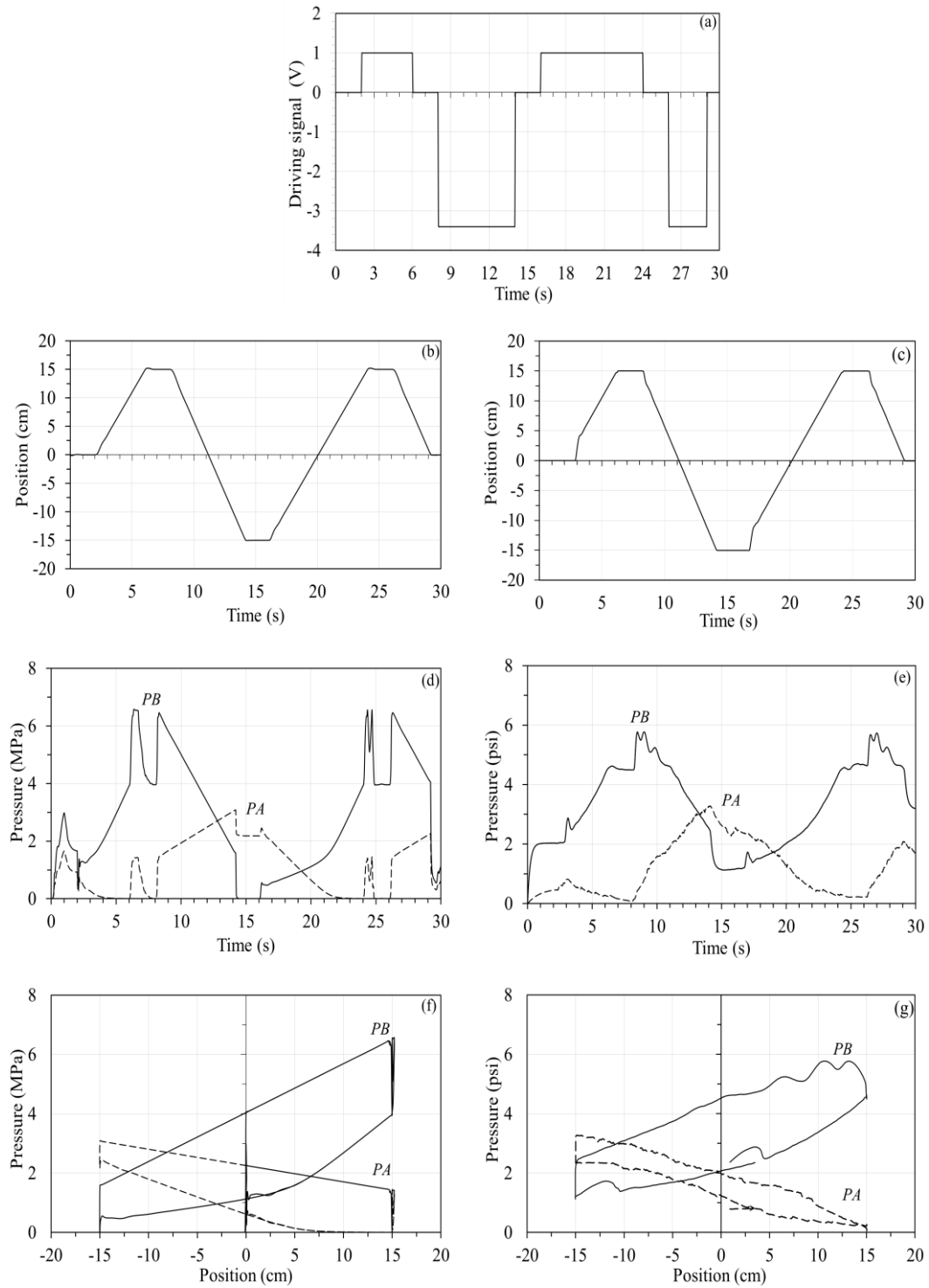
Figure 5-3: (a) Signal to VFD and ideal rotational drive in simulation setup, (b) position response of the simulation and (c) the test rig, (d) pressure responses at cylinder ports versus time in simulation setup and (e) the test rig versus, (f) pressure responses at cylinder ports versus end-effector position in simulation setup and (g) test rig.

5.2. Effect of counterbalance settings on performance of the circuit

At the second step to study the effect of the counterbalance valve pilot ratio to energy consumption of the circuit and pressure responses at the cylinder ports, pressure settings of two counterbalance valves are set to 3.4 MPa and 5.5 MPa, the same square signal is (see Figure 5-3 a) applied to ideal angular velocity source and pilot ratio of counterbalance valves are set to 3, 6 and 10. Figure 5-4(a) to (b) shows pressure at the cylinder ports versus end-effector position. Circuits with higher pilot ratio work with lower pressures at the cylinder ports and consume less power to perform the same motion of end-effector. Figure 5-4 (d) shows the delivered hydraulic power to ports of counterbalance valves by the hydraulic pump. By raising the pilot ratio from 3 to 10, pump delivered hydraulic power drops from 34 W to 22 W.

As the third test to study the effect of pressure settings on energy consumption of the circuit and cylinder ports' pressures, pilot ratios are fixed to 3 and settings of counterbalance valves at port A and port B of the cylinder are set to 1.7 MPa-3 MPa, 3.4 MPa-6.1 MPa, 5.1 MPa-9.2 MPa and simulation setup run when the same square signal is (see Figure 5-3 a) applied to ideal angular velocity source. Figure 5-5(a), (b) and (c) show the pressure plots of cylinder ports versus end-effector position. As it is shown by the trends in the pressure settings, pressure plots shift up when the pressure settings raise. Figure 5-5(d) presents the change of average delivered hydraulic power to the counterbalance valves' ports when the cylinder performed the same pattern of motion shown in Figure 5-3(b) and when the pressure of the counterbalance valves were set to different values. By increasing the pressure settings, the pump delivers more power to the circuit for the same pattern of load motio
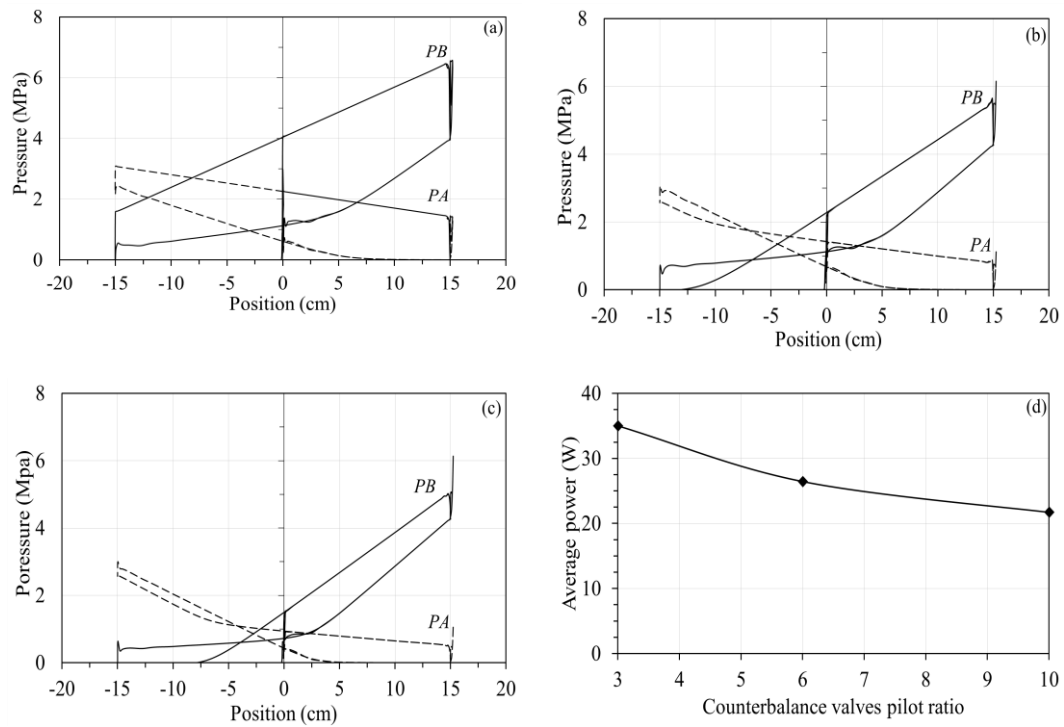
Figure 5-4: Pressure responses of the cylinder ports versus the end-effector position when pilot ratio is (a) 3, (b) 6, (c) 10, (d) changes of average pump delivered hydraulic power to cylinder when the counterbalance valve pressure settings are 3.45 MPa and 5.5 MPa.
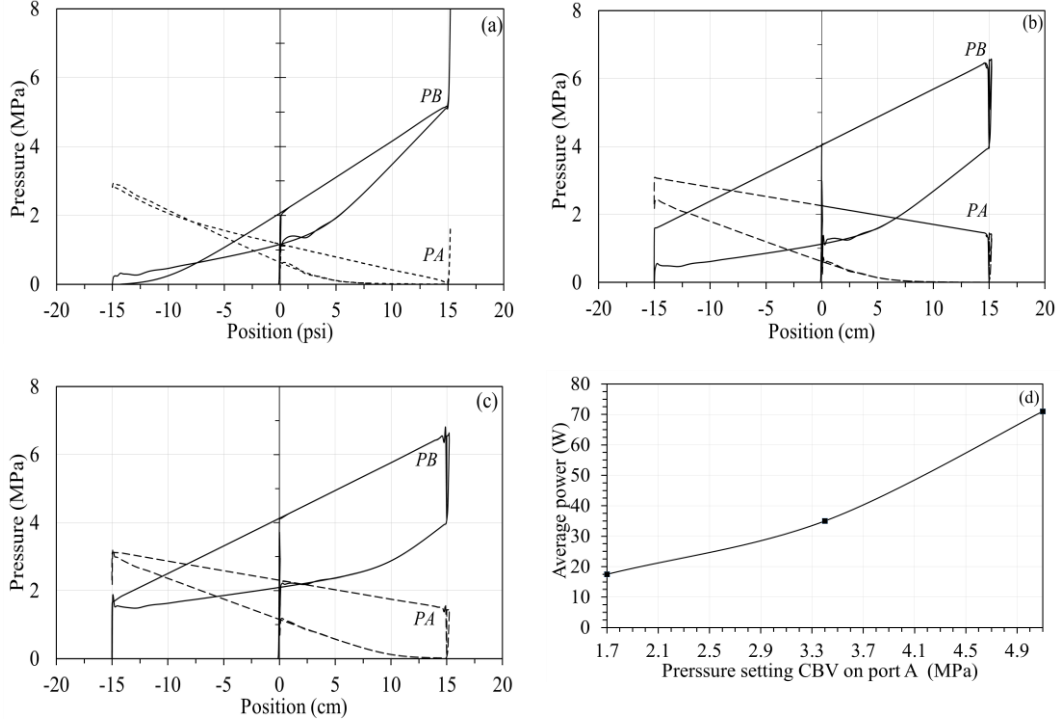
Figure 5-5.:Pressure at the cylinder ports versus end-effector position when pilot ratios fixed to 3 and pressure settings of counterbalance valves were (a) 1.7 MPa, 3.0 MPA (b) 3.4 MPa, 6.1 MPa, (c) 5.1 MPa, 9.2 MPa, (d) pump delivered hydraulic power for different settings of counterbalance valves.

5.3. Comparing energy consumption of proposed and valve controlled circuits

To calculate the delivered hydraulic power to the cylinder in proposed circuit, following equation can be used.

$$W_h = Q \times \Delta P \tag{8}$$

Where Q is the pump flow rate and can be obtained by multiplying the piston speed to the effective piston area and ΔP is the differential pressure of both sides of the hydraulic pump. In the case of the test rig, the pump is submerged in oil, and therefore it is a reasonable assumption to make that the suction port pressure is equal to the tank pressure and is almost zero. By reading the port pressures of the pump, ΔP is equal to *Pa* (see Figure 5-5 a) when the pump feeds port A of the cylinder and is equal to *Pb* (see Figure 5-5 b) when it feeds port B of the cylinder (also see Figure 5-2 a).

50

In conventional hydraulic circuits, the pump feeds a constant pressure fluid to the throttling valve ports; meanwhile the throttling valve controls pressures and flow rates of fluid to cylinder ports. In a valve controlled hydraulic circuit, the average delivered power to the throttling valve (W_{vav}) is calculated using the following equation [48]:

$$W_{vav} = \frac{(A_a + A_b)\, V_l\, P_s}{\pi} \qquad (9)$$

where P_s is the hydraulic power source pressure and V_l is the speed of the load (end-effector of the cylinder). The gear pump of the proposed circuit for the motion showed in Figure 5-3(a) consumed 37.7 W (see Figure 5-6). To calculate this energy, equation (8) was used by considering the pressures' readings at the ports of the pump and calculated the velocity of the end-effector of the cylinder. Using this equation, a prediction of the energy required by a pressure compensated pump to delivered power to a throttling valve (W_{vav}) to perform the same pattern of motion was made to be 183.6 W. In a valve-controlled hydraulic circuit equipped with a load sensing pump, when the load is assistive, the cylinder is uncontrollable [49]. Assuming that in the future, the uncontrollability issues using load sensing pump for assistive loads is solved, the theoretical studies have indicated that the energy required to produce the same pattern of motion in the same load condition is about 2% greater than the proposed circuit. Compared to our proposed circuit, valve controlled circuits equipped with load sensing pumps are expensive and require more complicated supporting hydraulic elements than an off-the-shelf gear pump that was used for the proposed test rig.
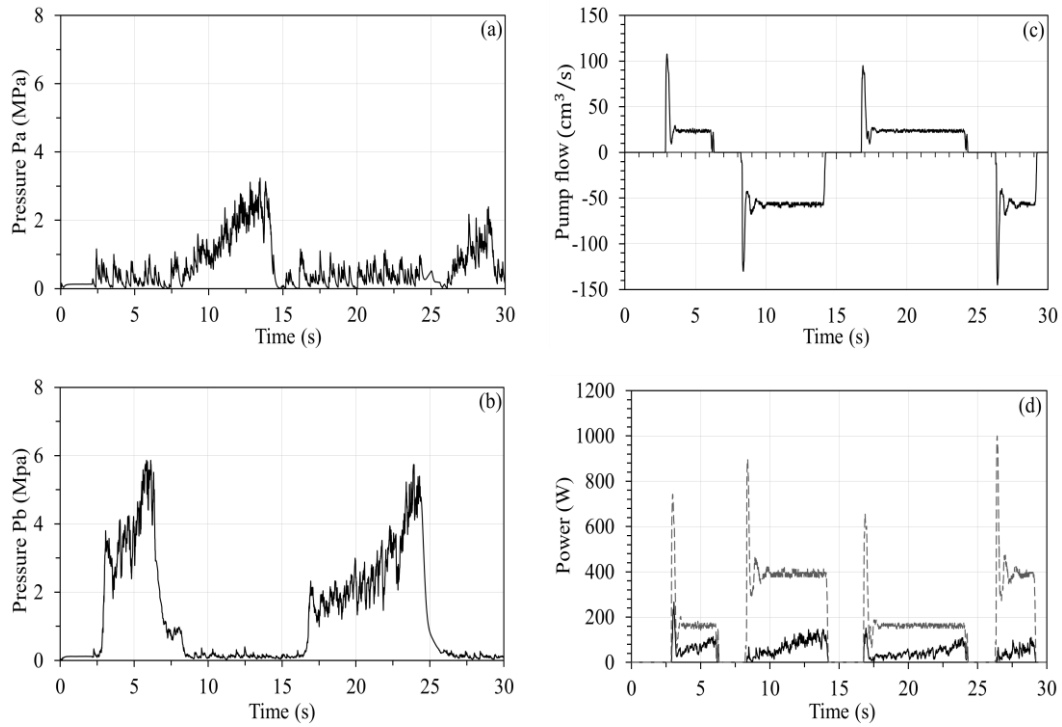
Figure 5-6.:Pressure readings at (a) port a and (b) port b of pump, (c) flow of the pump and (d) pump delivered hydraulic power (shown by solid line) and power required by a value controlled circuit to complete the same task given in Figure 5-3 (c) (shown by dashed line).

5.4.Pump-controlled hydraulic double rod cylinder

Figure 5-7(a) shows the schematic of a pump-controlled circuit for a double rod cylinder. Control loop is closed on readings of position sensor of cylinder end-effector with a proportional gain. Control signal governs the speed of the variable speed ideal motor as the prime mover. Simhydraulic setup simulation of the circuit is shown in Figure 5-7(b). Simhydraulic blocks used in Figure 5-7(b), symbols used in Figure 5-7(a) along with their simulation parameters are presented in Table 5-3. Pressure of accumulator tank was set to 35 KPa three different loads shown in Figure 5-1 applied to the simulation setup and position responses are presented in Figure 5-8. When the constant load as a non-switching load (see Figure 5-1 b) is applied to simulation setup and the desired tracking position signal is like Figure 5-1 (a), the average position error is 0.116 cm with standard deviation of ±0.074. Figure 5-8 (a)

52

shows the desired position and position response of simulation to constant load. When a square switching as an interim switching load like Figure 5-1(c) is applied to end-effector in simulation setup the average position response error is 0.166 cm with standard deviation of ± 0.155, Figure 5-8(b) shows the desired and position response of the simulation to the square swathing load Figure 5-1(c). When the load is a sinusoidal as a smooth switching (see Figure 5-1.d) the average of position error is 0.137 with standard deviation of $\pm$ 0.134 (see Figure 5-8. c and d).

To compare the performances of four previously mentioned pump controlled circuits, their responses under smooth changing switching load (sinusoidal load force) will be compared. Figure 5-9(a) presents the desired position and position response of the end-effector of the cylinder when the load is like Figure 5-9(b). Pressure responses at the cylinder ports are shown in Figure 5-9(c) and (e), position error of the simulation is shown in Figure 5-9(d). Figure 5-9(f) is the plot of pressure at port B versus pressure at port A of the cylinder. As it is shown in this plot some pressure protect two sides of the cylinder against sudden switching load. In other words in the case of sudden load force changing pressures two sides of cylinder protect the load against uncontrollable vibrations.
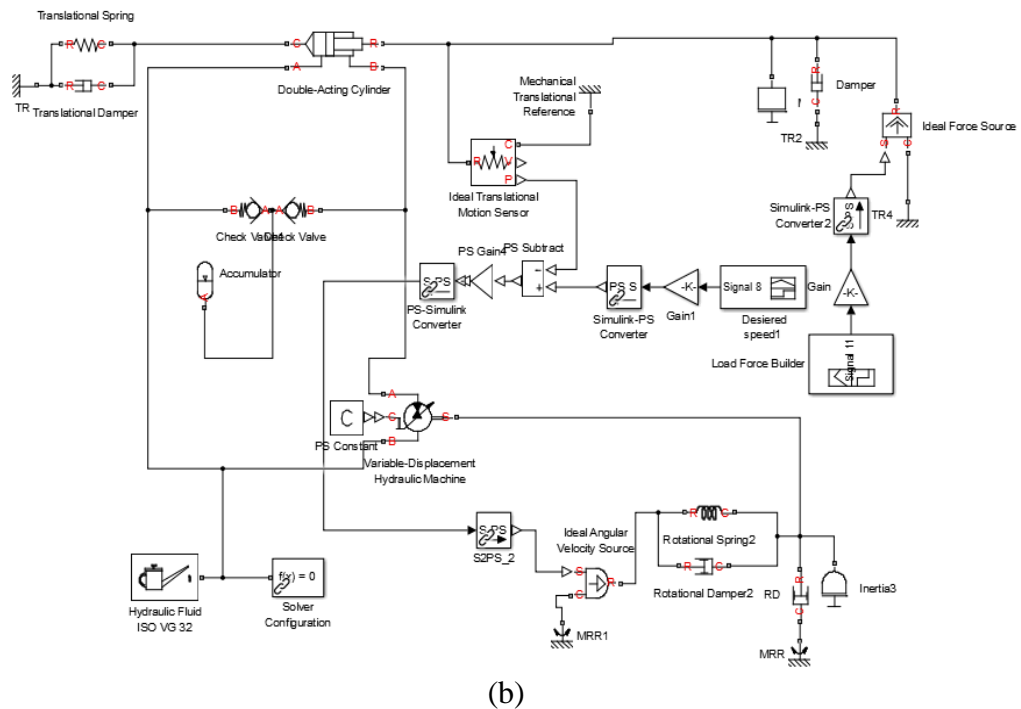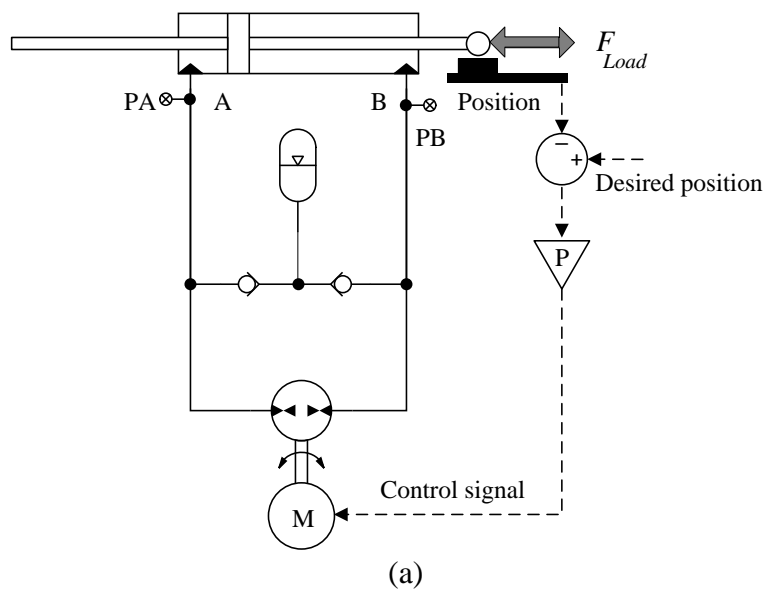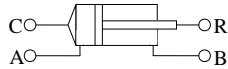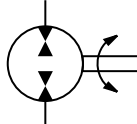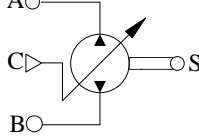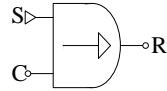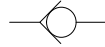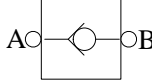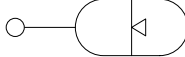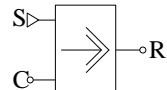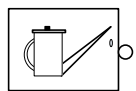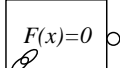
Figure 5-7: (a) Schematic of a pump-controlled double rod cylinder circuit, (b) simulation setup Matlab Simhydraulic blocks.

Table 5-3: Schematic circuit blocks, Simhydraulic blocks and parameters

Schematic	Simhydraulic block	block name	Parameters
	C○——○R A○——○B	Double rod cylinder	$A_A = A_B = 15.22$ cm^2 Stroke= 60 cm
	A○ C▷——○S B○	Hydraulic machine	Displacement=39.65 cm^3/rev Nominal pressure=17.2 MPa Maximum shaft velocity 188 rad/s
M	S▷——○R C○	Prime mover	Ideal angular velocity source
	A○——○B	Check valve	Max. passing area=1.93 cm^2, Cracking pressure=34KPa, Max. opening pressure= 15 KPa, Flow discharge coefficient=0.7 Critical Reynolds number=12 Leakage area=10^{-12} cm^2
		Accumulator tank	Capacity=0.25 m^3, Preload pressure= 552 KPa, Specific heat ratio=1.4, Initial volume=0.025 m^3, Structural compliance= 1×10^{-13} m^3/Pa
⟷ F_{Load}	S▷——○R C○	Load force	Ideal load force against end-effector (N)
		Hydraulic fluid	ISO VG 32 (Esso UNIVIS N 32)
	$F(x)=0$	Matlab Solver type	Ode 15s (stiff/NDF)

Figure 5-8: (a) Desired position and position response of simulated double rod circuit when the load force is constant like (b), (c) desired and position response of circuit to square switching load like (d), (e) desired and position response of the double rod circuit to sinusoidal switching load like (f) , dashed lines are desired position and solid lines are position response, (g) average and standard deviation of position response error of three different tests.
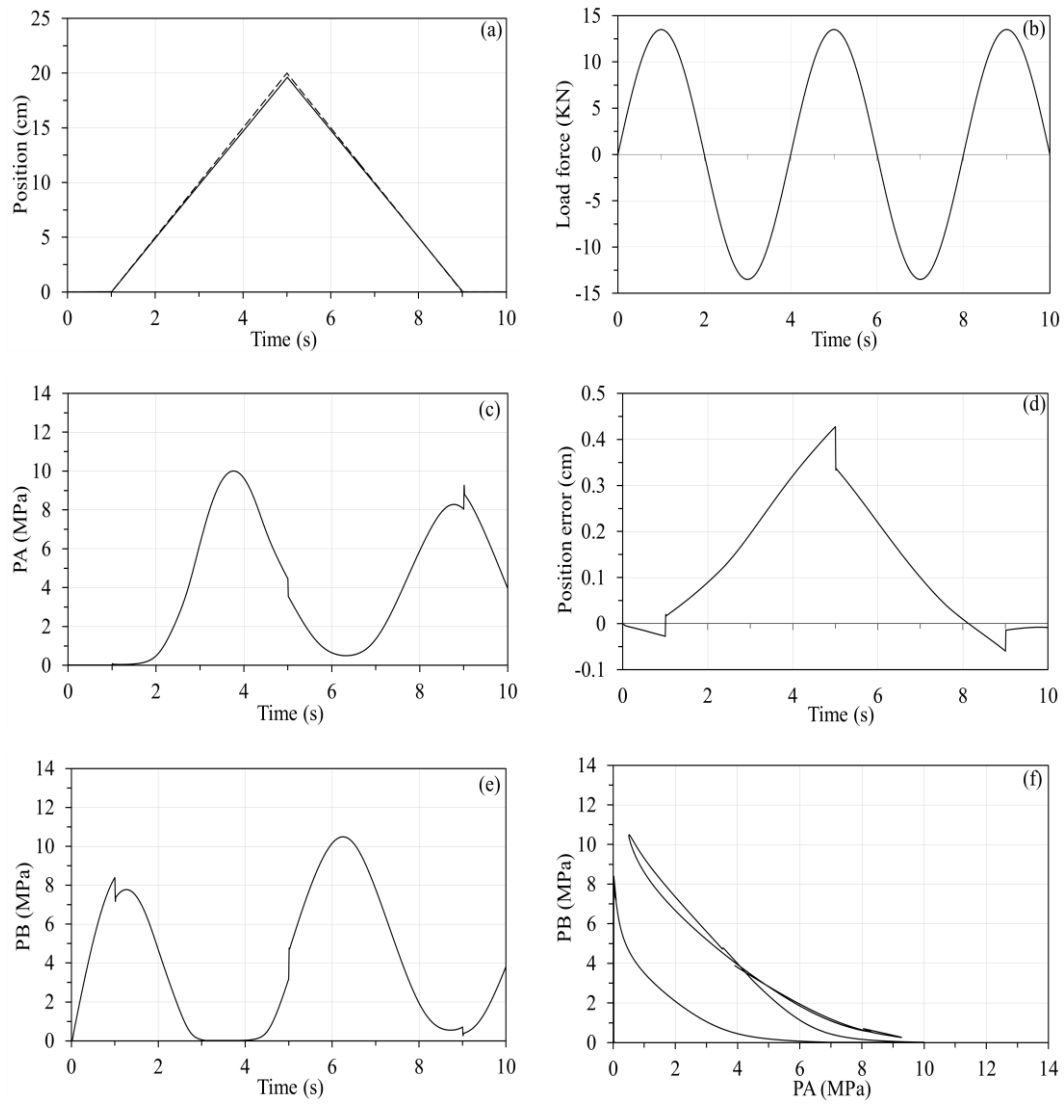
Figure 5-9: Simulation results of the pump-controlled double rod cylinder when the load is switching (a) desired position is presented by dashed line and position response of the end-effector id shown by solid line, (b) load force against end-effector, (c) pressures at the ports of cylinder versus time, (d) pressure at port B versus pressure at the port A of cylinder, (e) cylinder ports pressures versus end-effector position and (f) control signal of controller.

5.5. The circuit using one-pump and a three-port two-position valve

In this section, the simulation results of the circuit shown in Figure 5-10 (a) under the influence of non-switching load (Figure 5-11. b), smooth switching load Figure 5-11.f) and fast changing square load forces shown in Figure 5-11(d) are presented when the control loop is closed with a proportional gain. Simhydraulic simulation setup of the circuit uses the same size of cylinder and pump as the test rig. To prevent cavitation the accumulator, the tank pressure is set to 150 kPa, and to tune the proportional gain of the controller, the same non-switching constant load shown in Figure 5-11(b) is applied to circuit when the desired position signal is like dashed line of Figure 5-11(a) and the average position error is less than 0.4 cm with standard deviation of ± 0.22. Comparing position responses shows when the load is fast switching (square) the position response experiences undesirable and uncontrollable vibrations that were addressed in chapter 2. Figure 5-11(g) shows when the load is fast switching the average error of its position response raised to 2.47 cm with standard deviation of ± 2.39. As it is presented in Figure 5-11 (g) when the load is sinusoidal the end-effector tracks smoothly the desired position signal (average position error is 0.43 cm with standard deviation of ± 0.51.

To study the tracking performance and behavior of this circuit when the load is sinusoidal switching like Figure 5-12 (b), responses of simulation are shown in Figure 5-12 series. It is shown in Figure 5-12(a) the position response of the end-effector of the cylinder track the desired position signal. By comparing Figure 5-12 (c) and (e), at $t=2.5s$, 5s and 7.8s, both ports of the cylinder connect to the low-pressure side of hydraulic circuit. Figure 5-12(d) shows the plot of pressure at the port B versus pressure at port A of cylinder. As it is seen in this figure always one pressure is always equal to the low pressure of the hydraulic circuit and at any point in time, if

58

the load switches heavily from resistive to assistive, before the controller take action switch the position of three-port two-position valve (see Figure 5-10.a) it is only the low pressure that prevents the load from free falling. To improve the uncontrollability of this circuit in the case of switching loads low pressure of the circuit needs to be raised, more pressure more stability. By raising the low pressure the circuit consumes more energy to perform also the circuit needs a pressure source like a charge pump or an accumulator tank to keep up the low pressure at the safe level. Also in real world each pump needs very low pressure hydraulic oil available for case of the pump. In this case, having three different pressure levels for each pump-controlled or electro-hydrostatic circuit make it expensive, complicated and then not attractive for industrial applications. Figure 5-12(d) shows the position response error and Figure 5-12(g) presents the three-port two-position valve spool position for this simulation. Any delay on action of this valve make the circuit more unstable under switching loads.

(a)

(b)

Figure 5-10. (a)Schematic of a pump-controlled circuit using a three-port two position solenoid valve, and (b) simulation setup using Matlab Simhydraulic blocks.
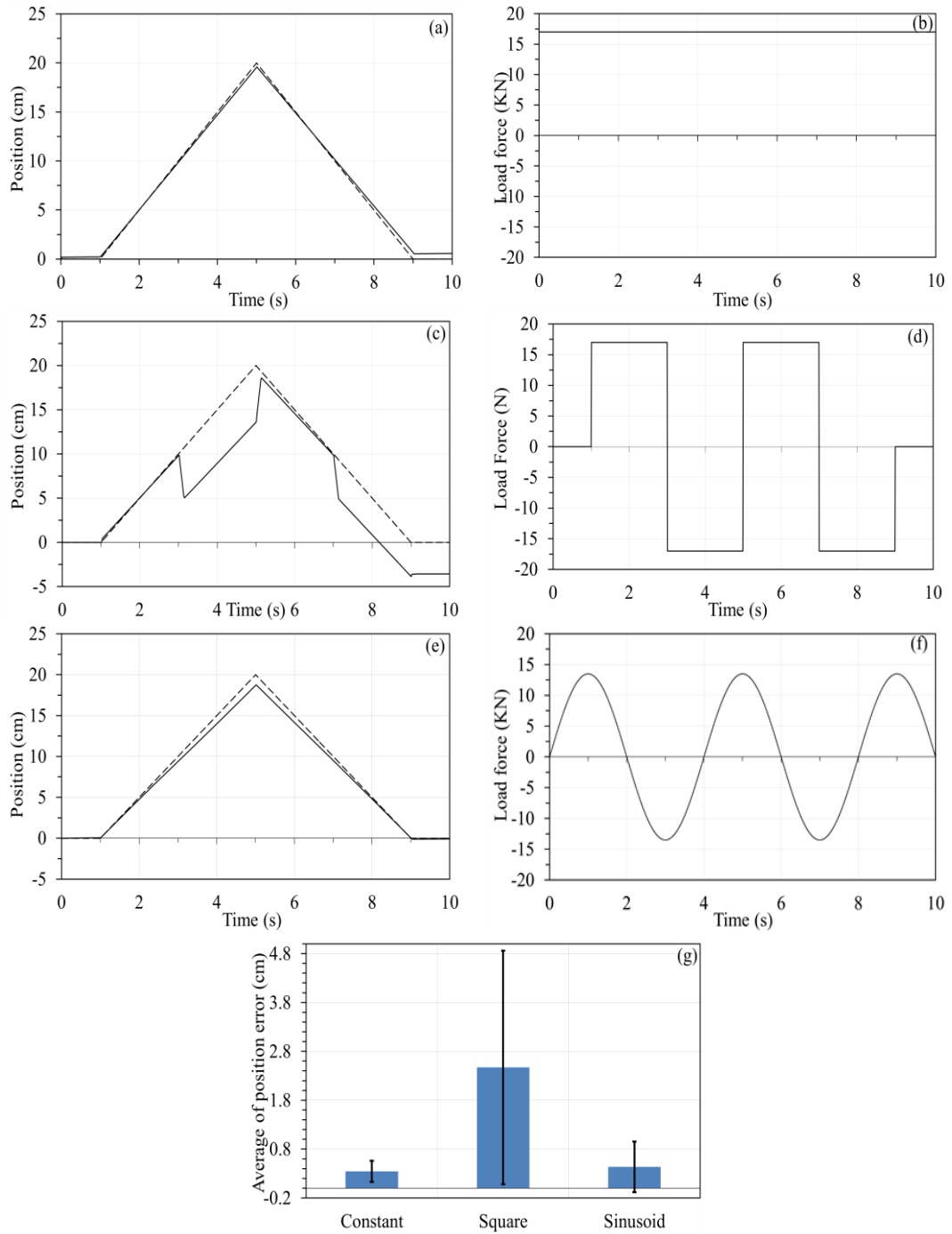
Figure 5-11. (a) Desired position signal and position response of simulated pump controlled circuit using three-port two position valve when the load force is constant shown in (b), (c) desired and position response of circuit to square switching load shown in (d), (e) desired and position response of the circuit to sinusoidal switching load shown in (f), (g) average and standard deviation of position response error of three tests.
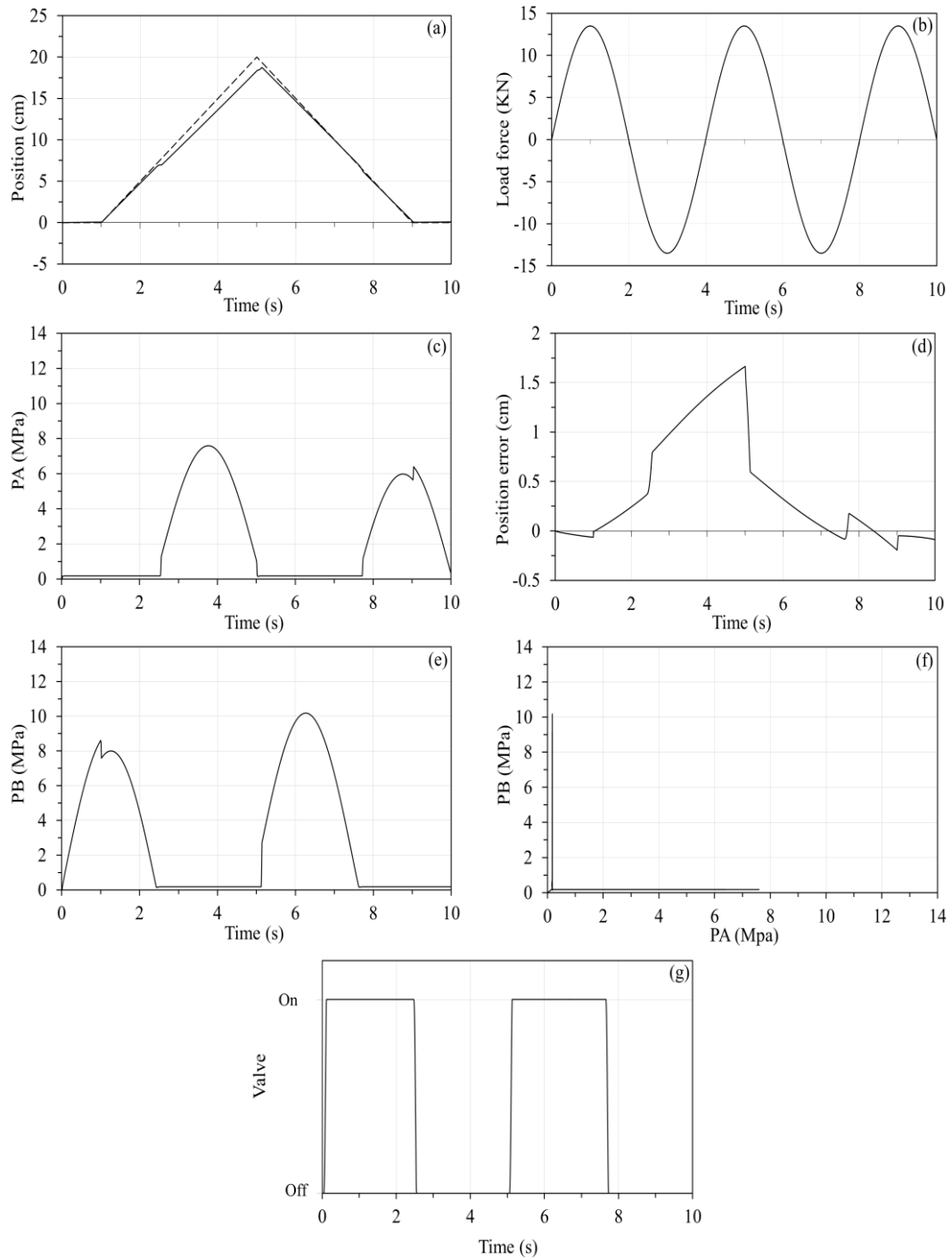
Figure 5-12. Simulation results of a pump-controlled single rod circuit using a three-port two-position valve; (a) desired and position response of the end-effector are shown by dashed and solid lines when load force is like (b), (c) pressure response at port A of cylinder, (d) position response error, (e) pressure response at ports B of the cylinder, (f) pressure at port B versus pressure at port A of the cylinder, (g) spool position of the three -port two-position valve.

5.6.The circuit using one-pump and two pilot check valves

To simulate the circuit shown in Figure 5-13(a) and compare the results with other circuits, same cylinder and pump used in test rig are chosen and Matlab Simhydraulic tools are used to setup simulation shown in Figure 5-13 (b).To prevent cavitation, pressure of the accumulator tank is set to 35 kPa and the proportional gain of controller is tuned to keep the average position error less than 0.4 cm with standard deviation of ±0.21 (see Figure 5-14.g). Figure 5-14 (a) shows the desired position and position response of the circuit when the same sinusoidal switching load shown in Figure 5-14 (f) is applied to the simulation setup. The end-effector tracks the desired position signal smoothly (see Figure 5-14.e), the average position error is 0.36 cm with standard deviation of ±0.41 (see Figure 5-14.g). By applying the square force load shown in Figure 5-14 (d) as a fast changing switching load to the end-effector of cylinder the position response of the circuit experiences some chattering, the average position error is 0.99 cm with standard deviation of ±0.67 (see Figure 5-14.g). Figure 5-14 (c) briefly shows uncontrollable load chattering at following moments; $t=$ 3s ,5s and 7s.

To study this circuit under switching load, pressure and position responses of the simulation setup under sinusoidal load force is presented in Figure 5-15 series. Figure 5-15 (a) again shows the desired and position response of the circuit when the load force is like Figure 5-15 (b). Figure 5-15 (c) and (e) present the pressure responses at the cylinder ports versus time and comparing two plots shows at $t=$ 3s, 5s and 7s both ports experience same pressure of the accumulator tank (lowest pressure of the circuit). At these moments two pilot check valves changed their position and at the same time both ports of cylinder are connected to the tank. Figure 5-15 (f) presents the plot of pressure at port B versus pressure at port A of the cylinder. As it is shown

in Figure 5-15 (f) when suddenly load force change the direction, pilot check valves need some time to change their position and during transition time end-effector moves uncontrollably. To improve the performance of the circuit when the load switches the low pressure side of the circuit needs to be raised. Higher pressures improve the control on end-effector and at the same time the energy consumption of the circuit get worse. Like previous circuit in real life the circuit using this method needs three level of pressure, low level for pump case drain (atmospheric pressure), and higher level to improve the controllability of the end-effector also work pressure to perform the work. It makes the circuit more expensive and complicated. Figure 5-15 (d) shows the position error of the end-effector versus time.
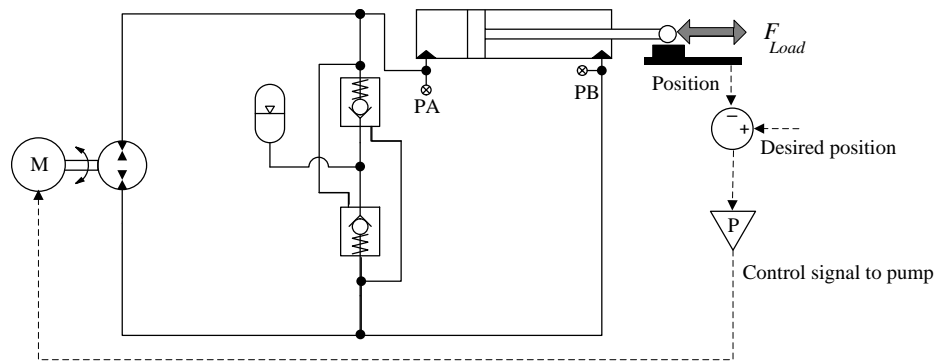
(a)
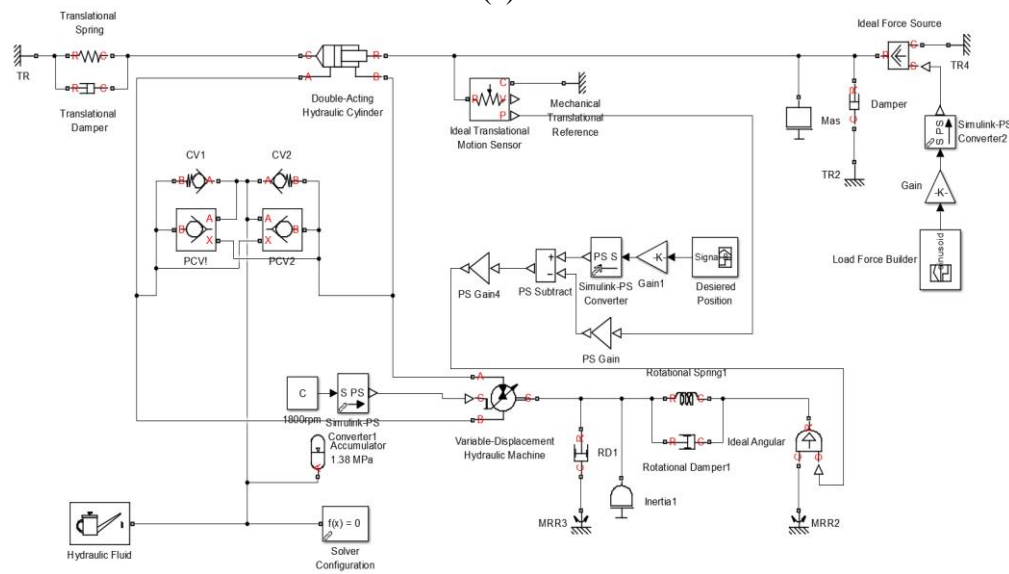
(b)

Figure 5-13. (a)Schematic of a pump-controlled circuit using two pilot check valves (b) simulation setup using Matlab Simhydraulic blocks.
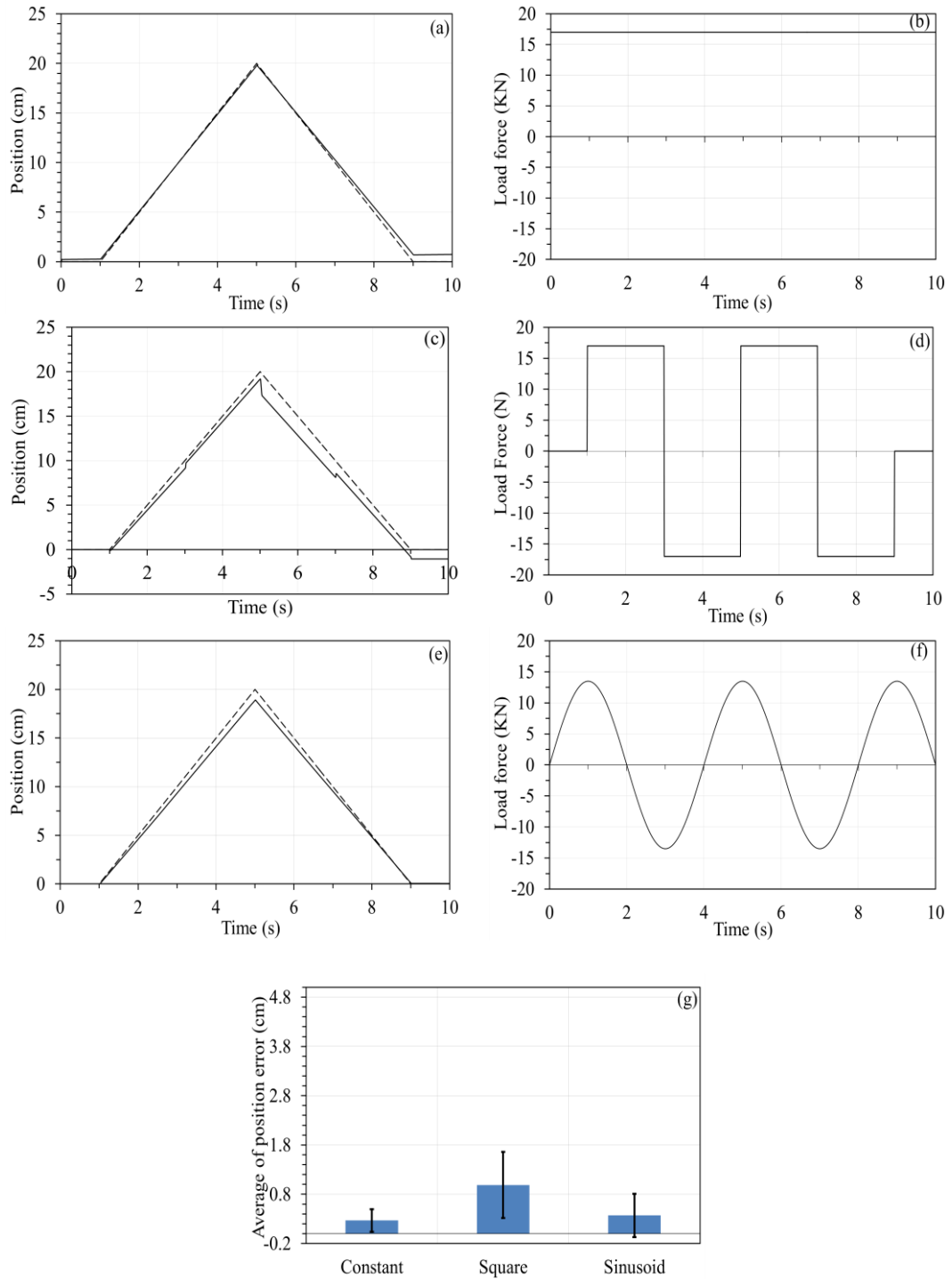
Figure 5-14: (a) Desired position signal and position response of simulated pump controlled circuit using two pilot check valves when the load force is constant shown in (b), (c) desired and position response of circuit to square switching load shown in (d), (e) desired and position response of the circuit to sinusoidal switching load shown in (f), (g) average and standard deviation of position response error of three tests.
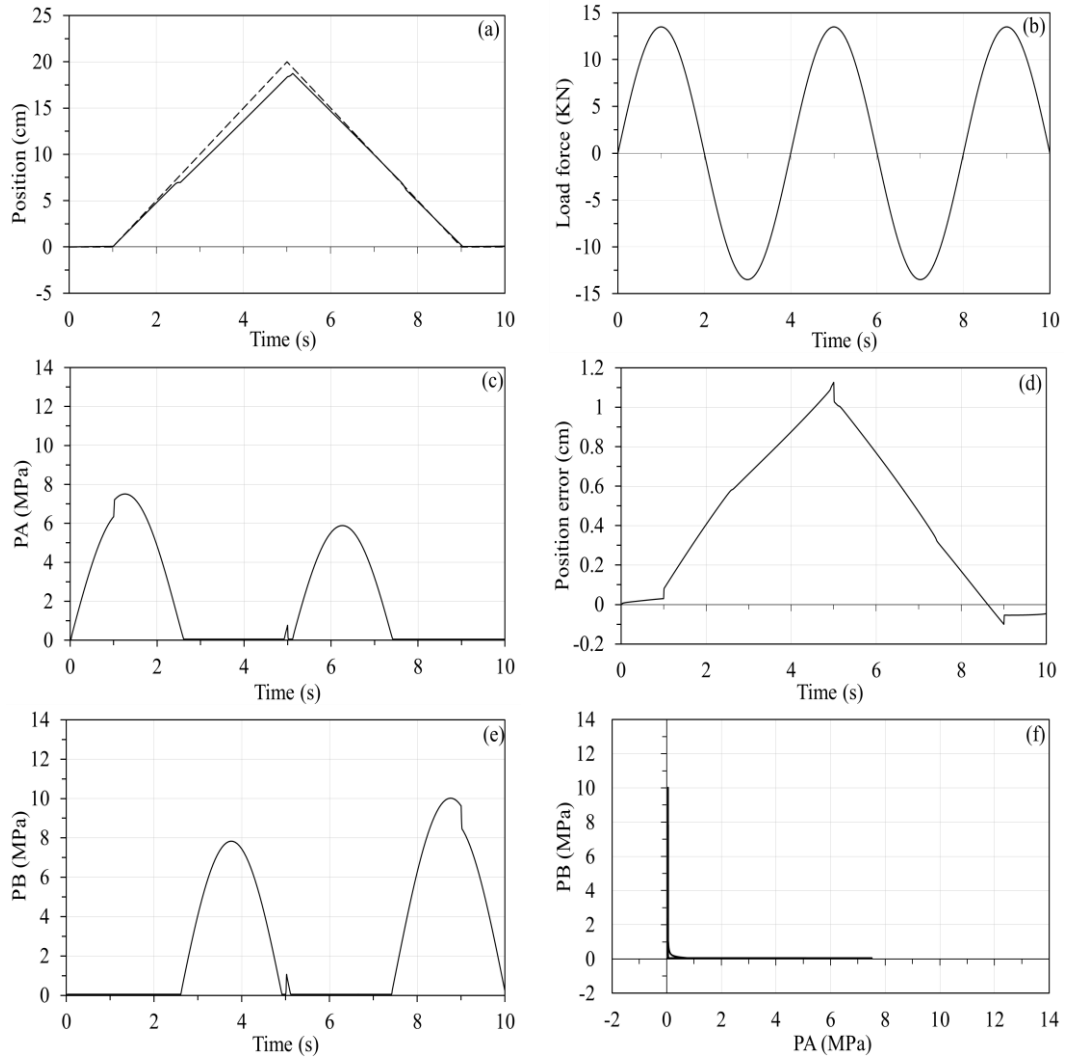
Figure 5-15:Simulation results of a pump-controlled single rod circuit using two pilot check valves; (a) desired and actual position of end-effector are shown by dashed and solid lines, (b) load force against the end-effector (c) pressure at port A of cylinder versus time, (d) error of position response versus time, (e) pressure of port B of cylinder versus time, (f) port B pressure versus pressure at port A of cylinder.

5.7. Proposed circuit

To compare the performance of proposed circuit Figure 5-16 (a) under switching loads its simulation setup using Matlab Simhydraulic tools is created and is presented in Figure 5-16 (b). Same cylinder, pump and counterbalance valves sizes used in test rig are chosen for simulation setup blocks and proportional gain of the control loop is tuned by applying the constant non-switching load shown in Figure 5-17 (b) applied

to simulation and the average position response error of end-effector of cylinder is less than 0.4 cm and standard deviation of position error is ±0.27 cm. Pressure settings of counterbalance valves set to 9.2 MPa for port A and 5.1 MPa for port A of cylinder. In real life pressure of counterbalance valve set to keep the maximum possible load at its position with no effort from pump. In this case the prime mover is ideal and assistive load cannot rotate the pump's shaft in reverse direction. Counterbalance valves prevent the circuit working in motoring mode. As the second step of this test series two same square (Figure 5-17d) and sinusoidal switching (Figure 5-17f) loads is applied to simulation setup and position responses are smooth (see Figure 5-17c and e). The mean value of position error to for square switching load is 0.39 cm with standard deviation of ±0.16 and for sinusoidal load force is 0.14 cm with standard deviation of ±0.13.

To study and compare the behavior of the proposed circuit with three previously studied circuits, responses of the proposed circuit when the load force is sinusoid are presented in Figure 5-18 series. Figure 5-18(a) presents the desired position and position response of the simulation setup when the switching load is like Figure 5-18(b). Figure 5-18(d) shows the poison response error of the end-effector versus time and Figure 5-18(f) presents spool position of the solenoid valve versus time. Pressures responses at the cylinder ports are shown in Figure 5-18(c) and (e). Comparing these plots shows two sides of the cylinder are never connected to the tank at the same time. Figure 5-18(g) shows pressure response at port B versus pressure at port A of the cylinder, it shows that the pair of pressures at two sides of the cylinder supports the load position effectively. Sudden change of load force cannot any sudden and uncontrollable motion of end-effector. As mentioned settings of the counterbalance valves are critical in making the circuit controllable and energy

efficient. Behavior of a counterbalance valve was introduced in the previous section, by raising pressure at one port of pump, pressure raise at the pilot port of opposite counterbalance valve and resistive pressure against flowing out of oil from the low pressure counterbalance valve decreases. Pair of check valves and internal leakage of the pump keeps pump ports pressures at tank pressure when the circuit is in the rest and counterbalance valves keep pressures at cylinder ports at the setting pressures.

To compare the performance of proposed circuit, circuit with three-port two-position valve and the circuit with two pilot check valves with the electro-hydrostatic circuit for double rod cylinder their cylinder pressure plots are presented in Figure 5-19. Desired position signal, load force against end-effector, cylinder and pump type and sizes are all the same. Comparing Figure 5-19(a) and (d) shows, pressure two sides of cylinder support the end-effector position against uncontrollable changes when the load force switches fast. Figure 5-19(b) and (c) shows the behavior of two other electro-hydrostatic circuits against fast switching load are the same. Always one side of cylinder connects to the low pressure side and in the case of fast load force switch suddenly and uncontrollably end-effector moves till the controller of circuit take action and compensate the variation of the load.

(a)

(b)
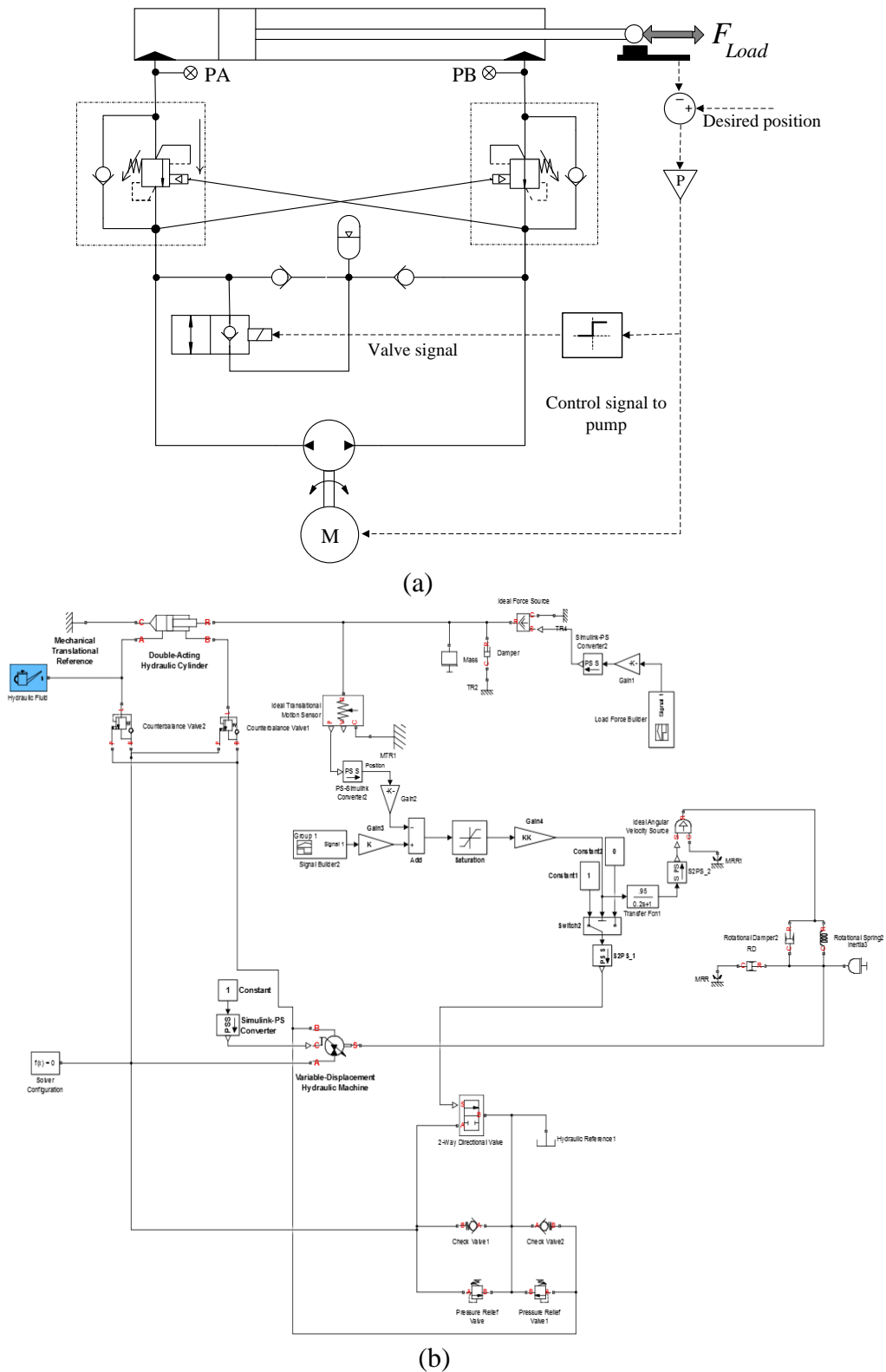
Figure 5-16: (a)Schematic of the proposed circuit using two counterbalance valve (b) simulation setup using Matlab Simhydraulic blocks.
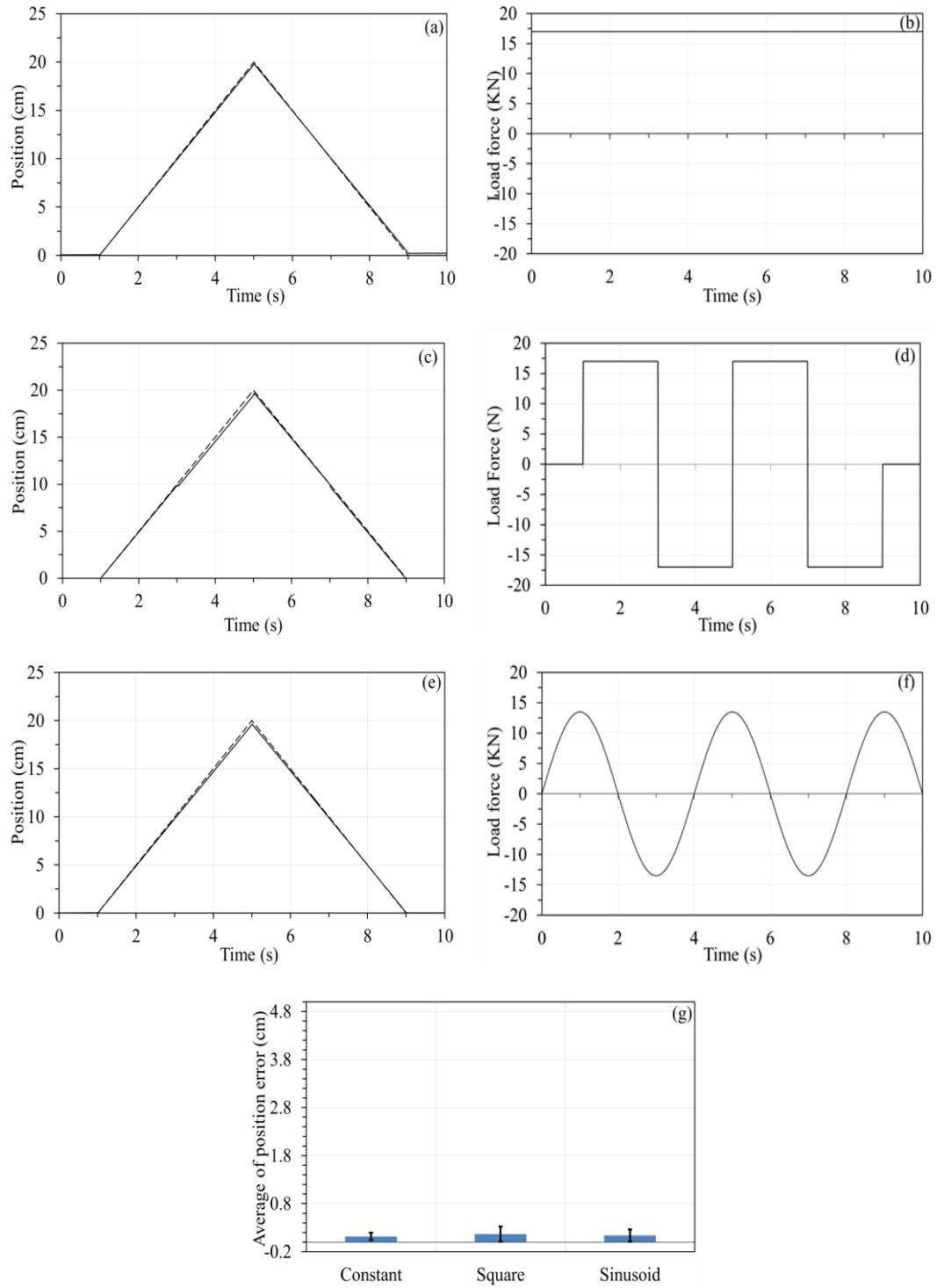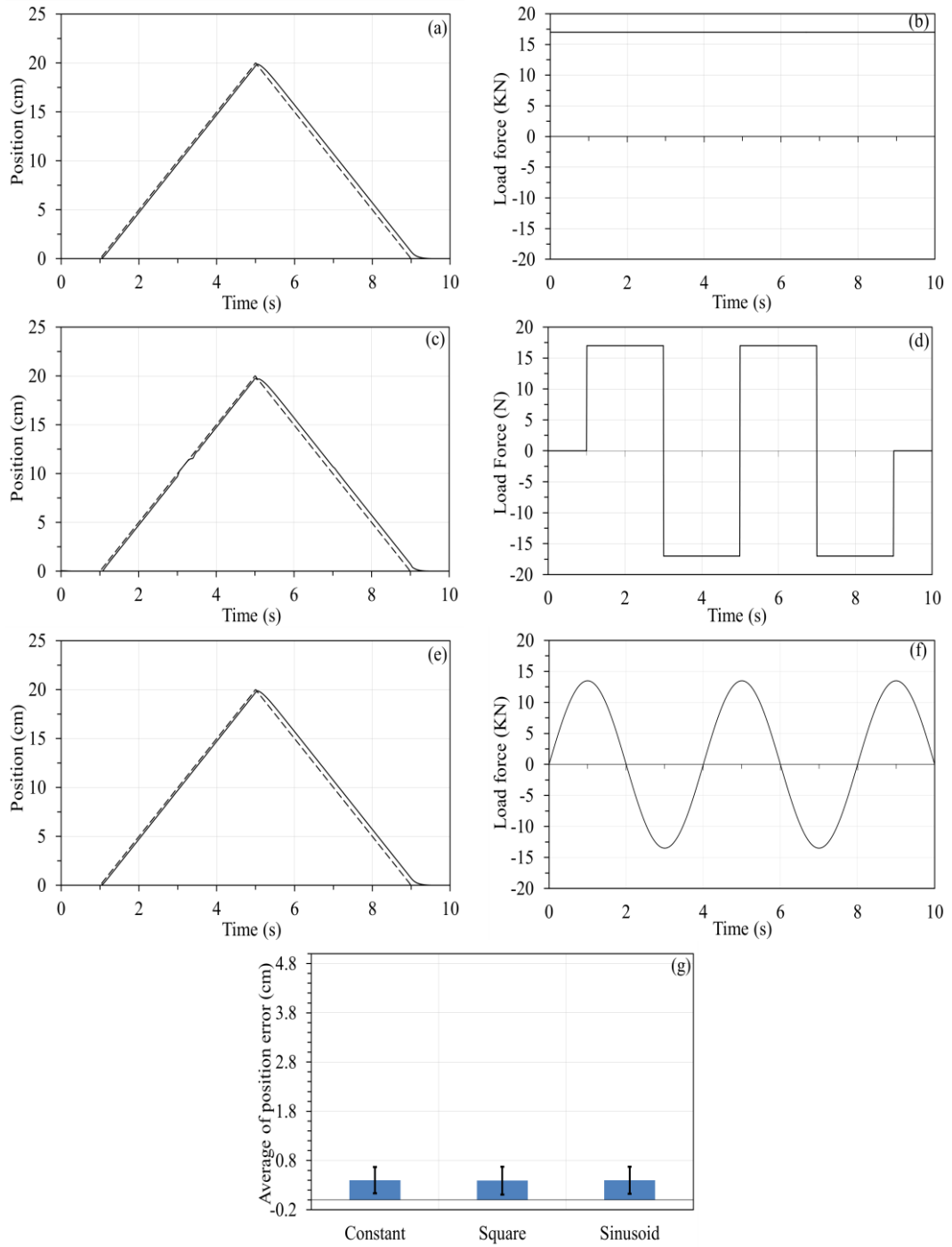
Figure 5-17:(a) Desired position signal and position response of simulated proposed circuit when the load force is constant as shown in (b), (c) desired and position response of circuit to square switching load shown in (d), (e) desired and position response of the circuit to sinusoidal switching load shown in (f), (g) average and standard deviation of position response error of three tests.
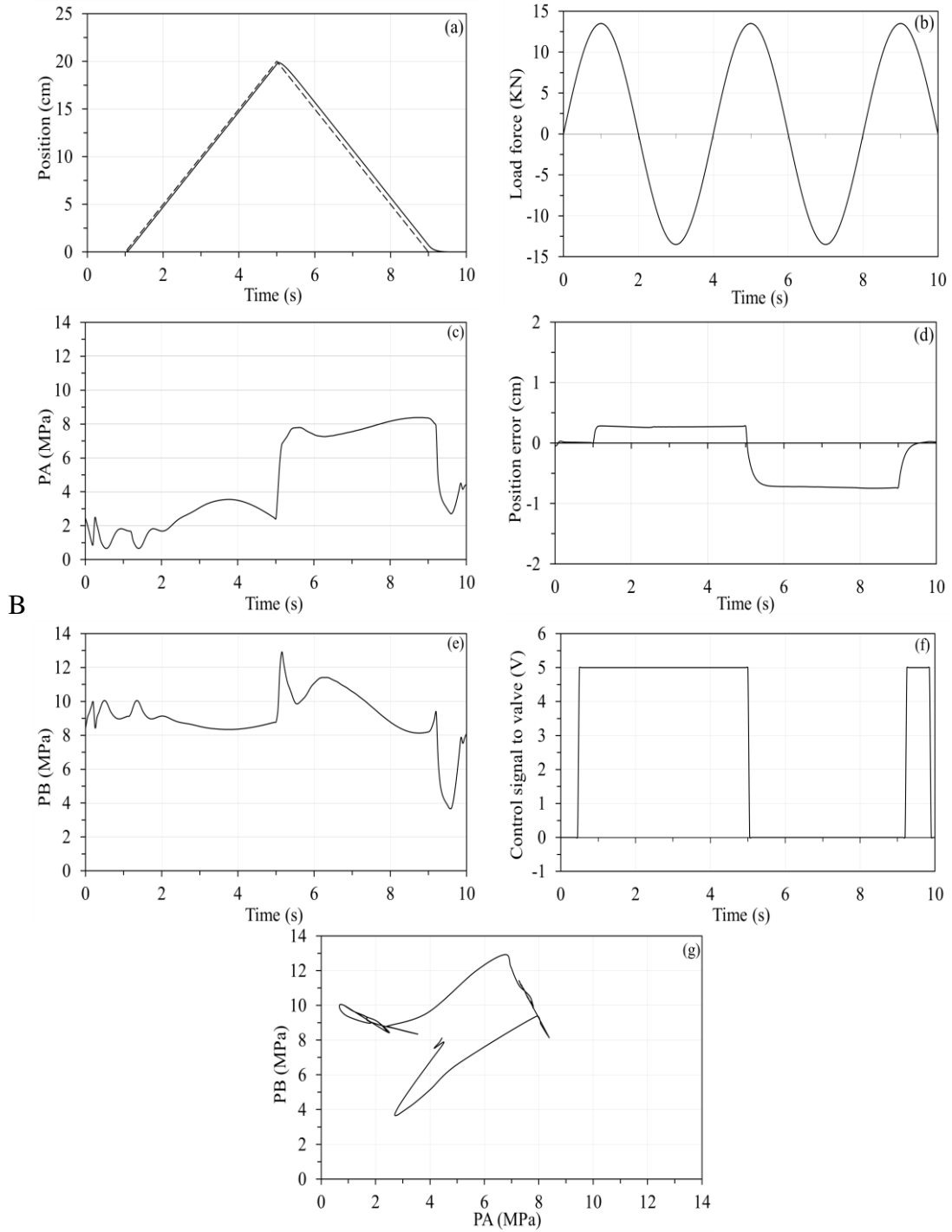
Figure 5-18: Simulation results of the proposed circuit using two counterbalance valves; (a) desired and actual position of end-effector are shown by dashed and solid lines, (b) load force against the end-effector (c) pressures at port A of cylinder versus time, (d) position error of the circuit, (e) pressure at port B of cylinder versus time, (e) control signal to solenoid valve, (g) port B pressure versus port A pressure of the cylinder.
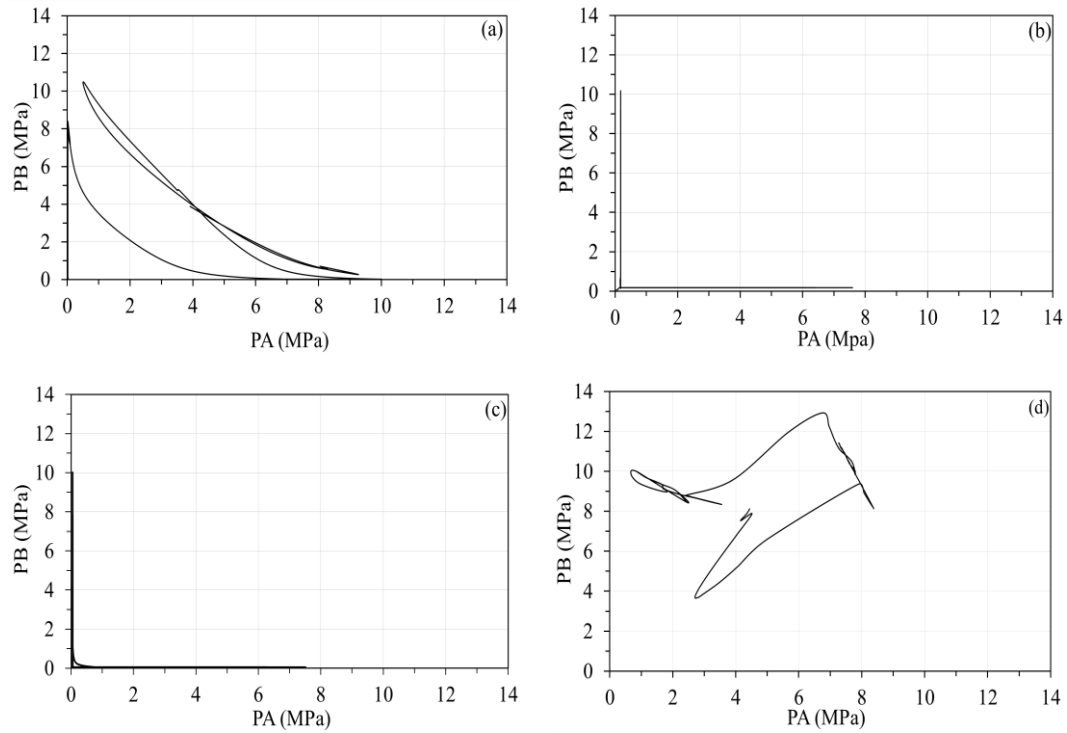
Figure 5-19: (a) Double rod cylinder circuit pressure plot, (b) one pump circuit with a three-port two-position solenoid valve pressure plot, (c) pressure plot of circuit with one pump and two pilot check valves , (d) the proposed circuit cylinder ports pressure plot.

5.8.Summary

To evaluate the accuracy of the simulation tools, the test rig, presented in Chapter 4, was simulated with Matlab Simhydraulic tools. The same tracking signal applied to the test rig was used in the simulated model of the system. The responses of pressure and position signals were compared to verify that the accuracy of the simulation models. The simulation studies also showed that by increasing the pilot ratio of counterbalance valves (from 3 to 10), the hydraulic power, delivered by the pump, decreased by a ratio of 30%. Moreover, by increasing pressure settings of the counterbalance valves, the pump delivered more hydraulic power. In industrial applications, however, the pressure setting of counterbalance valves is set to maintain

the end-effector position at possible extreme conditions with no effort from the pump or other controlling valves.

Counterbalance valves prevent hydraulic circuit from recycling hydraulic energy. Energy consumption of the proposed circuit was also compared with a valve controlled circuit. The delivered hydraulic energy was calculated and compared to the energy required by a pressure compensated pump to perform the same motion. Results indicated that the proposed circuit for the case of tested pattern of motion was 80% more efficient than the valve controlled circuit. The efficiency of the proposed circuit depends on many factors including pattern of motion, setting of counterbalance valves, and type of counterbalance valves.

The proposed circuit, the circuit using a three-port two-position valve, and the circuit using two pilot check valves were then compared with the circuit for double-rod cylinder. The commonly used pump controlled circuit was considered as the benchmark for further comparisons. All four circuits were simulated by applying the same sizes of the cylinder and the pump. For the case of the double rod cylinder, both areas of the cylinder had the same area as the rod side of the single rod cylinder. Control loops of all circuits were closed in response to readings of the end-effector of cylinders using a proportional gain. Three constant non-switching, sinusoidal switching and a square load force as a fast changing load were applied to the above circuits. Results showed uncontrollability on the end-effector of cylinders for the case of two pilot check valves and three-port two-position valve. The performance of the proposed circuit was comparable with the circuit for the double rod cylinder.

CHAPTER 6

EXPERIMENTAL EVALUATIONS OF THE
PROPOSED CIRCUIT

Performance of the proposed circuit is experimentally investigated with two sets of tests using the test rig. The first set of experiments evaluates the performance of the proposed circuit under non-switching loads and the second set evaluates the performance of the proposed circuit under switching loads. In the first set, the performance of the circuit for lifting applications is first evaluated by attaching the lifting load setup to test rig. To improve the efficiency of the circuit, the counterbalance valve, on the cap side of the cylinder, is removed. The counterbalance valve, on rod side of cylinder, sets to keep the maximum load at its position when the prime mover is switched off. A periodical square position signal (desired) is applied for 300 s. The control loop of the test rig is closed on readings of the end-effector linear position transducer with a proportional gain that is tuned to achieve the lowest position steady state error. The tuned proportional gain is used for all tests with lifting load setup except the test with the circuit with no counterbalance valve. Pressure settings of the counterbalance valve is set to keep the load at its position with no effort

from the prime mover and the hydraulic pump, the test will show the consistency of position response of the circuit for lifting applications like industrial tote dumpers.

In the second step, to study the effect of the size of the weight load to position response when the proposed circuit is setup as an industrial lifter, a square position signal is applied to the circuit with three different weight loads, position responses and position steady state errors. Thirdly, to study the effect of the counterbalance valve on performance and responses of the proposed circuit when the load is lifting, the second counterbalance valve will be removed and a periodic variable amplitude trapezoid desired position signal is designed and will be applied to the proposed circuit with and without one counterbalance valve.

Afterwards, a sinusoidal desired position signal is applied to the test rig with weight load. The energy consumption of the whole hydraulic circuit is then compared with the delivered power by the pump. Next, the pair of spring load will replace the lifting load setup and the second counterbalance valve will be connected to the port of cylinder. A variable amplitude square desired position signal is designed and will be applied to the test rig the way that the circuit experiences a non-witching load. Counterbalance valves will be set the way that when each spring is fully compressed, the end-effector stays at its position with no effort from prime mover. The proportional gain of the controller will be tuned for the lowest possible steady state position error and responses of the circuit will be presented and evaluated. The same tuned proportional gain and settings of counterbalance valves will be used for all tests with the pair of spring loads. The proposed circuit will be evaluated for switching loads. Three different desired position periodical signals are designed to study the tracking performance, energy consumption of the circuit and sensitivity of the position response to the frequency, shape and range of motion. Periodic signals

consist of sinusoidal (to perform a smooth motion with variable velocity for end-effector), trapezoid (to perform a smooth motion with constant speed) and square (as a fast changing signal to be followed by the end-effector of cylinder).

Next, three mentioned signals with unique amplitude will be applied to the test rig in five deferent frequencies, and responses of the proposed circuit will be compared. After that, test frequency of signals will be fixed and tests will run for five different ranges of end-effector motion (amplitude). Finally, the tracking performance of the proposed circuit, when the frequency of desired position signal is variable, will be qualitatively studied. To perform the test for each pattern of motion, five different frequencies will be applied to the circuit when the amplitude is constant. Also the frequency of motion will be fixed and five different amplitudes will be applied as series for each pattern of motion.

6.1. Test the consistency of the position response for lifting applications

To validate the performance of the circuit, when the load is non-switching, the lifting load setup (shown in Figure 6-1) is attached to the test rig and the control loop is closed on readings of the end-effector position transducer. A periodic square desired position signal with frequency of 0.032 Hz and amplitude of 40 cm is designed and applied to the circuit for a time period of 300 s (see dashed line in Figure 6-2.a). The proportional gain of controller is tuned to get the smallest steady state error of the position response when the maximum load of 136 kg is attached to the load setup. The tuned proportional gain will be used for all tests of the circuit with one counterbalance valve and lifting loads. Test results shows the position response of the circuit is consistent and repetitively follows the tracking signal. Figure 6-2(a) shows two periods of the desired and actual position response of the system between 144 s and

77

224 s. Delay, rise and settling times of the system response in both the up and down strokes are also shown in Figure 6-2(a). The delay response of about 0.4 s was attributed to the response delay of the variable frequency drive (VFD), inertia of the rotating parts of pump-motor unit and compressibility of the oil. Figure 6-2(b) shows the magnified view of the highest steady state error of the position response. The small amount of voltage control signal was created by the steady state error. When the load was at rest, steady state errors created a low control signal, the electromotor rotated the pump shaft in low RPM, built up pressure that was not enough to overcome to the weight of the load and the low flow of oil was consumed by internal leaks of the pump. In Figure 6-2(c) and (d), pressure readings at the cylinder ports are presented. The period starts with a downward stroke. For lowering the load, the pump was needed to build up pressure at the pilot port of the counterbalance valve. This excessive pressure opens the line between port b of the pump and port B of the cylinder in Figure 6-1. When the pressure at the pilot port of the counterbalance valve reaches to 2.1 MPa, the counterbalance valve opens the circuit. Furthermore, as long as the pump feeds port A of the cylinder and pressurizes the pilot port of the counterbalance valve, the counterbalance valve remains open. In Figure 6-2(d), the first peak of pressure PB shows that more pressure was generated in chamber B than chamber A which is attributed to the piston area difference and the load induced pressure. The second peak of pressure at 148 s is present due to the effect of the load dynamics and compressibility of the hydraulic fluid when the cylinder stopped. To raise the load, the pump feeds fluid to port B of the cylinder through the check valve of the counterbalance valve (Figure 6-1). Pressure PB builds up to overcome the load dynamics and friction forces, and performs the upward motion. When the load reaches to the maximum position, the pump stopes at $t = 162.5$ s, and the check valve of the

counterbalance valve is closed. Small low pressure ripple shows the effect of load dynamics and the fluid compressibility.
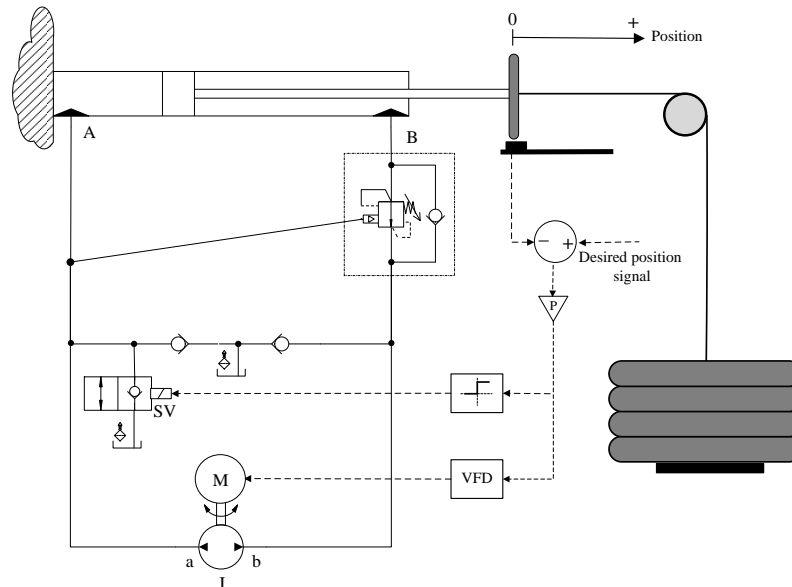
Figure 6-1: Schematic of the circuit with one counterbalance valve for lifting applications.

At the resting up position (for example 163 s to 176 s), pressure at port A is equal to the tank pressure and pressure at port B is stabilized at the backpressure of the load against the counterbalance valve. Figure 6-2(e) shows the upward and downward velocity of the load and Figure 6-2(f) demonstrates the acceleration of the end-effector of the cylinder. Figure 6-2(b) shows the highest steady state error of the response is $\pm$0.034 mm when the desired displacement is 40 cm ($\pm$0.00085% of stroke).
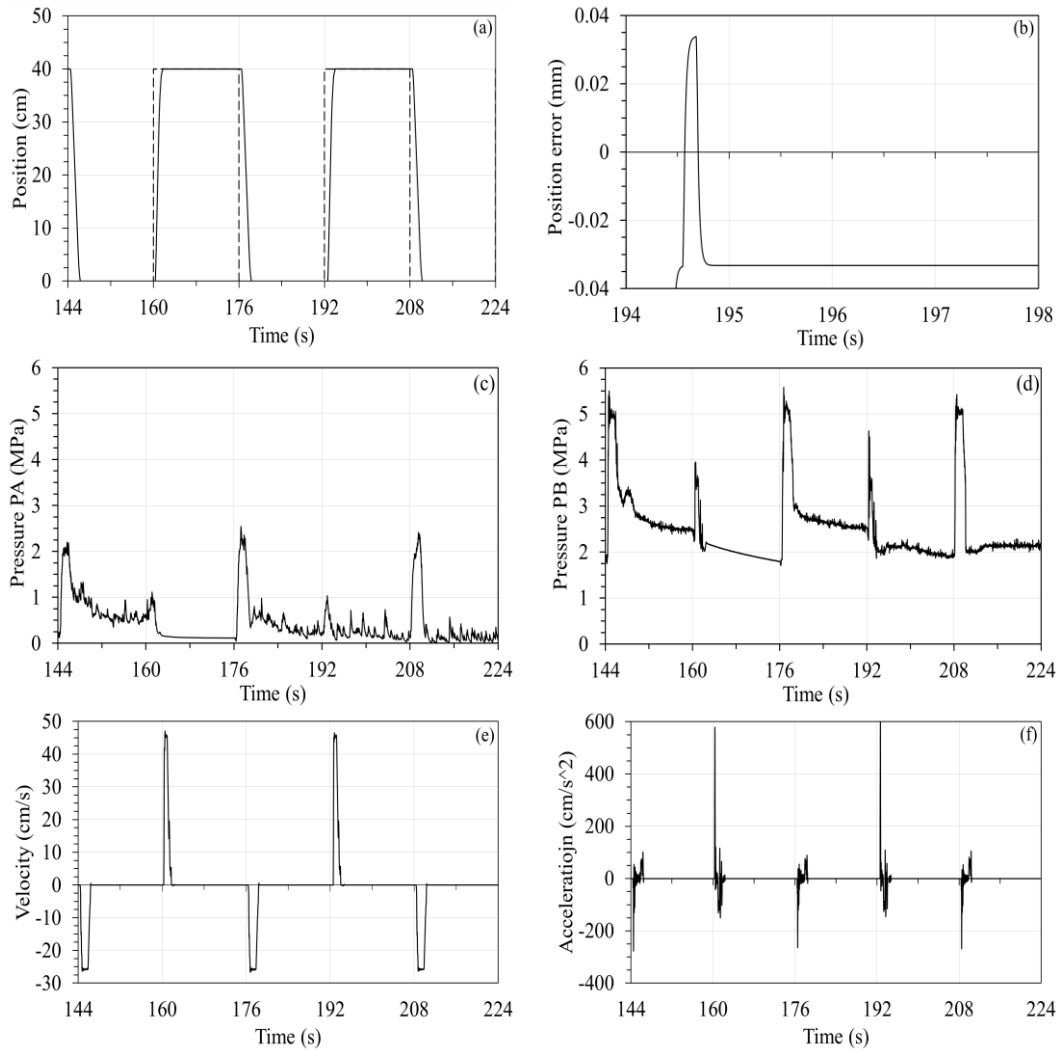
Figure 6-2: (a) Desired position showed by dashed line and position response is presented by solid line, (b) highest steady state error of the end-effector, (c) pressure at port A of cylinder,(d) pressure at port B of cylinder, (e) speed of the end-effector versus time, (f) acceleration of the end-effector versus time.

6.2.Test the sensitivity of position response to the weight of load

In the second test of the test rig with one counterbalance valve for lifting applications, to examine the effect of load changes to the response of the hydraulic circuit, three different loads are applied to the circuit in Figure 6-1. Position responses of the circuit under the same gain of the proportional controller are recorded when the desired position is a square signal. Figure 6-3(a) shows the desired and actual positions of the circuit for loads 9, 68 and 136 kg. Figure 6-3(b) shows the magnified

position error response of the circuit for those three different loads. Experimental results prove that the steady state error of position response of circuit is not sensitive to the load size.
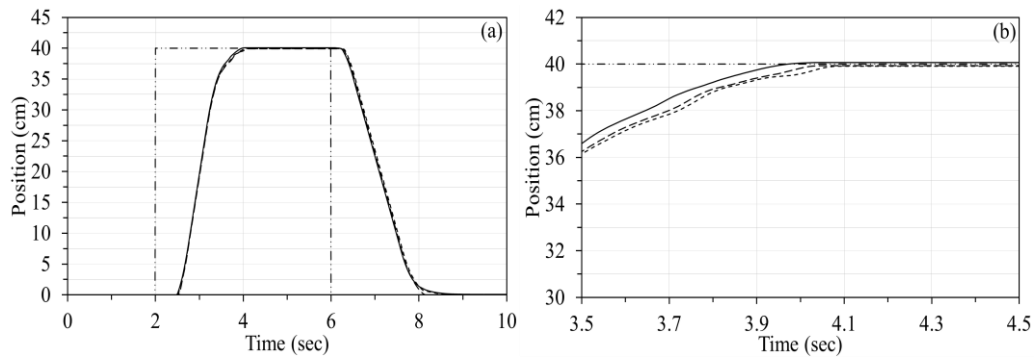
Figure 6-3:(a) Desired position signal presented by dashed line and position responses for three different loads are shown by solid lines, (b) magnified view of position response shows by raising the weight of the load position response experience slightly higher position error.

6.3. Study the effect of counterbalance valve to responses of the circuit

In the third test the last counterbalance valve is removed and the response of this circuit is compared to the response of the circuit with one counterbalance valve when the load is set to 136 kg, and when the same desired position signal and closed loop proportional controller is applied. For the circuit without the counterbalance valve, the proportional gain is tuned to get the best possible position response.

Figure 6-4(a) shows the desired and actual position of the circuit with the counterbalance valve and Figure 6-4(b) shows the desired and actual position of the circuit without the counterbalance valve. Comparison between Figure 6-4(a) and Figure 6-4(b) shows how controllable and stable the circuit with the counterbalance valve was compared with the circuit without the counterbalance valve. Figure 6-4 (c) shows the pressure readings at port A of the cylinder for the circuit with the counterbalance valve (CBV) and Figure 6-4 (d) presents the plot of pressure at port A

of cylinder for the circuit without the counterbalance valve. Comparing Figure 6-4(c) and Figure 6-4(d) shows that in the absence of the counterbalance valve, pressure at the port *A* of the cylinder is lower in compare to the circuit with the counterbalance valve. This extra pressure in the circuit with the counterbalance valve is needed to keep the valve open in lowering motions. The test shows that the counterbalance valve can make the circuit controllable when the load is assisting and reduces the pump power consumption in rest positions. Figure 6-4(e) presents the pressure readings at port B of the cylinder for the circuit with the counterbalance valve and Figure 6-4(f) presents the pressure readings at port B of the cylinder for the circuit without counterbalance valve. Comparing Figure 6-4(e) and Figure 6-4(f) shows the counterbalance valve is needed more pressure at port B of the cylinder to perform the motion and while in absence of the counterbalance valve, the pump is needed more energy to build up pressure to keep the load at the rest position. Ripples of *PB* plot in Figure 6-4(e) and Figure 6-4(f) shows the pulsation effect due to the usage of a gear pump and possibly the dissolved air in the hydraulic oil. The internal leakage of the pump, inertia of rotating parts of the electromotor and pump, poor performance of variable frequency drive (VFD) at low speed, lack of mechanical or magnetic break of electromotor and response delay of VFD are the main factors causing poor performance of the circuit without a counterbalance valve.

With one counterbalance valve   Without counterbalance valve
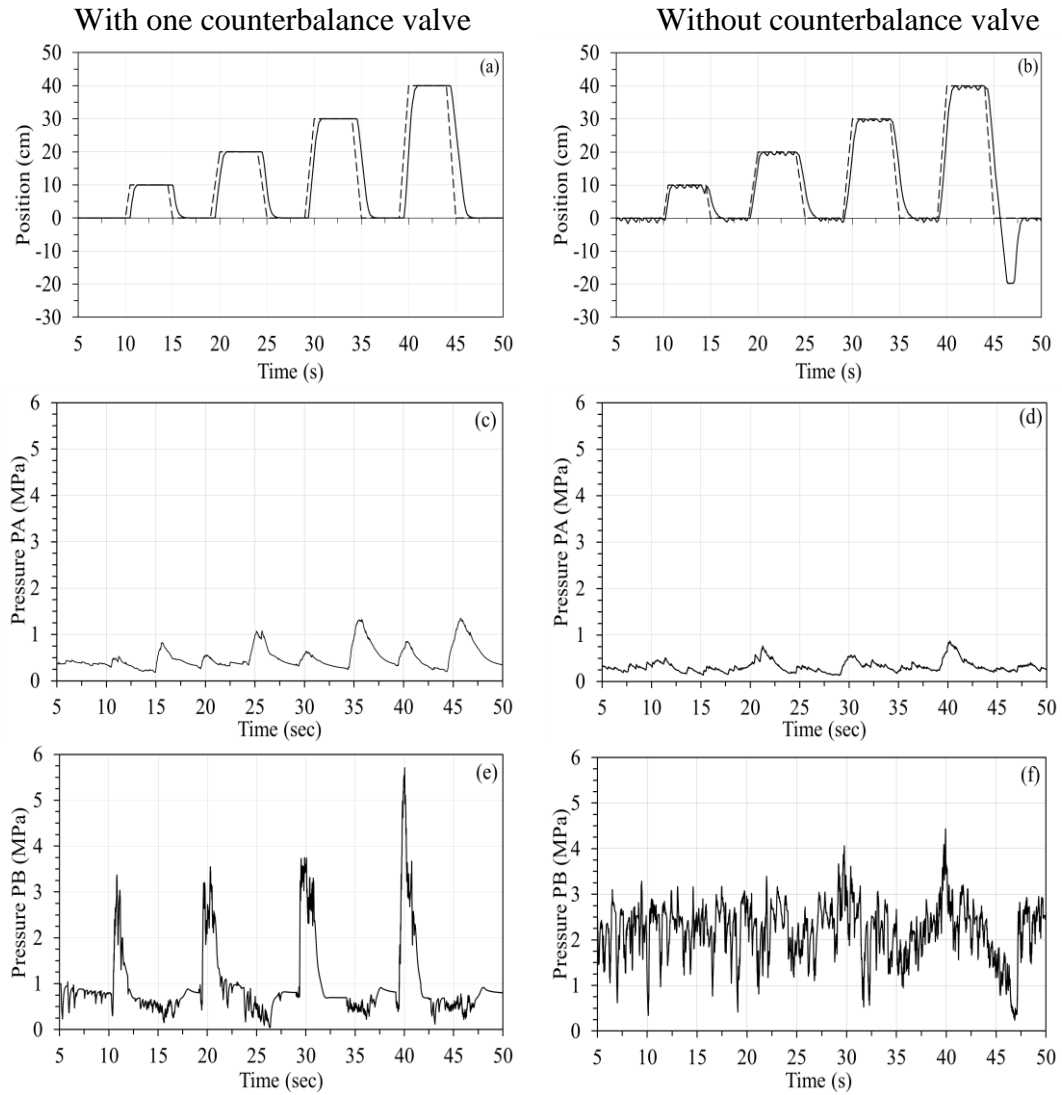
Figure 6-4: (a) actual (solid line) and desired (dashed line), circuit with CBV, (b) actual and desired positions, circuit without CBV, (c) pressure at port A of the cylinder and actual position (dashed line), circuit with CBV,(d) pressure at port A of the cylinder , circuit without CBV, (e) pressure at port B of the cylinder, circuit with CBV (f) pressure at port B of the cylinder, circuit without CBV

6.4. Energy consumption of circuit for lifting application

As the fourth test to study the energy consumption of the test rig with one counterbalance valve, a sinusoidal desired position (amplitude; $X_l = 0.4$ m and angular velocity; $\omega = 1$ rad/s) is applied to the proposed circuit when the load is 136

83

kg and the control loop is closed. The electrical power consumption of the prime mover and delivered the hydraulic power to the cylinder by the pump are recorded and results are compared to amount of energy that is required if the same motion is provided by a valve control circuit.

In pump-controlled circuits, the pump produces only the needed pressure to perform the motion. In the proposed circuit, at rest, the counterbalance valve keeps the load in position and the prime mover does not need energy to overcome the load weight. While in motion, the delivered hydraulic power to the cylinder (W_h) in the proposed circuit can be calculated by expanding ($W_h = Q\Delta P$) and considering upward and downward motion of the load. The average rate of the power delivered by the pump to cylinder for pump-controlled circuit (W_h) in sinusoidal motion can be calculated by using the following equation:

$$x_l = X_l \sin \omega t \tag{10}$$

where x_l is the instantaneous position, X_l is the maximum travel, and ω denotes the angular velocity of the load. Therefore, the velocity is given by:

$$v_l = V_l \cos \omega t \tag{11}$$

where v_l and $V_l = \omega . X_l$ are the instantaneous and maximum speeds of the load, respectively.

To lift the load, the pump provides pressurized hydraulic fluid to the rod side of the hydraulic cylinder while it receives fluid from the tank. To lower the load, the direction of the hydraulic fluid reverses. The flow rate from the pump to the cylinder is given by:

$$Q = \begin{cases} A_b V_l \cos \omega t & for \ \cos(\omega t) \geq 0 \\ A_a V_l \cos \omega t & for \ \cos(\omega t) \leq 0 \end{cases} \tag{12}$$

where Q denotes the instantaneous flow rate. A_a and A_b represent the effective areas

of cap side and rod side of the piston, respectively.

The instantaneous power delivered by the pump to the cylinder using Equation (8), W_h *is* calculated using the following:

$$W_h = \begin{cases} (P_b - P_a)A_b \, V_l|\cos \omega t| & for \; \cos(\omega t) \geq 0, & 0 \leq t \leq \dfrac{T}{2} \\ (P_a - P_b)A_a \, V_l|\cos \omega t| & for \; \cos(\omega t) \leq 0, & \dfrac{T}{2} \leq t \leq T \end{cases} \tag{13}$$

The average power delivered by the pump to the cylinder W_{hav} is calculated based on one motion cycle, and given by:

$$W_{hav} = \frac{1}{T} \int_0^T W_h \, dt \tag{14}$$

where, $T = \dfrac{2\pi}{\omega}$ is the time period.

Therefore, the average power consumption of the proposed circuit W_{hav} is calculated using the following:

$$W_{hav} = \frac{1}{T} \left(\int_0^{\frac{T}{2}} (P_b - P_a)A_b \, V_l|\cos \omega t| \, dt + \int_{T/2}^T (P_a - P_b)A_a \, V_l|\cos \omega t| \, dt \right) \tag{15}$$

where, T is the cycle period of the motion, A_a and A_b are the effective areas of the cap side and rod side of the piston, V_l is the rod-end maximum speed that is the maximum of the numerical differentiation of position transducer readings and ω denotes the angular velocity of the load.

Figure 6-5(a) shows the sinusoidal desired position and the actual position response of the circuit in the time period of 4 s to 18 s. VFD response delay, Inertia of the rotating parts of the electromotor-pump unit, pump internal leakage and fluid compressibility were sources of the response delay of the circuit when the load changed its direction of motion. In upward motion, the circuit needed about 0.5 s to build up enough pressure to overcome the load-induced pressure to open the check valve of the counterbalance valve. In lowering motion, the pump needed about 0.4 s to

85

gain enough reverse speed and build up pressure to open the counterbalance valve. During these delay periods, the load stayed in its position and does not follow the desired signal (see Figure 6-5a).

The power delivered by the pump to the cylinder is calculated by numerical integration using Eq. (15) where P_a and P_b were readings of pressure sensors at the pump ports. Also, the electric power consumption, which represents the total power consumption, is recorded through a wattmeter and the extracted data are shown in Figure 6-5(b). The slight difference between sinusoidal patterns of electric power consumptions and the delivered hydraulic power to the cylinder is attributed to the electric wattmeter accuracy. Figure 6-5(b), clearly, shows the effect of the counterbalance valve on energy consumption in the top and bottom positions of the load (instantaneous rest). At these two positions, the counterbalance valve is closed and the pump ports are depressurized. Figure 6-5(b) shows that the proposed circuit absorbed energy and worked in the pumping mode throughout the duration of the test. It is noticed that, the pump consumed more energy to open the counterbalance valve in the lowering mode than to the energy required to lift the load up. The value of the consumed energy in the lowering motion is related to the counterbalance valve characteristics (type, pilot ratio and initial setting), the load value, and the pattern of motion. As it is shown in Figure 6-5(b), when the load passes the midpoint of the stroke, the effect of the load inertia is perceived, and the pump consumes less energy to follow the desired position signal. At the maximum and minimum positions of the load, the electromotor consumes only the power needed to cover mechanical and electrical losses of the electromotor-pump unit. At these positions, the pump delivers no power to the cylinder (no movement therefore no power required). The average value of the power delivered by the pump to the cylinder is 167.1 W and is calculated

by substituting experimental readings to Eq. (11). Moreover, the mean value of consumed electric power, measured using a wattmeter, is 280.5 W. This shows that the efficiency of the proposed circuit is 60%. Using Eq. (4) and assuming that the maximum pump pressure value needed to lift the load in the valve controlled circuit would be almost the same as that recorded in the pump control circuit (2.5 MPa), the power that a valve control circuit needs to perform the same motion for the load can be predicted. For the valve control circuit, a pump with a 3.7 MPa constant pressure is selected, taking into consideration that the pump constant pressure is 1.5 times the maximum pressure needed in the circuit. The hydraulic power delivered by the pump to the throttling valve, is calculated using Eq. (5) and is found to be approximately 810 watts. This means that the proposed pump-controlled hydraulic circuit in Figure 6-1, consumes only 21% of energy that is required by a conventional valve controlled hydraulic circuit.

These power values are valid only for this smooth pattern of motion whiles the selected pump of this valve controlled hydraulic circuit is incapable of performing other faster patterns of motion used for other tests in this thesis. The test showed that the proposed circuit consumed 21% of required energy by a valve controlled circuit. Also, the efficiency of the proposed circuit was about 60% in comparison to the efficiency of a valve controlled circuit that has a value less than 31% [2].
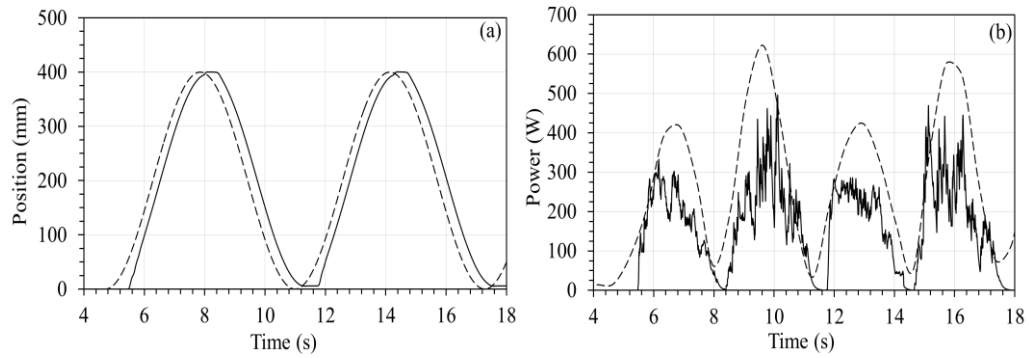
Figure 6-5: (a) Sinusoidal desired and actual positions. (b) Pump delivered hydraulic power to circuit and electric power consumption.

6.5.Tuning the proportional gain of the test rig for variable switching loads

To evaluate the proposed circuit with two counterbalance valves when the load is switching, set of two compression springs is replaced the lifting load setup (see Figure 6-6). The control loop is closed on readings of the end-effector linear position transducer with a simple proportional gain. A variable amplitude square desired position signal is designed (see dashed line in Figure 6-7.a) and applied to the circuit to tune the proportional gain and achieve smallest stady state position error. As it is shown in each step of motion, end-effector works aginst a pure resistive or a pure assistive force and the size of the force is equal to mutiplication of the end-effector position and stiffness of compression springs. Accuracy of the position response and pressure readings of the circuit are presented in the Figure 6-7 series. Figure 6-7(a) shows the desired and position response of the circuit. The control signal is shown in Figure 6-7(b). Comparing the first and second pair of control signal peaks shows the effect of the different areas of both sides of the piston, different settings of the two counterbalance valves and delay of the VFD on the control of the electric induction motor. Not only did the VFD have an almost 0.25 s delay in circuit response, the inertia of rotating parts of the prime mover and pump also added 1 more second in delay when changing the direction of rotation of the electromotor. To get the quickest and most efficient response, the overshoot for position response was avoided. Two

88

different propotional gains were chosen for the forward and backward motion of the cylinder end-effector. Position response error of the cylinder end-effector versus time is shown in Figure 6-7(c). Figure 6-7(c) shows the steady state error of the position response of the circuit. The highest steady state error of the response is magnified in Figure 6-7(d). The highest steady state error of the circuit for this test is less than 0.058 mm. Figure 6-7(e) and (f) are presenting pressure responses at the cylinder ports. Picks of presssure shows the effect of inertia of rotating parts and pressure settings of counterbalance valves.

Figure 6-6: Schematic of the test rig setup with the pair of spring load.

Figure 6-7: (a) Desired position shown by dashed line and position response shown by solid line, (b) control signal to VFD, (c) position error, (d) magnified largest steady state error, (e) pressure readings at port A of cylinder, (f) pressure reading at port B of cylinder.

6.6. Effect of frequency and pattern of motion to responses of the circuit when the load is switching

To study the sensitivity of the position response and the energy consumption of the proposed circuit to the pattern and frequency of motion, three different signals are chosen. A sinusoidal signal as a smooth and variable speed pattern of motion, a trapezoidal signal to test the responses of the circuit when the pattern of motion is

90

smooth and speed of end-effector is constant for each segment of signal, and a square desired position signal to study the system responses to fast desired position signals. For all tests, the amplitude of the desired position signal is 15 cm and the frequencies are 0.05, 0.1, 0.2, 0.3 and 0.4 Hz. and controller settings are not changed. Two counterbalance valves are set to keep the load (springs compressed) with no effort from the prime mover. The rod side counterbalance valve pressure is set to 5.2 MPa and at the cap side seating is 2.8 MPa. For all tests of this section, the settings of two counterbalance valves will not change.

6.6.1. Applying sinusoidal desired position signal(amplitude=15 cm)

Figure 6-8 shows the position responses of the proposed circuit when the amplitudes of sinusoidal desired position signals are fixed to 15 cm and frequencies are 0.05, 0.1, 0.2, 0.3 and 0.4 Hz. It is shown; by increasing the frequency of the desired position signal to 0.4 Hz the position response does not follow the tracking signal properly. Asymmetric position response of the position response is the result of asymmetric areas two sides of piston, delay of response of variable frequency drive, different proportional gains for retraction and extraction of cylinder, data acquisition board limit (± 10 V) and different settings two counterbalance valves on two ports of cylinder. Figure 6-8(e) shows the asymmetric position response of the end-effector. Figure 6-9 shows the position response error of the proposed circuit for scenarios showed in Figure 6-8. They show how raising the frequency of sinusoidal desired position signal affects the error of the position response. Figure 6-8(f) shows the comparative mean values and standard deviations of position response errors when the signal is sinusoidal and the constant amplitude is 15 cm.
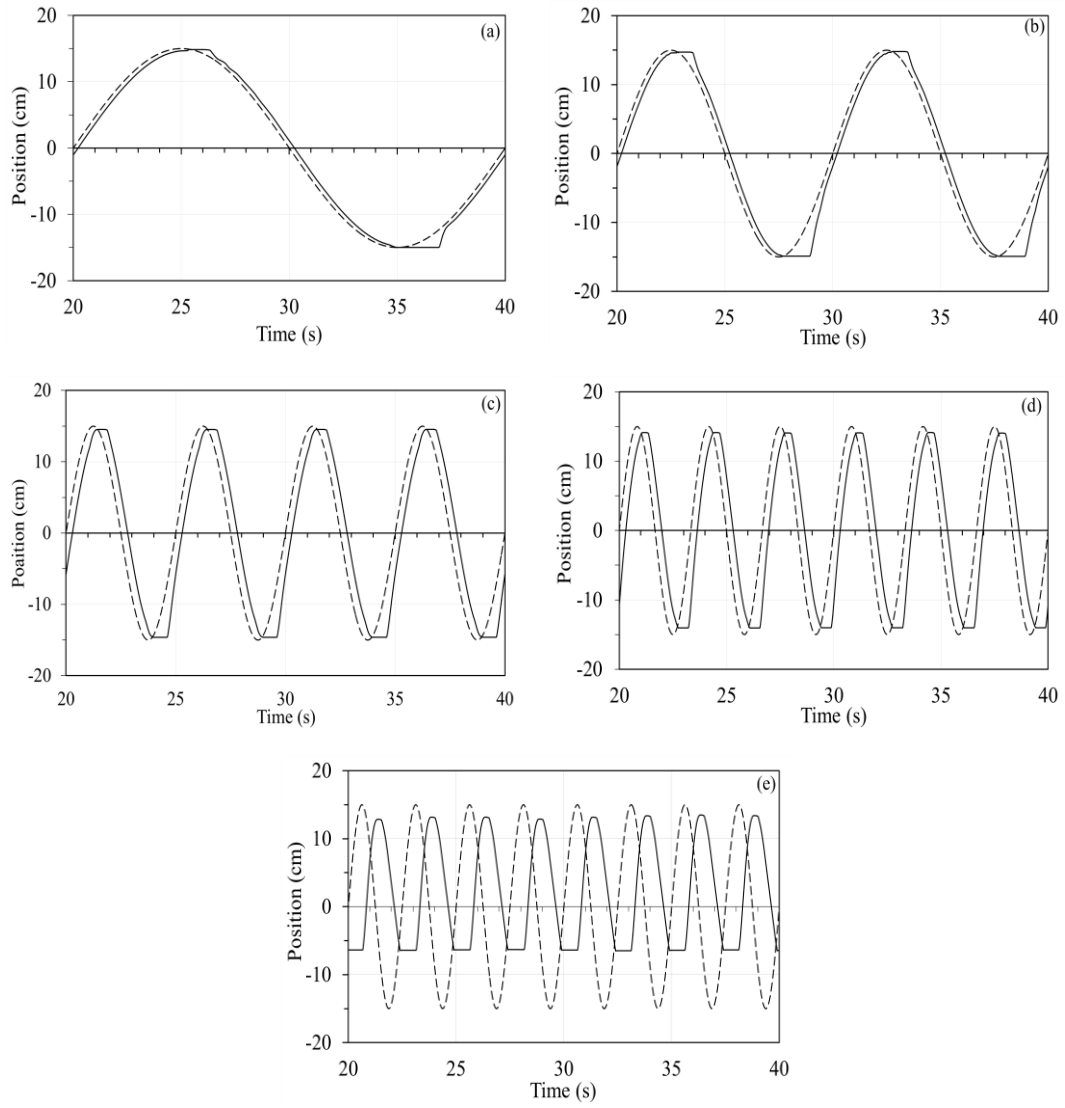
Figure 6-8.:Desired sinusoidal position signals (dashed) and position responses (solid) of the proposed circuit when the amplitudes are fixed to 15 cm and frequencies are; (a) 0.05 Hz, (b) 0.1 Hz, (c) 0.2 Hz, (d) 0.3 Hz and (e) 0.4 Hz.
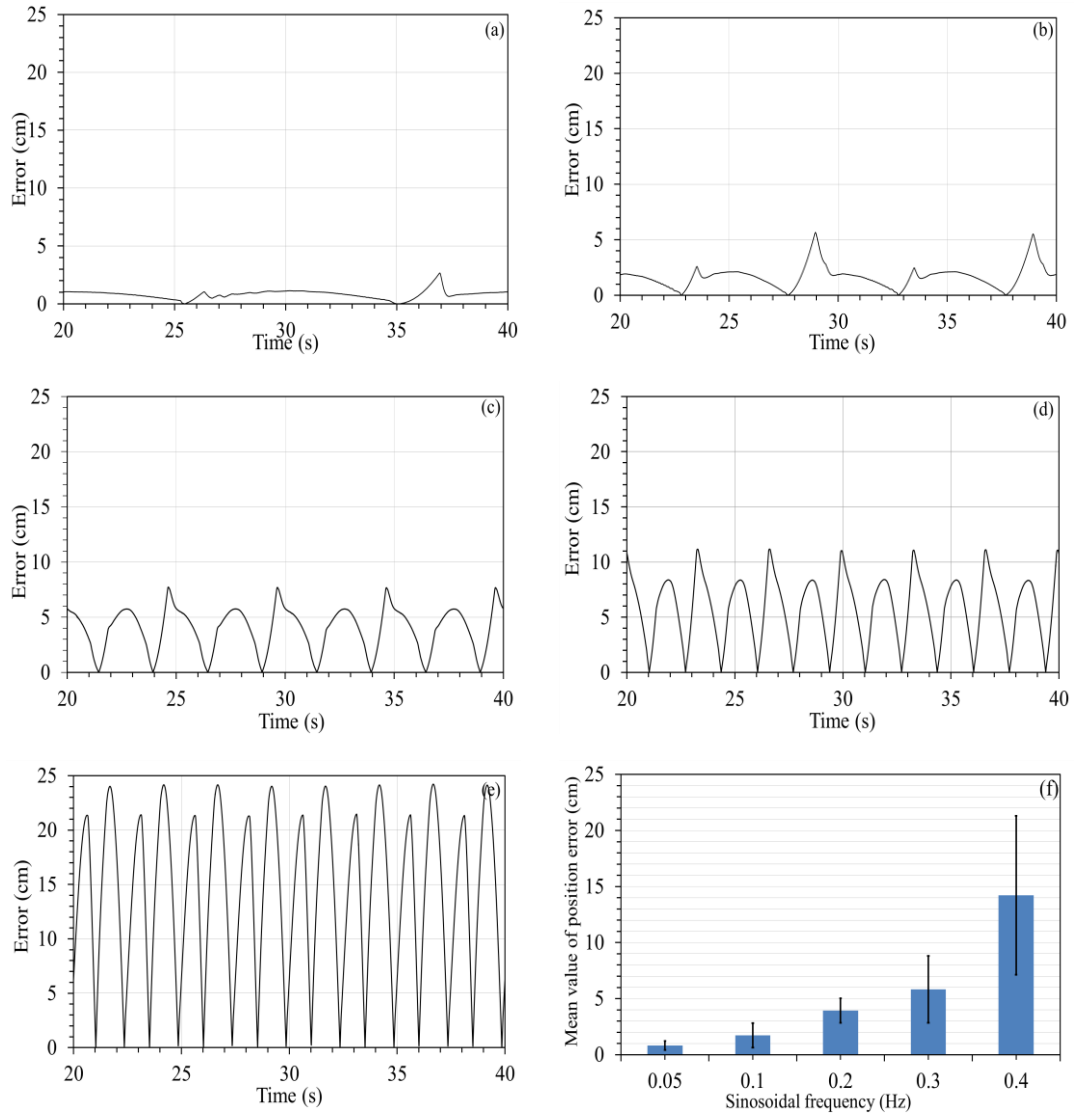
Figure 6-9:Positionn response errors of the proposed circuit to sinusoidal tracking signals with amplitudes of 15 cm and frequencies of (a) 0.05 Hz, (b) 0.1 Hz, (c) 0.2 Hz, (d) 0.3 Hz and (e) 0.4 Hz, (f) mean value and standard deviation of position error versus frequency of sinusoidal desired position signal.

Set of Figure 6-10(a) to (e) represent the pressure behavior of the cylinder of the proposed circuit against the end-effector position of the cylinder when the desired position is sinusoid and the frequency is changed from 0.05 Hz to 0.4 Hz. Comparison of Figure 6-10(a) to Figure 6-10(e) shows that by increasing the frequency of the desired position signal working pressures on both sides of the cylinder slightly

increased and the pump feeds more power into the ports of the cylinder to achieve almost the same performance.

Figure 6-11(a) to (e) shows pressure at port A versus pressure at port B of the cylinder when the desired position signals are sinusoidal with fixed amplitude of 15 cm and frequencies changed from 0.05 Hz to 0.4 Hz.

Pressure readings at the pump ports and records of the end-effector position transducer delivering hydraulic power to the cylinder for these tests are calculated by taking into consideration the fact that in pump-controlled hydraulic circuits, the pump produces only the needed pressure to perform the motion and internal leakage of the pump is negligible. In the proposed pump-controlled circuit at rest, the counterbalance valves keep the load in position with no effort from the prime mover. While in motion conditions, the hydraulic power delivered by the pump to the cylinder (W_h) can be calculated by ($W_h = \Delta P Q$), where Q is the pump flow rate and can be obtained by multiplying the piston speed to the effective piston area. Average delivered hydraulic power to the ports of the counterbalance valves are calculated over 60 s tests and the results are summarized in Figure 6-12 . In Figure 6-12(a) solid line presents the variation of average pump delivered hydraulic power to the circuit when the frequency of the end-effector sinusoidal motion raises and dashed line presents the variation of delivered power by a pressure compensated pump to ports of the throttling valve to perform the same motion. Figure 6-12(b) shows by raising the frequency of the sinusoidal motion the relative efficiency of the proposed circuit relate to a throttling valve circuit decreased from 68% to 40%.
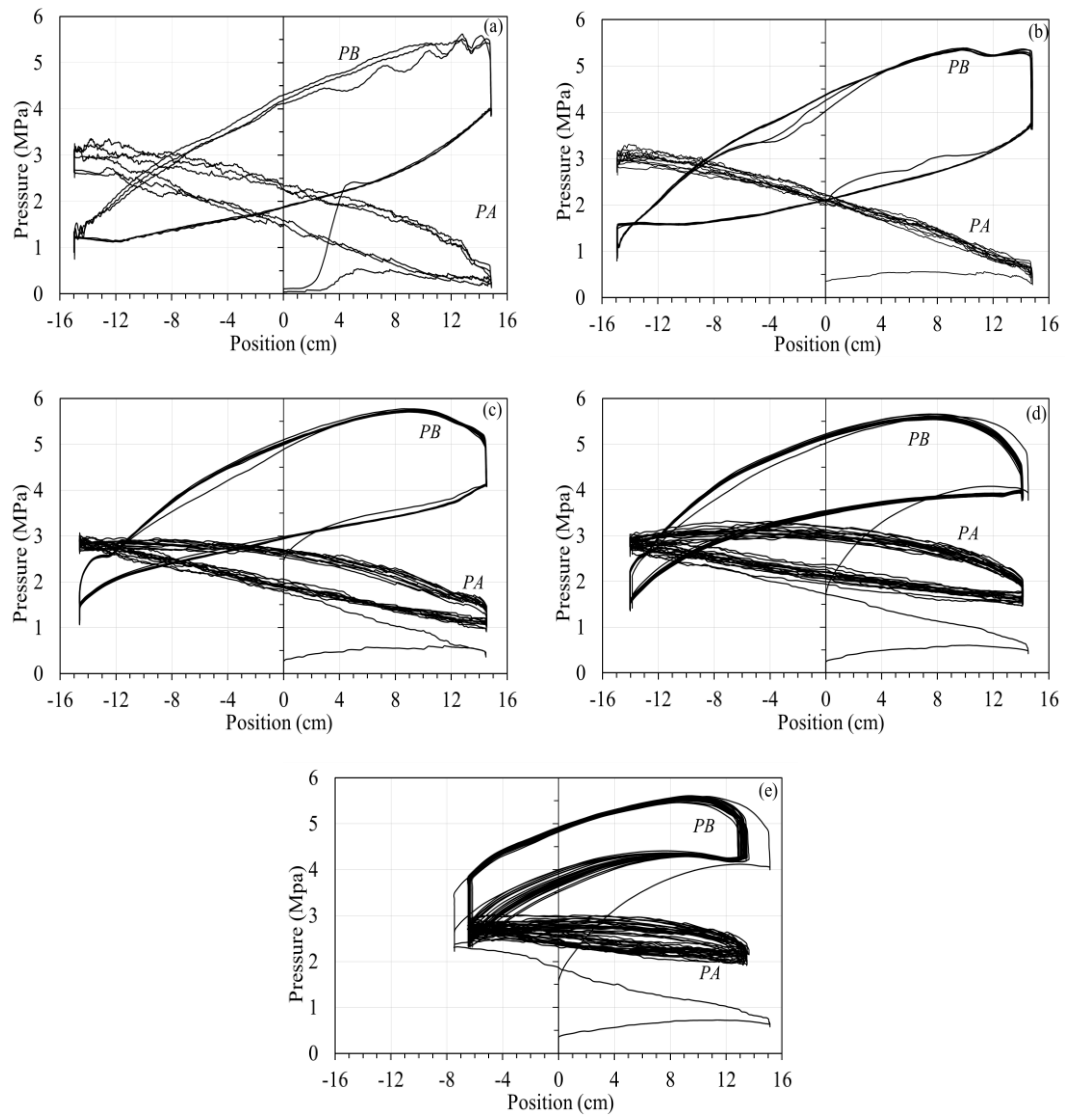
Figure 6-10:Pressure readings at ports versus end-effector position of the cylinder, when the desired position signals are sinusoidal with amplitude 15 cm and frequencies of (a) 0.05 Hz, (b) 0.1 Hz, (c) 0.2 Hz, (d) 0.3 Hz and (e) 0.4 Hz.
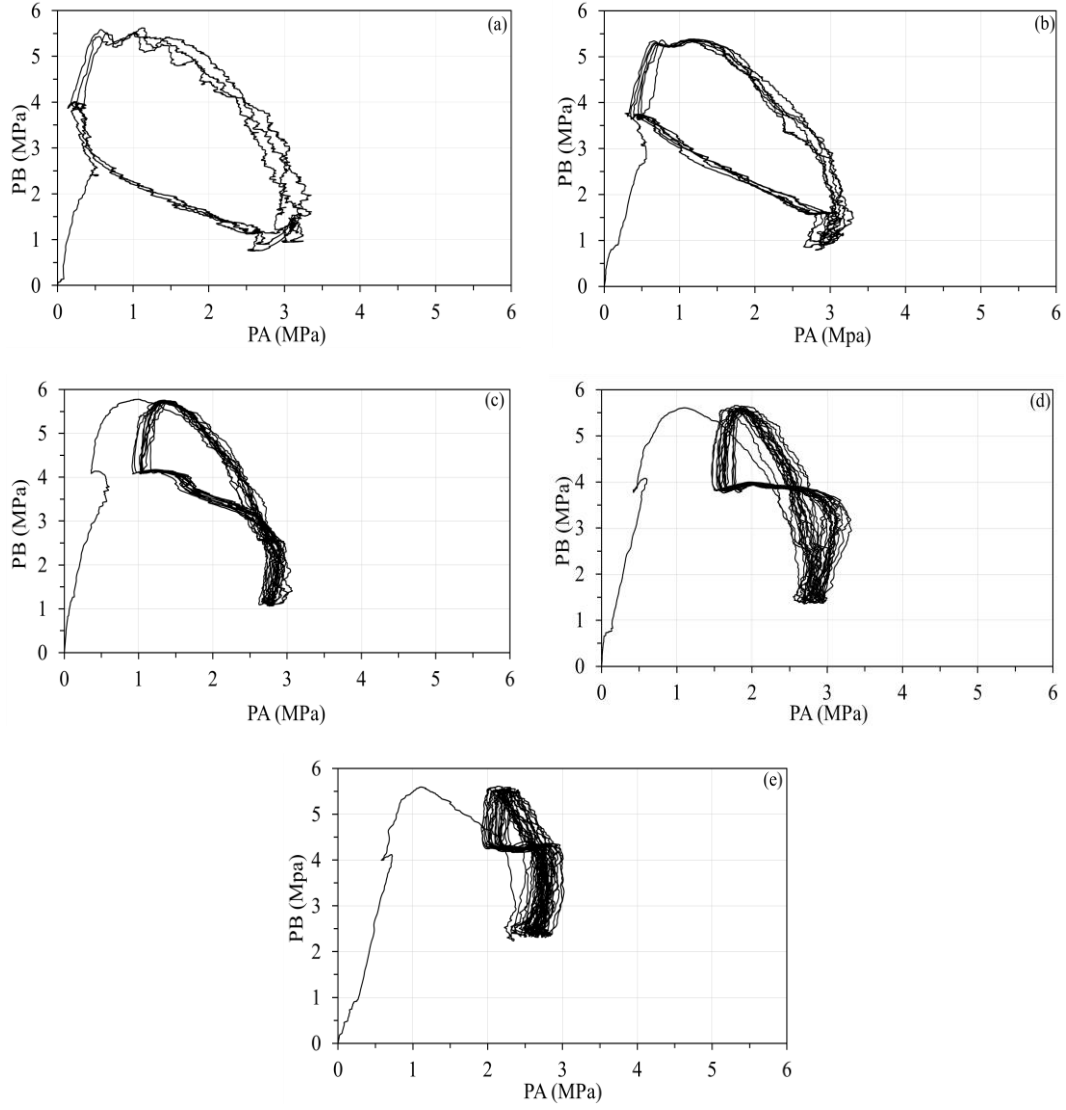
Figure 6-11.Pressure at port A versus port B of the cylinder when the desired position signal were sinusoidal, the cylinder stroke were fixed to 30 cm and frequencies were; (a) f=0.05 Hz, (b) f=0.1 Hz, (c) f=0.2 Hz, (d) f=0.3 Hz and (e) f=0.4 Hz.
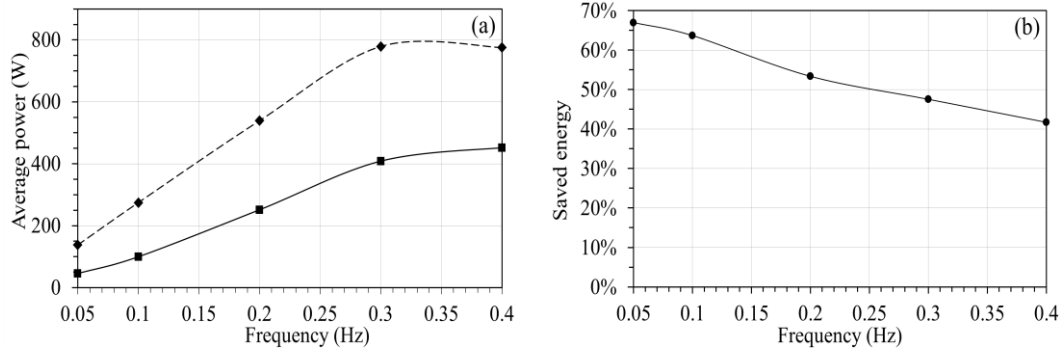
Figure 6-12 (a) Average pump delivered hydraulic power to cylinder in test rig is showed by solid line and dashed line is the power required by a valve controlled circuit pressurized with a pressure compensated pump performs the same pattern of motion, (b) relative efficiency of the proposed circuit in compare to a valve control circuit.

6.6.2. Applying square desired position signal (amplitude=15 cm)

In the next step, square desired position signals with fixed amplitude of 15 cm and frequencies of 0.05, 0.1, 0.2, 0.3 and 0.4 Hz are applied to the test rig with no changes on controller gain and counterbalance valves settings. Duration of each test is 60s and the positon responses and pressures at pump and cylinder ports are recorded. Figure 6-13 series shows the position response of the test rig to the previously mentioned square desired position signals and as it is seen by raising the frequency the tracking performance of test rig get worse. As seen in Figure 6-13(e), when the frequency is 0.4 Hz the end-effector does not follow the tracking signal. Figure 6-14 series shows the position response errors of the proposed circuit in different frequencies and amplitudes of 15 cm of the desired position square signal. Figure 6-14(f) shows how by increasing the frequency when the tracking signal is square the mean value and standard deviation of position response error increased. At a frequency of 0.4 Hz the average of position error increased and standard deviation decreased. Declining of standard deviation shows the steady state error of the position response at high and low stop points are affected and increased. Figure 6-15(a) shows how increasing the frequency of the desired square position signal effects the average hydraulic power

97

delivered to the cylinder in the proposed circuit and compare it to average hydraulic power required to feed ports of a throttling valve by a pressure compensated pump to perform the same load motions. As Figure 6-15(b) shows, comparative energy efficiency of the proposed circuit for frequencies higher than 0.05 Hz to a valve controlled circuit is not as sensitive of sinusoidal desired position (compare Figure 6-15b and Figure 6-12b).
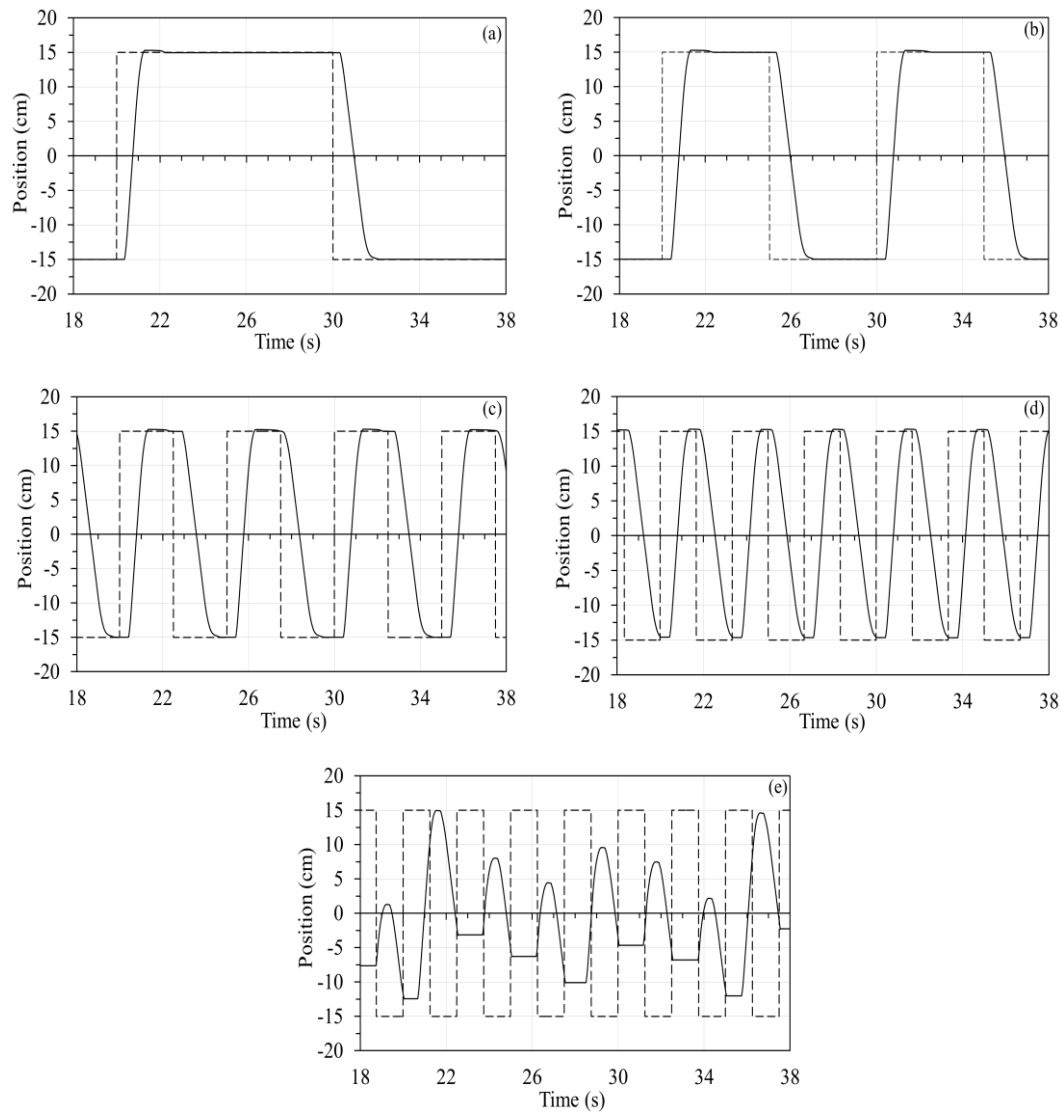
Figure 6-13. Position response of the proposed circuit to square desired position signal when the amplitudes set to 15 cm and frequencies are (a) f=0.05 Hz, (b) f=0.1 Hz, (c) f=0.2 Hz, (d) f=0.3 Hz, (e) f=0.4 Hz., dashed lines are desired position signal and solid lines are position response of the proposed circuit.
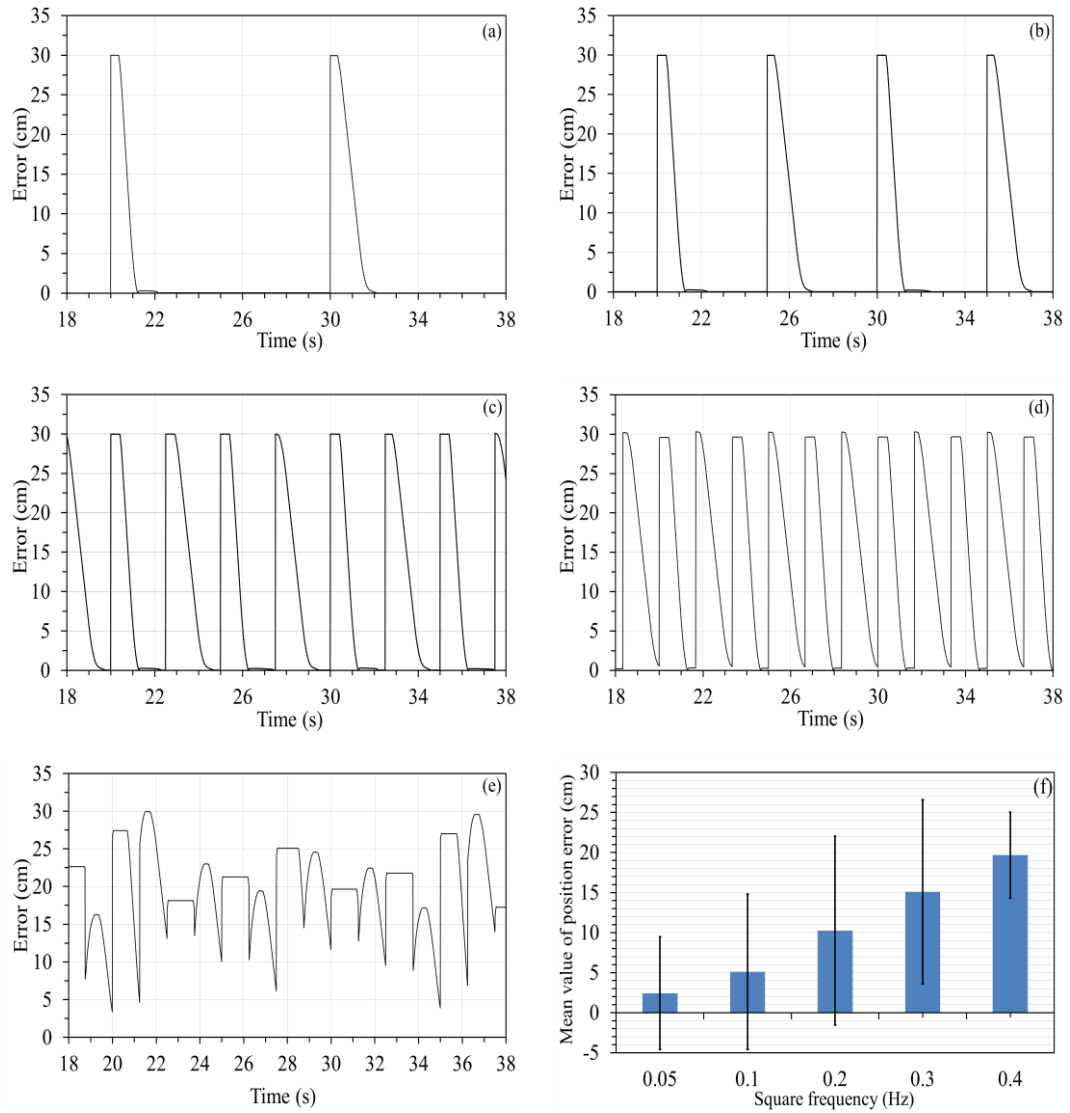
Figure 6-14 Position error of the proposed circuit when amplitude of the desired position signal was 15 cm and (a) f=0.05 Hz, (b) f= 0.1 Hz, (c) f=0.2 Hz, (d) f=0.3 Hz, (e) f=0.4 Hz.
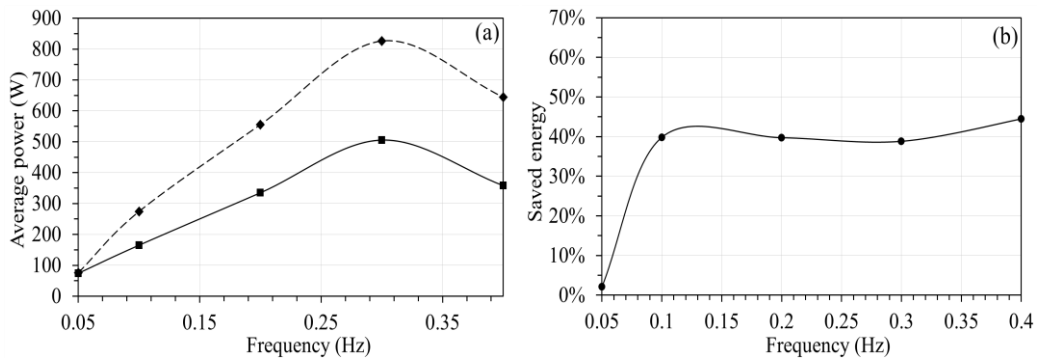
Figure 6-15. (a) The average delivered hydraulic power (solid) to circuit when the and frequency is raised from 0.05 to 0.4 Hz, and the required average hydraulic power for a valve controlled circuit to perform the same tasks, (b) relative energy efficiency of the proposed circuit over the valve controlled circuit in different frequencies.

6.6.3. Applying trapezoidal desired position signal (amplitude of 15 cm)

The third step of tests with a variable frequency desired position signal, a trapezoid desired position signal is chosen and the amplitude of the signal is set to 15 cm. Position responses and pressures of the proposed circuit are recorded for 5 different frequencies of 0.05, 0.1, 0.2, 0.3 and 0.4 Hz. The proportional gain of the control loop was fixed for all test of this chapter. Figure 6-16 represents the position responses of the proposed circuit to trapezoid desired position signals. End-effector of the cylinder did not track the desired position signal properly when the frequency of it reaches to 0.4 Hz (see Figure 6-16e). Figure 6-17 shows the shape of position response error of the end-effector to the same trapezoidal signals. Figure 6-17(f) shows by increasing the frequency of the trapezoidal signal mean value of the position error increased. Figure 6-18(a) presents the comparative graph of energy saving between the proposed circuit, and a pressure compensated pump feeding a throttling valve to perform the same action for load. Figure 6-18(b) illustrates the sensitivity of the average saved energy of the proposed circuit to the frequency of a trapezoidal desired position signal. By increasing the frequency of the end-effector motion the proposed circuit shows less efficient in compare to valve controlled circuit.
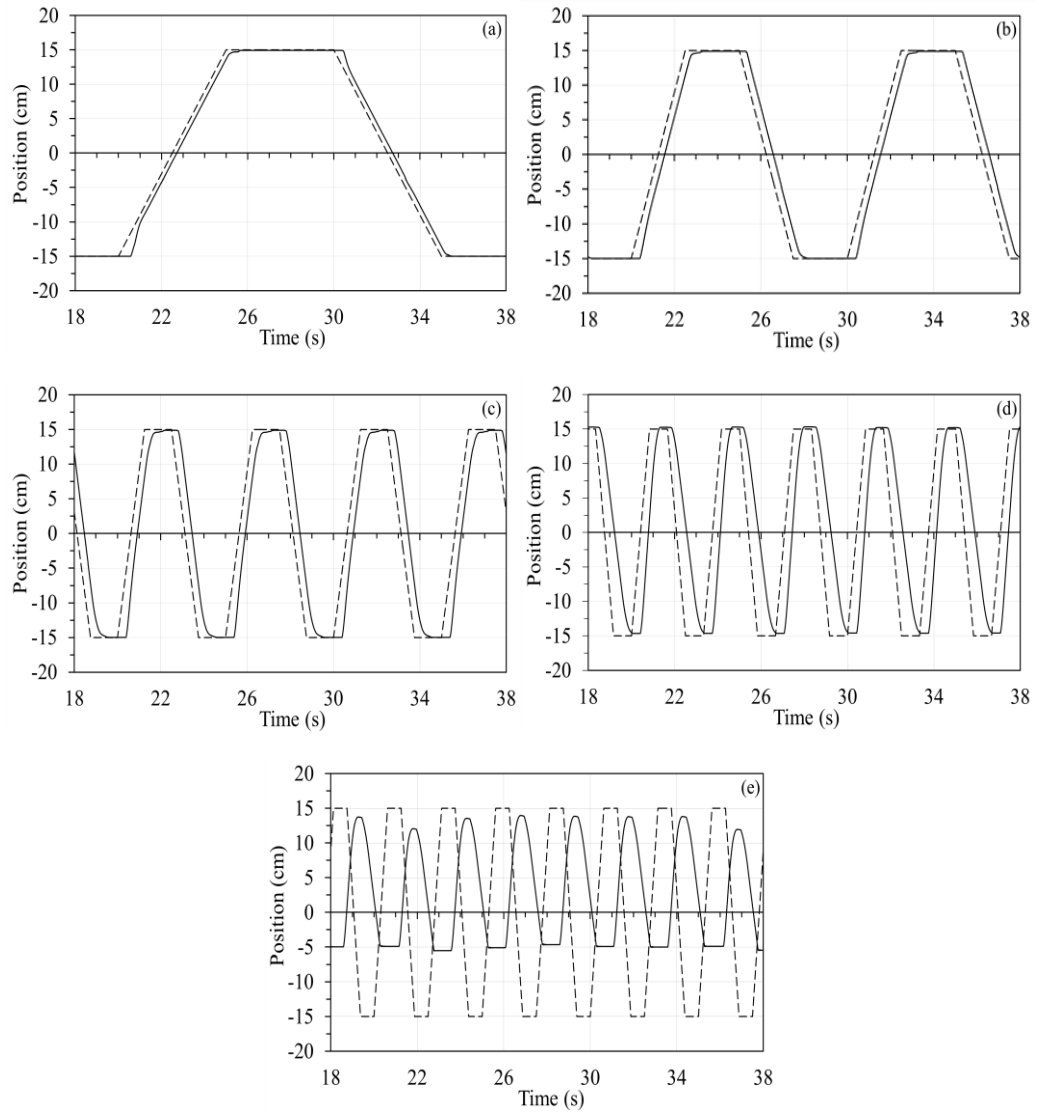
Figure 6-16. Position responses of the proposed circuit to trapezoidal desired position signals when amplitude fixed to 15 cm and frequency are (a) f= 0.05 Hz, (b) f= 0.1 Hz, (c) f=0.2 Hz, (d) f=0.3 Hz, (e) f=0.4 Hz, dashed lines are desired position signals and solid lines are position response of the proposed circuit.
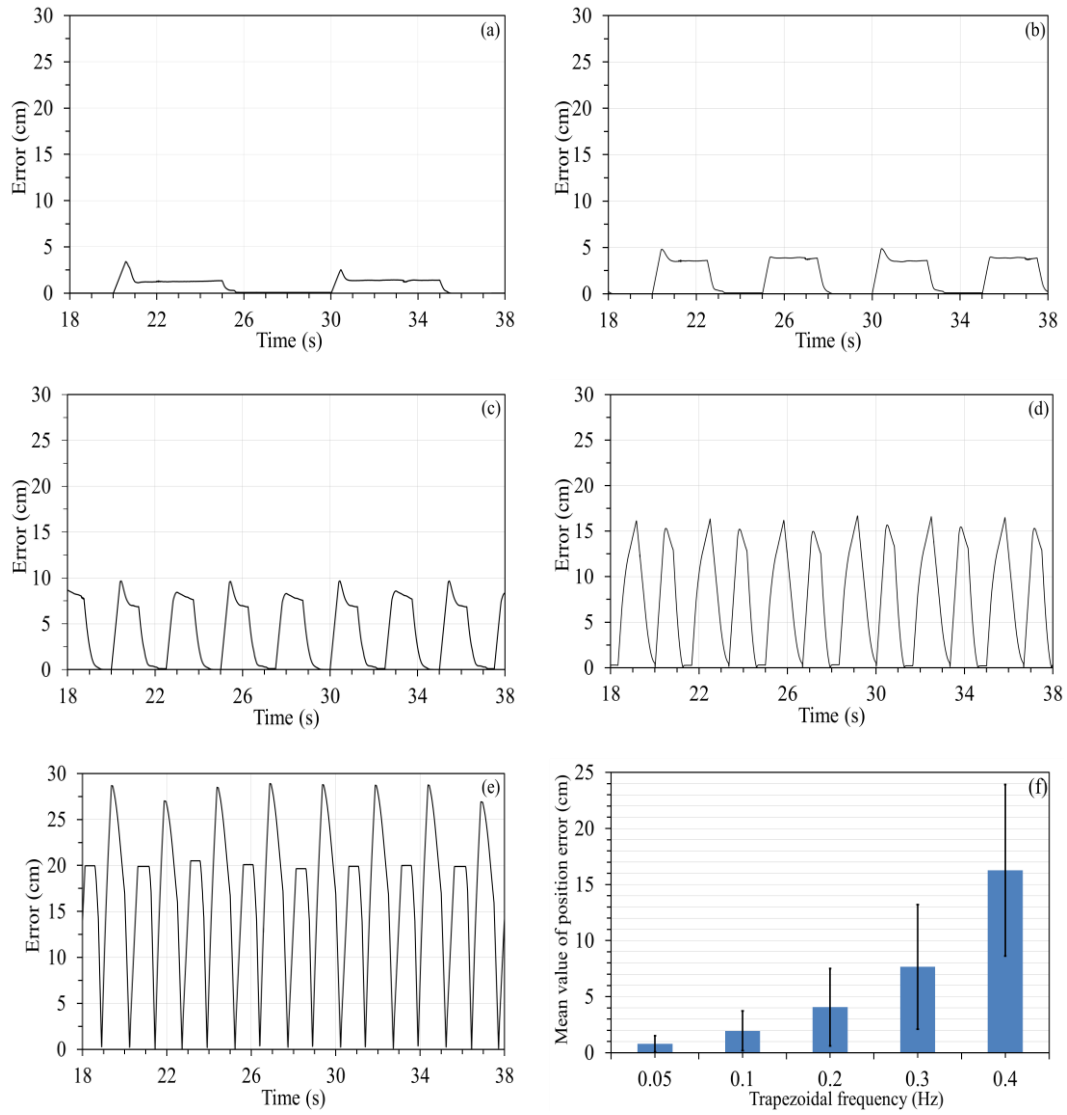
Figure 6-17: Position response error of the proposed circuit when the desired position signal is trapezoid with amplitude 15 cm and frequencies are (a) f=0.05 Hz , (b) f=0.1 Hz, (c) f=0.2 Hz, (d) f=0.3 Hz, (e) f=0.4 Hz, (f) mean value of and standard deviation of the position response error for tests with trapezoidal signals.
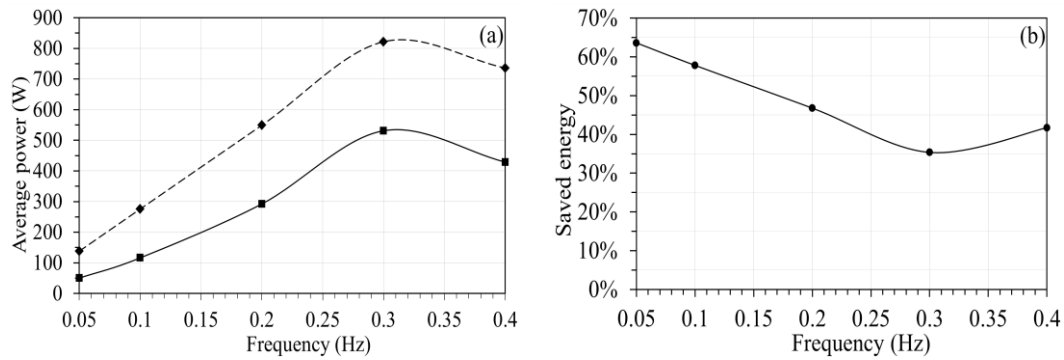
Figure 6-18: (a) Average delivered hydraulic power to the cylinder in proposed circuit for different frequency of trapezoid signals shows by solid line and the average amount of required hydraulic power from a pressure compensated pump for a throttling valve to perform the same performance showed by dashed line, (b) relative power saving of the proposed circuit to a throttling circuit when the desired signal is trapezoid and frequency is changing.

6.6.4. The proposed circuit responses and pattern of motion when amplitude is fixed and frequency is changed

To study the effect of the pattern of desired position signal to position response of the proposed circuit mean values and standard deviations of the position response error of the proposed circuit in different frequencies and amplitude of 15 cm summarized in Table 6-1 and Figure 6-19 series. As it is shown, by raising the frequency, sinusoidal and then trapezoidal tracking signals offer less average position errors, and square pattern of motion has the highest errors. In conclusion when the tracking performance is important the proposed circuit needs to track smoother signals and if the lowest steady state error is the required performance of the circuit trapezoidal tracking signal is a better choice.

Table 6-2 and Figure 6-20 compare average of the delivered power to the counterbalance ports by the pump under three tracking signals of sinusoidal, trapezoidal and square in different frequencies. In lower frequencies, smoother signals perform more energy efficient responses. The square tracking signal has performs the lowest efficiency and lowest tracking performances.

103

Table 6-1: Mean values and standard deviation of position errors for tested scenarios when amplitudes are fixed to 15 cm.

Frequency (Hz)	Sinusoid	Trapezoid	Square
0.05	0.82±0.39	0.79±0.73	2.43±7.40
0.1	1.72±1.09	1.95±1.77	5.09±9.69
0.2	3.94±2.03	4.06±3.44	10.25±11.86
0.3	5.83±2.99	7.66±5.56	15.09±11.47
0.4	14.23±7.08	16.27±7.65	19.67±5.42
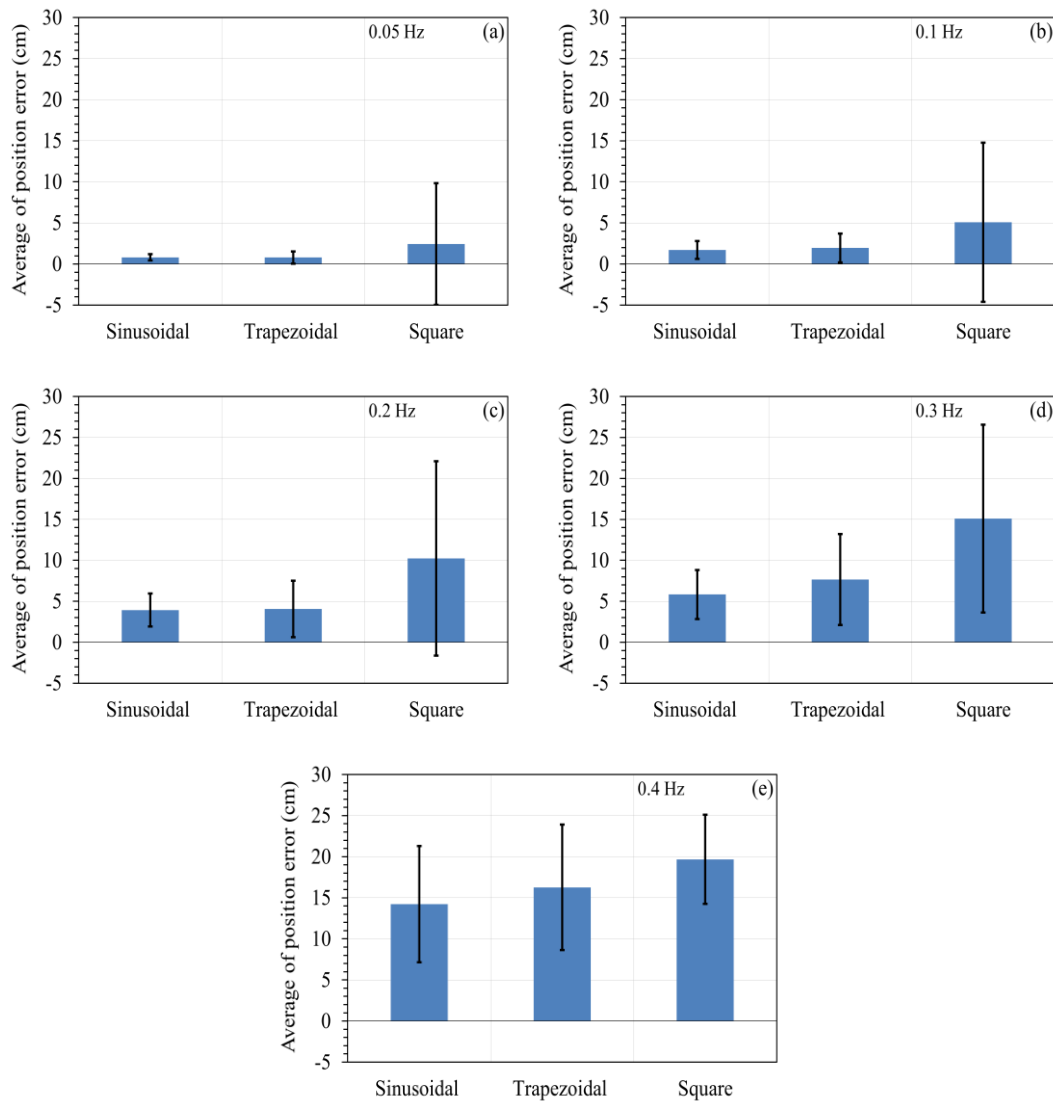
Figure 6-19 :Comparative average position response errors of the proposed circuit when sinusoidal, trapezoidal and square signals are applied with amplitude of 15 cm and frequencies of (a) 0.05 Hz, (b) 0.1 Hz, (c) 0.2 Hz, (d) 0.3 Hz and (e) 0.4 Hz .

Table 6-2: Mean values and standard deviation of average delivered hydraulic power for tested scenarios when amplitudes are fixed to 15 cm.

Frequency (Hz)	Sinusoid	Trapezoid	Square
0.05	45.6±32.41	50.33±53.88	74.2±252.00
0.1	99.83±79.99	116.28±122.75	165.00±45.23
0.2	251.57±185.29	292.38±298.33	334.84±488.89
0.3	408.75±323.90	531.26±559.47	505.50±535.01
0.4	452.16±481.91	428.83±478.80	357.89±435.34
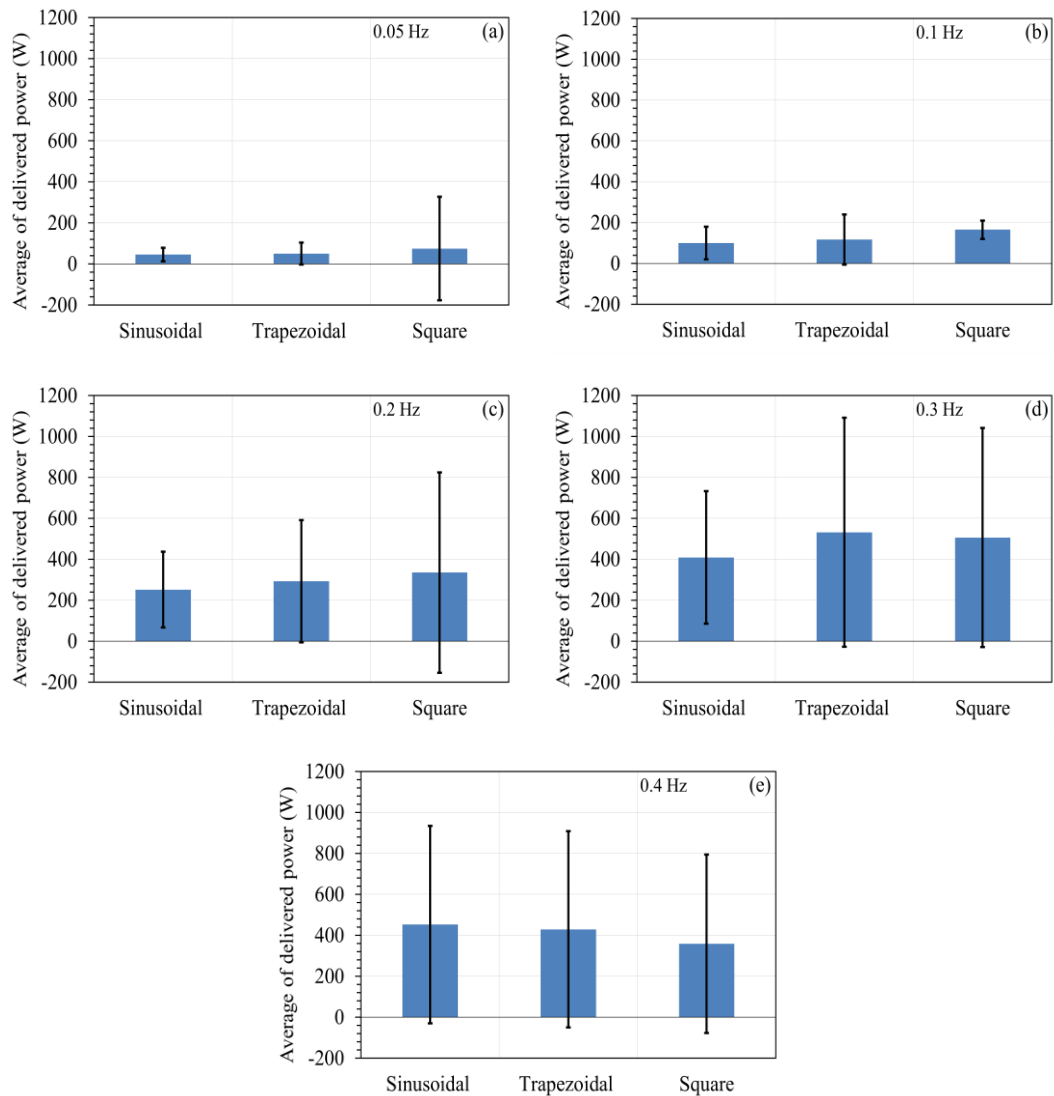
Figure 6-20: Comparative average energy consumption of the proposed circuit when sinusoidal, trapezoidal and square tracking signals are applied with amplitude of 15 cm and frequencies of (a) 0.05 Hz, (b) 0.1 Hz, (c) 0.2 Hz, (d) 0.3 Hz and (e) 0.4 Hz.

6.7. Effect of amplitude to position response

To study the sensitivity of the position response and energy consumption of the proposed circuit to the amplitude of the tracking signal, three set of tests are designed. Pattern of periodic signals are sinusoidal, square and trapezoidal with a frequency of 0.1 Hz and amplitudes of 4 cm, 8 cm, 10 cm, 15 cm and 20 cm. Results of tests are presented in the next section. As mentioned earlier in this text, proportional gain and counterbalance valve settings are all the same in this chapter.

6.7.1. Applying sinusoidal desired position signal (f=0.1 Hz)

Figure 6-21(a) to (e) shows sinusoidal desired position signals and position response of the proposed circuit when frequency is 0.1 Hz and amplitudes are (4, 8, 10, 15, and 20 cm) and tests are performed for 60 s. The variable frequency drive response delay, inertia of rotating parts of electromotor and pump and pressure settings of counterbalance valves changed the shape of the position responses plots when the end-effector changes its direction of motion. Figure 6-21(f) summaries the mean value and standard deviation of position response errors in different amplitudes, by raising the amplitude by factor of 5 (from 4 cm to 20 cm) average position error raised the factor of 5 (from 0.55 cm to 2.26 cm). Figure 6-22 presents plots of pressures at ports of cylinder versus end-effector position. By increasing the amplitude of the motion, springs are compressed more and they create more force against end-effector. More force induces more pressure in chamber of the cylinder. Rod side of cylinder works with higher pressure attributed to smaller effective area of piston. More pressure is needed in order to retract the spring load cylinder when the amplitude of motion is increased.

106

Figure 6-23 shows pressure at port A of the cylinder versus pressure at port B of the cylinder in different amplitudes. As shown, by increasing the amplitude when the frequencies are fixed, the pressure work space (pressure loop area) of the cylinder expands (see Figure 6-23). The position of the end-effector of the cylinder and the pressures at pump ports are recorded for all tests and the average hydraulic power delivered to the cylinder is calculated for different amplitudes which are shown by solid line in Figure 6-24(a). Also, for the scenario of using a throttling valve and a pressure compensated pump powering the same cylinder, the average delivered hydraulic power to throttling valve is calculated and showed by the dashed line in Figure 6-24(b). This figure shows that the proposed circuit consumes less power in comparison to the throttling valve that is pressurized with a pressure compensated pump system in different amplitudes of the sinusoid position pattern.
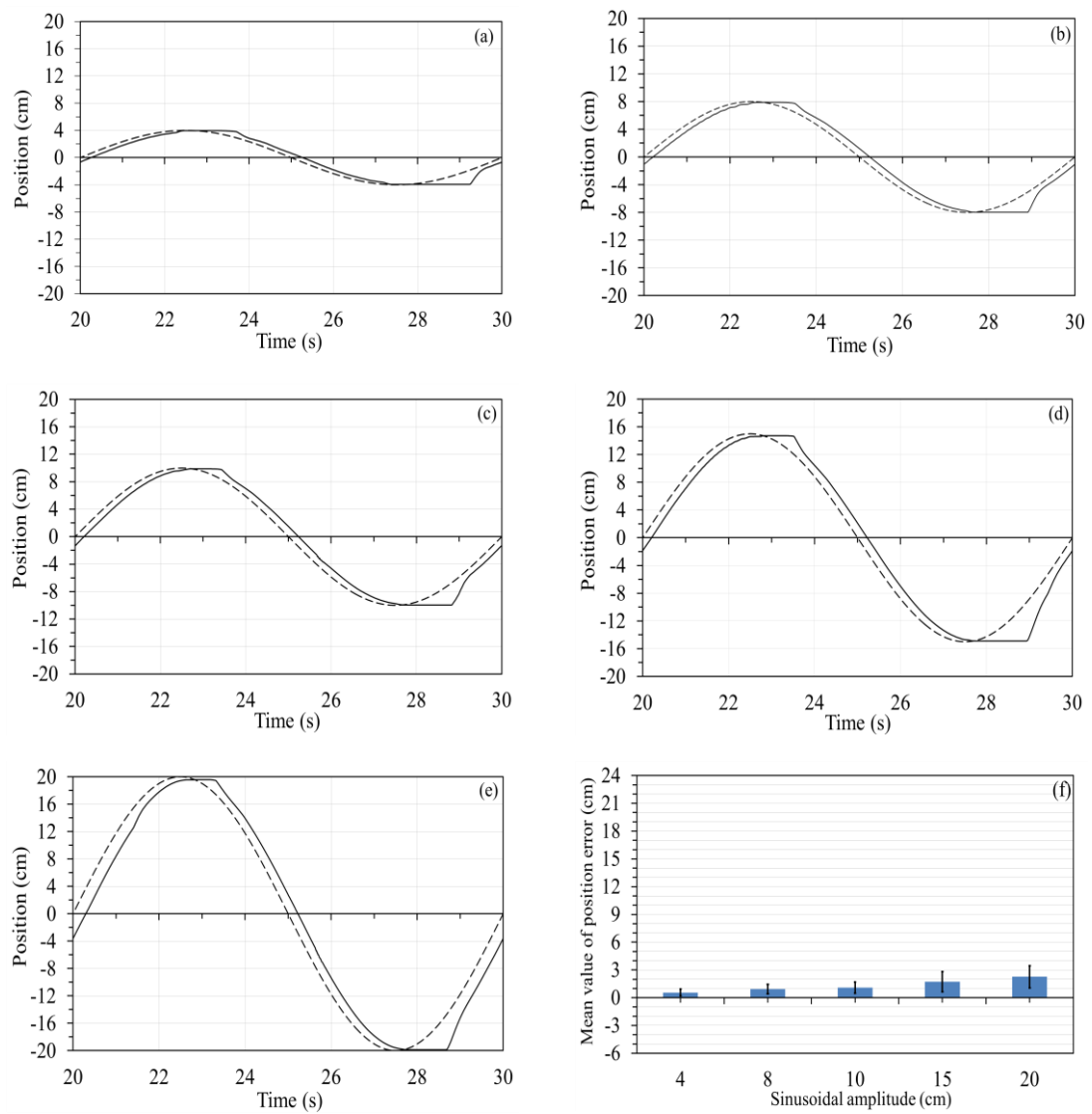
Figure 6-21: Desired sinusoidal position signals are showed by dashed and position responses are showed by solid lines, when frequencies are 0.1 Hz and amplitudes are (a) 4 cm, (b) 8 cm, (c) 10 cm, (d) 15 cm and (e) 20 cm and (f) the mean value and standard deviation of average position response errors for different amplitudes.

108
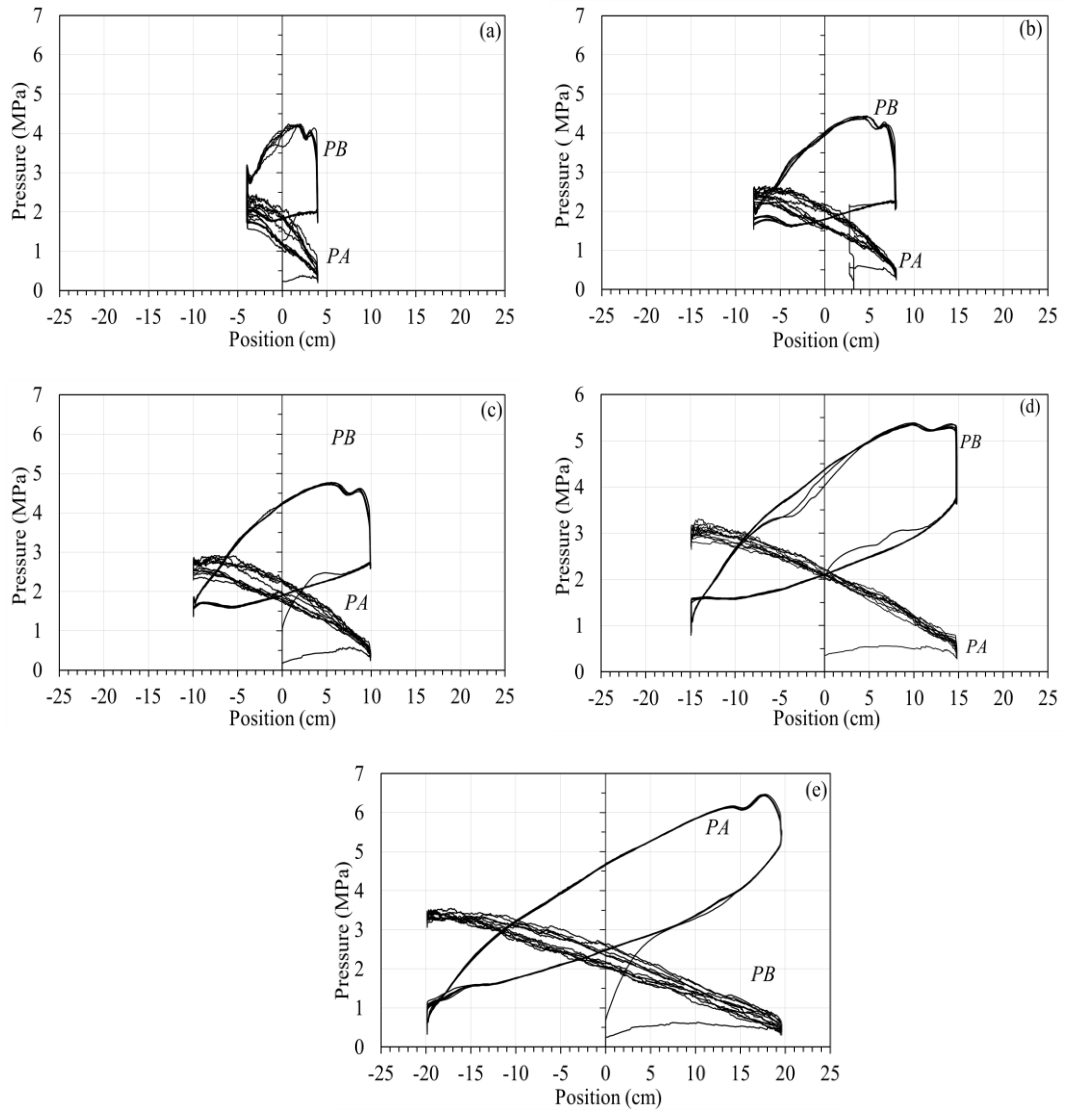
Figure 6-22: Pressures at ports of the cylinder versus end-effector position when the frequency of the desired position signal is fixed to 0.1 Hz and amplitudes are (a) 4 cm, (b) 8 cm, (c) 10 cm, (d) 15 cm and (e) 20 cm.
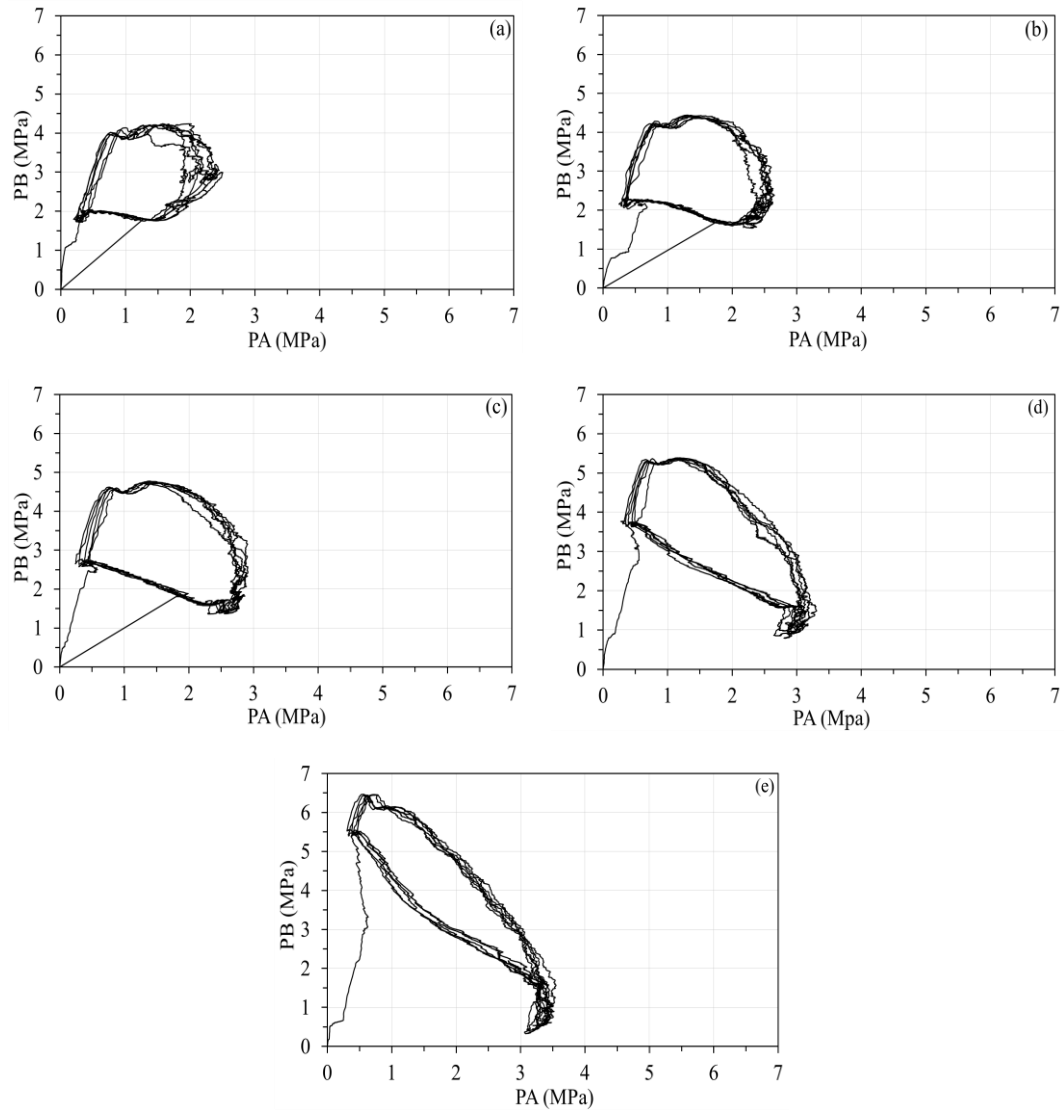
Figure 6-23 Pressure surface of the cylinder is the pressure at port A versus the pressure at port B of the cylinder when frequency of motion was fixed to 0.1 Hz and amplitude was (a) 4 cm, (b) 8 cm, (c) 10 cm, (d) 15 cm and (e) 20 cm.
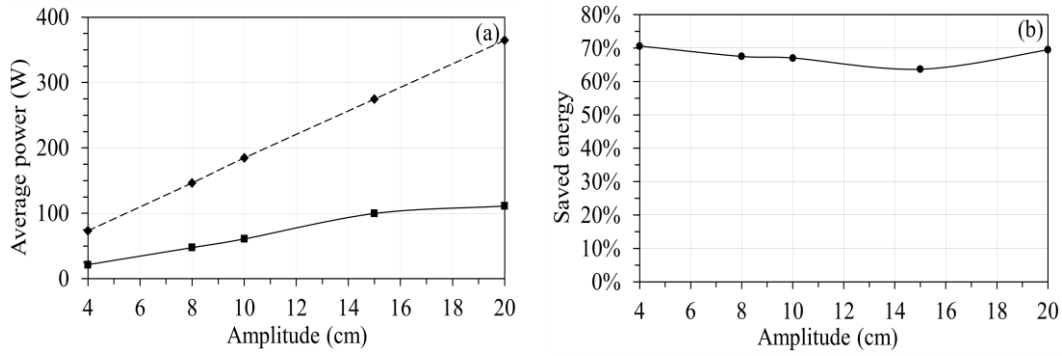
Figure 6-24.(a) The average of delivered hydraulic power to the cylinder in different amplitudes (solid line) and the average of required hydraulic power from a pressure compensated pump for a throttling valve to perform the same motion (dashed line), (b) amount of saving energy by using the proposed circuit in compare to throttling system in different amplitudes.

6.7.2. Applying square desired position signal (f=0.1 Hz)

For the second test of this series, a fixed frequency square signal with different amplitudes (4, 8, 10, 15 and 20 cm) are applied to the proposed circuit and the results presented in the Figure 6-25(a) to (e). Figure 6-25(f) summaries the mean value and standard deviation of position response errors in different amplitudes, by increasing the amplitude from 4 cm to 20 cm the mean value of the position response error is increased from 1 cm to 8 cm. Figure 6-26 shows the energy performance of the proposed circuit when the desired position signal is square with fixed frequency and the amplitude is changed. As seen in Figure 6-26(a) by increasing the amplitude of the desired signal, the average hydraulic power delivered to the cylinder by the proposed circuit and the required power for the throttling valve in a pressure compensated pump increases also. Figure 6-26(b) shows that by increasing the amplitude of the desired signal in a fixed frequency, the percentage of improving efficiency of the proposed circuit in relation to a throttling system decreases (from 58% at 4 cm to 38% at 20 cm).
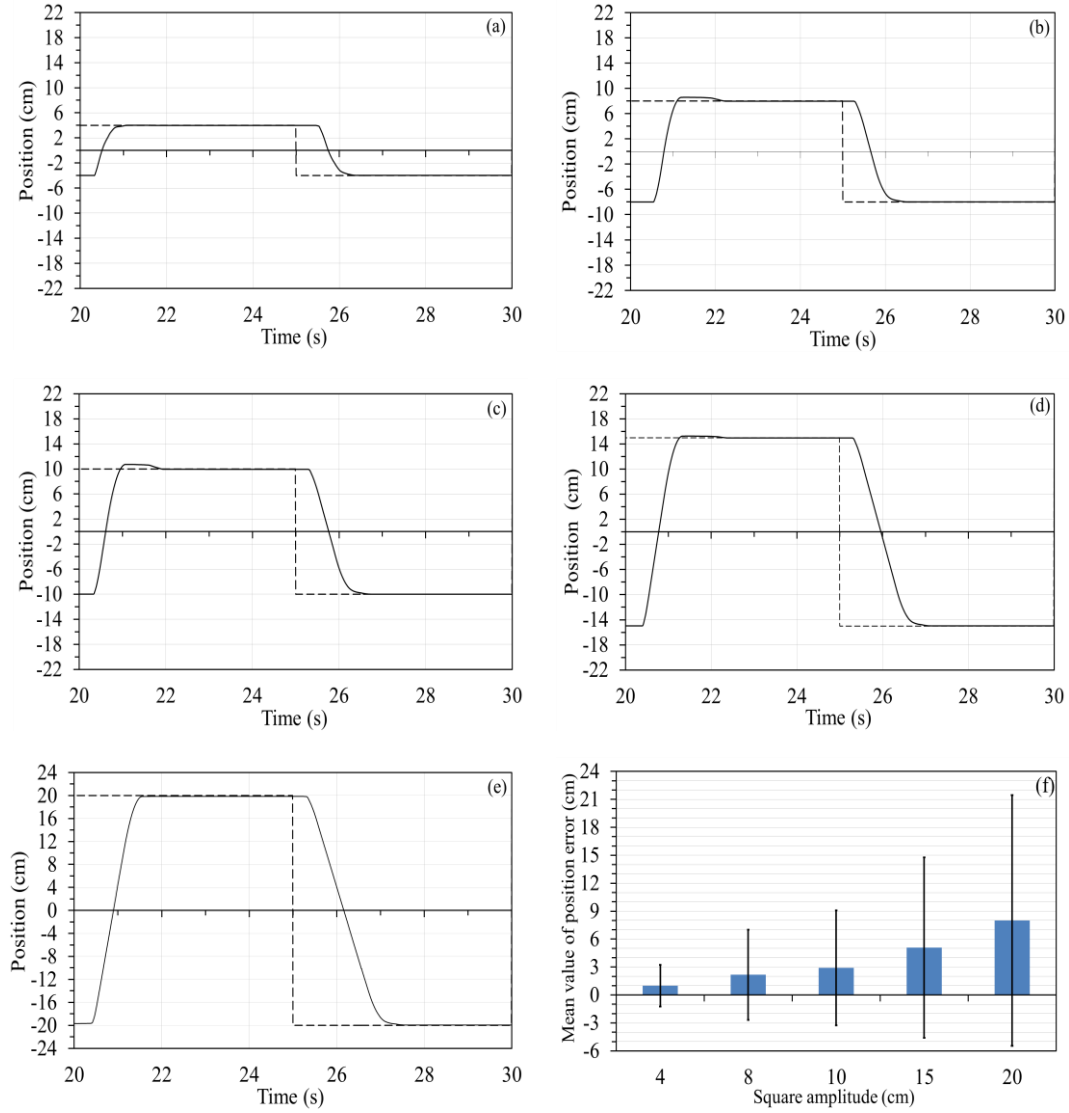
Figure 6-25: Desired position signals presented by dashed line and position responses of the proposed circuit showed by solid lines, frequency of desired position signals are fixed on 0.1 Hz and amplitudes are (a) 4 cm, (b) 8 cm, (c) 10 cm, (d) 15 cm and (e) 20 cm, (f) shows mean values and standard deviations of position response errors of the proposed circuit in different amplitudes.
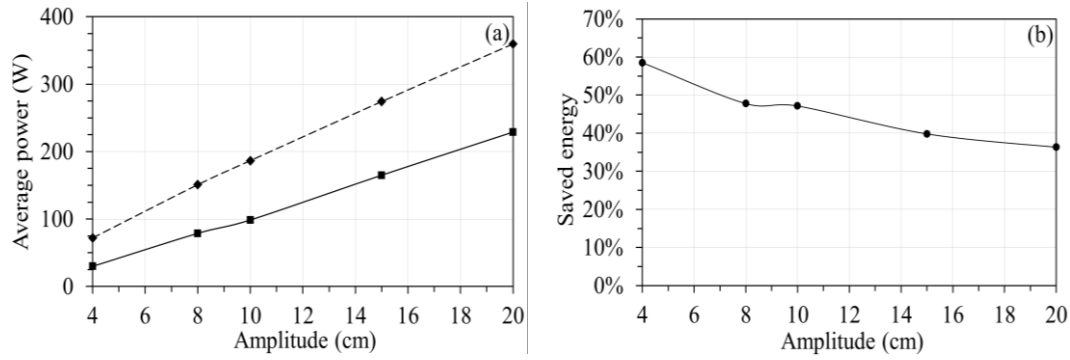
Figure 6-26: (a) Average pump delivered hydraulic power to cylinder in different amplitudes (dashed line) and required power from a pressure compensated pump to throttling valve to perform same motion, (b) comparative energy efficiency of the proposed circuit in compare to a throttling system.

6.7.3. Applying trapezoidal desired position signal (f=0.1 Hz)

In third series of tests, fixed frequency (0.1 Hz) trapezoidal desired position signals with different amplitudes (4, 8, 10, 15 and 20 cm) are applied to the proposed circuit. Solid lines in Figure 6-27(a) to (e) represent the position responses of the proposed circuit to trapezoidal desired position signals when the frequencies are fixed to 0.1 Hz and amplitudes are (a) 4 cm, (b) 8 cm, (c) 10 cm, (d) 15 cm and (e) 20 cm. Figure 6-27(f) shows the mean value and standard deviations of position response errors of the proposed circuit when the amplitude changes, by increasing the amplitudes from 4 cm to 20 cm the mean value of position response error increased from 0.54 cm to 2.62 cm. The solid line in Figure 6-28(a) shows the average delivered hydraulic power to the cylinder of the proposed circuit when the frequency of the trapezoidal desired position signal is fixed to 0.1 Hz and amplitudes are 4, 8, 10, 15 and 20 cm. in Figure 6-28(a) dashed line denotes the average required power from a pressure compensated pump to a throttling valve to perform the same motions of the load. Figure 6-28(b) presents the amount of saved energy when using the proposed circuit in compared to a throttling system for different amplitude trapezoidal signals.

113
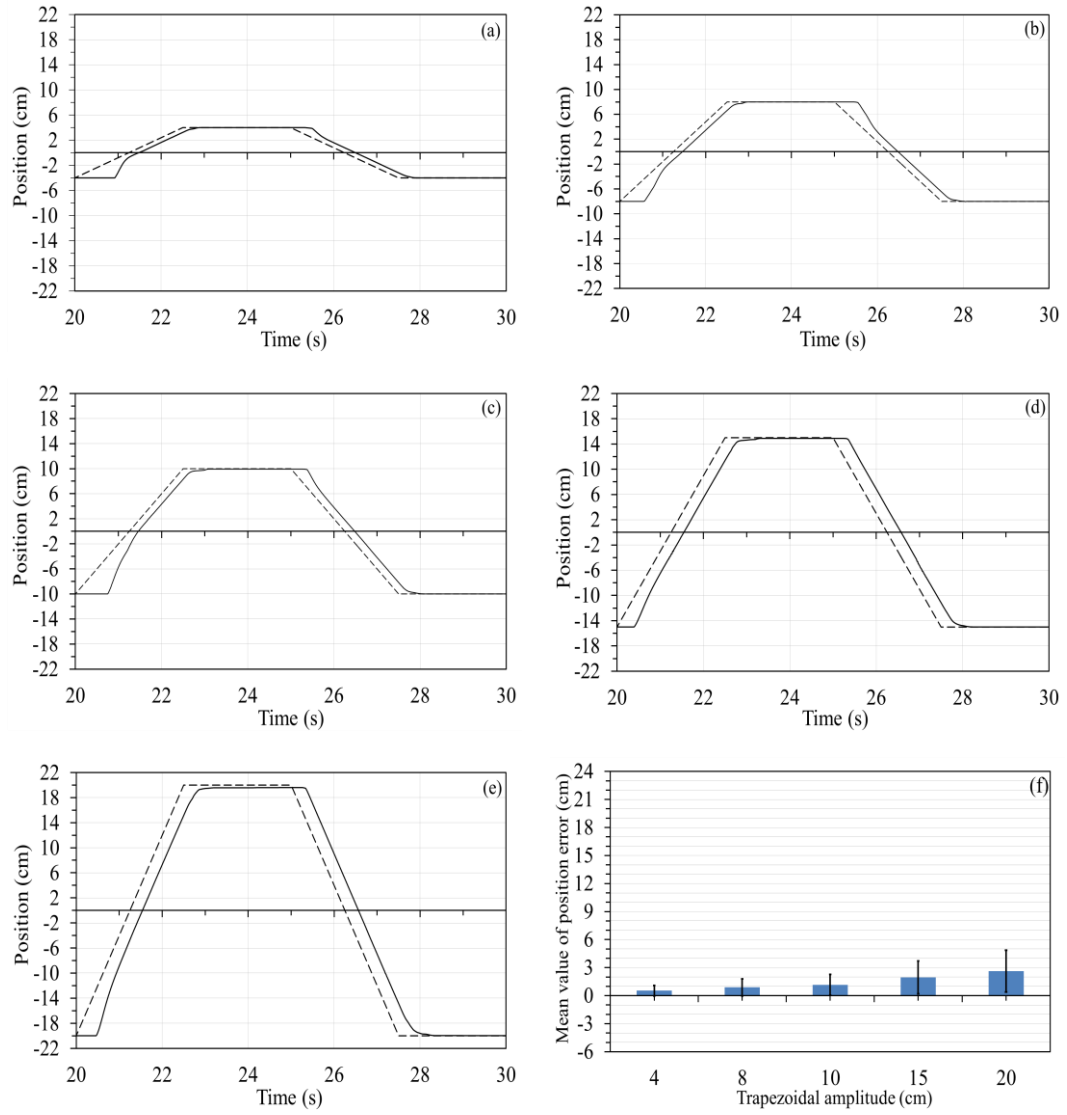
Figure 6-27:Trapezoidal desired position signals (dashed lines) and position responses (solid lines) of the proposed circuit and when the frequencies are fixed to 0.1 Hz and amplitudes are (a) 4 cm, (b) 8 cm, (c) 10 cm, (d) 15 cm and (e) 20 cm, (e) shows the mean value and standard deviation position errors.
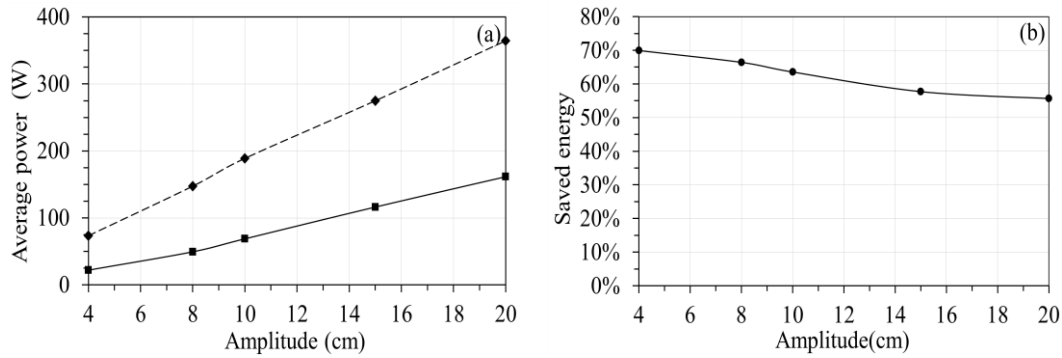
Figure 6-28:(a) Average pump delivered power in the proposed circuit (solid line) and in a pressure compensated pump of a throttling circuit to perform the same motions (dashed line) in different amplitudes (b) shows amount of saved energy by using the proposed circuit in compare to a throttling system for different amplitude signals.

6.7.4. The proposed circuit responses and pattern of motion when the frequency is fixed and amplitude changes

To show a better picture of the proposed circuit performance, average and standard deviation of position response errors and average of pump delivered power to the proposed circuit are rearranged by amplitudes and type of desired position signals. Table 6-3 and Figure 6-29(a) to (e) show the average and standard deviation of position response errors of the proposed circuit in different amplitudes and fixed frequencies 0.1 Hz. Average of position response errors of the circuit to sinusoidal and trapezoidal signals raised by factor of 4.1 and for square signals raised by factor of 8 when the amplitude raised from 4 cm to 20 cm. Also comparing standard deviations of the position response errors shows for sinusoidal desired position signals the standard deviation raised by factor of 3.2, for trapezoidal signals it is raised by factor of 4 and for the case of square signal it is raised by factor of 5.8. In conclusion the proposed circuit for smoother signals performs more accurate tracking performance.

Table 6-4 and Figure 6-30(a) to (e) present the pump average delivered hydraulic power to the proposed circuit in different amplitudes of desired position signal and three different signals of sinusoidal, trapezoidal and square. As it is shown when the

115

amplitude raised from 4 cm to 20 cm for the case of sinusoidal signal average of delivered hydraulic power raised by factor of 5.1, for trapezoidal signal raised by factor of 7.3 and for square signals, it raised by factor of 7.6. Smoother motions required less power to perform.

Table 6-3: Mean values and standard deviation of position errors for tested scenarios when frequencies are fixed to 0.1 Hz.

Amplitude (cm)	Sinusoid	Trapezoid	Square
Amp.=4 cm	0.55±0.37	0.54±0.56	1.00±2.33
Amp.=8 cm	0.92±0.51	0.89±0.91	2.17±4.84
Amp.=10 cm	1.10±0.61	1.15±1.21	2.92±6.17
Amp.=15 cm	1.72±1.09	1.95±1.77	5.09±9.69
Amp.=20 cm	2.26±1.19	2.62±2.23	8.00±13.46
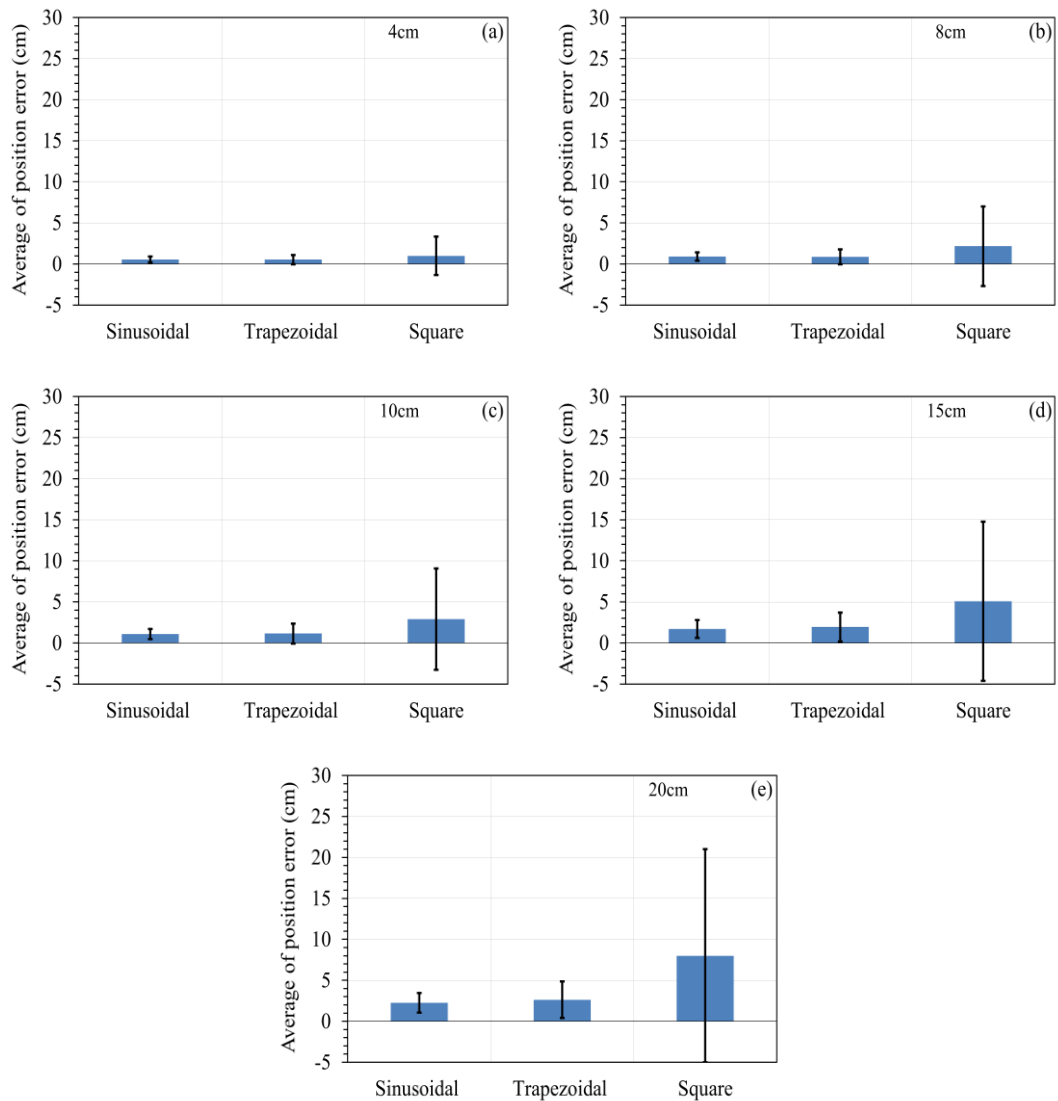
Figure 6-29: Comparative (sinusoidal, trapezoidal and square) average and standard deviation of position errors when the amplitude of desired position signals are (a) 4 cm, (b) 8 cm, (c) 10 cm, (d) 15 cm and (e) 20 cm and frequencies are set to 0.1 Hz.

Table 6-4: Mean values and standard deviation of average delivered hydraulic power for tested scenarios when frequencies are to 0.1 Hz.

Power (W)	Sinusoid	Trapezoid	Square
Amp.= 4cm	21.56±21.99	22.12±31.09	29.90±88.85
Amp.= 8 cm	47.62±35.97	49.54±57.73	78.82±228.24
Amp.=10 cm	60.87±45.19	68.89±84.07	98.64±268.38
Amp.=15 cm	99.83±79.99	116.28±122.75	165.00±455.23
Amp.=20 cm	111.20±72.67	161.57±169.82	229.00±762.77
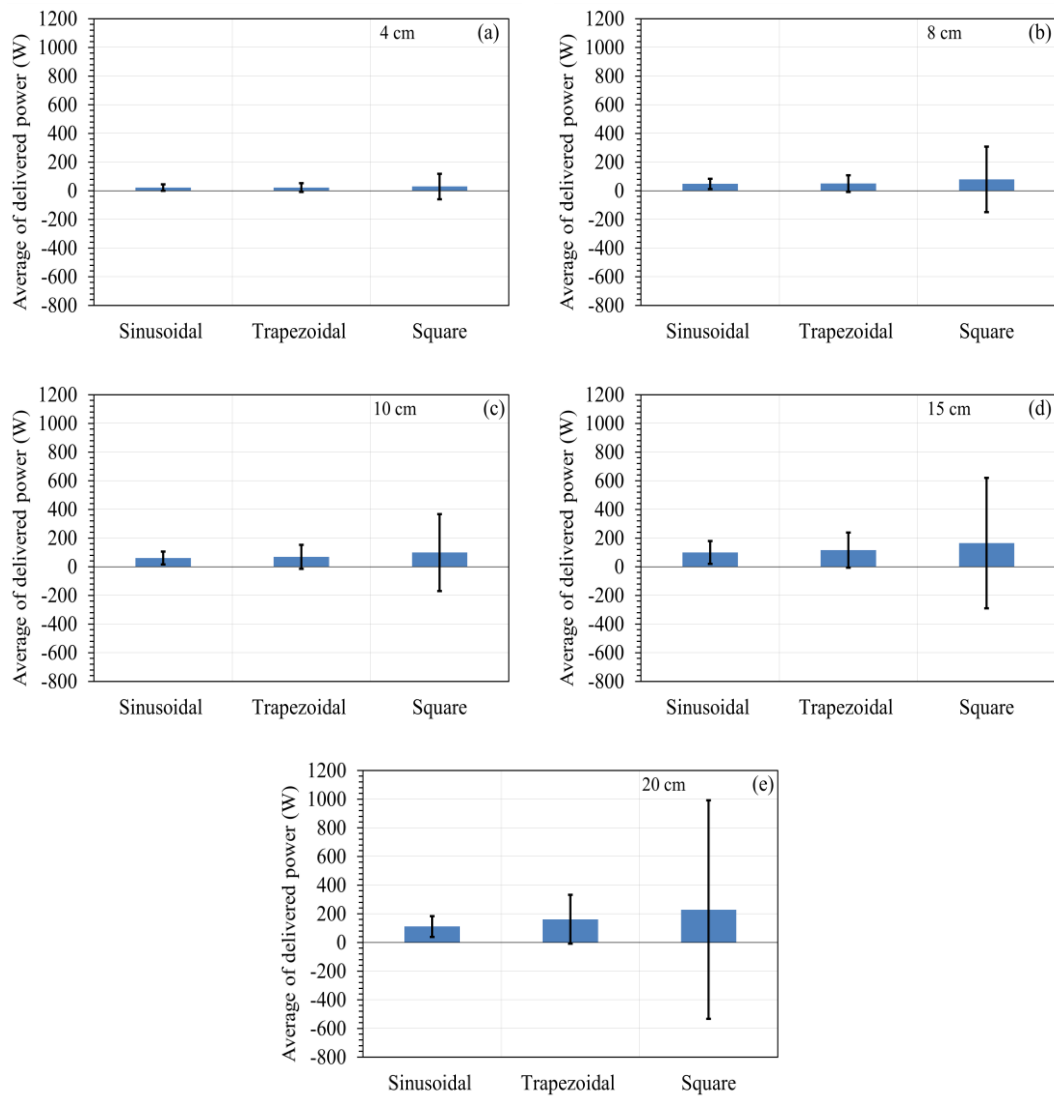
Figure 6-30: Comparative (sinusoidal, trapezoidal and square) average pump delivered hydraulic power to the cylinder of proposed circuit when the frequency of desired position signals set to 0.1 Hz and amplitudes are (a) 4 cm, (b) 8 cm, (c) 10 cm, (d) 15 cm and (e) 20 cm.

6.8. Tracking performance of the circuit when the signal has a series of frequencies and series of amplitudes

To validate the tracking performance of the proposed circuit when the desired position signal has a series of frequencies and series of amplitudes two more test are performing on the proposed circuit. First a fixed amplitude sinusoidal desired position signal with a series of frequencies is applied to the proposed circuit for 60 s. Figure 6-31(a) shows the desired position and position response of the circuit. Second, a fixed frequency sinusoidal desired position with a series of different amplitudes is applied to the proposed circuit; Figure 6-31(b) shows the desired position signal and position response of the circuit.

In the third test, fixed amplitude signal of 15 cm with a series of frequencies is applied to the proposed circuit for 60 s. The desired position signal and position response of the circuit are shown in Figure 6-31(c). The fourth test consisted of a fixed frequency 0.1 Hz square desired position signal with a series of amplitudes which is applied to the proposed circuit. Figure 6-31(d) shows the proposed position signal and the position response of the forth test.

In the fifth and sixth tests, two trapezoidal signals, first with fixed amplitude of 15 cm and same series of frequencies, and second with a fixed frequency of 0.1 Hz and same series of amplitudes are applied to the proposed circuit. Figure 6-31(e) and (f) present the desired position and position response of the proposed circuit to these trapezoidal signals.
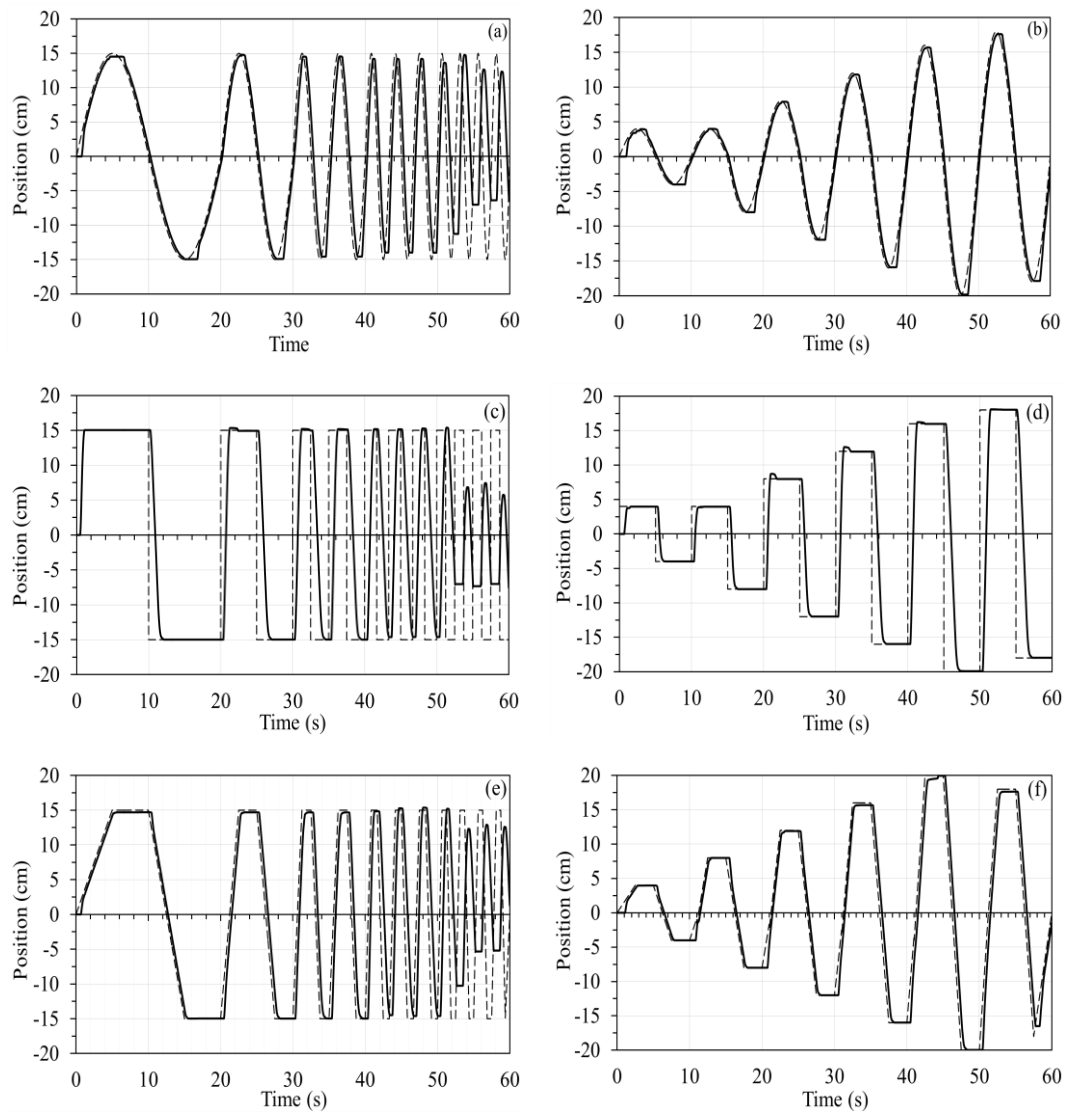
Figure 6-31:(a)Desired sinusoidal position signal with series of frequencies (dashed line) and position response of the circuit (solid line) , (b) desired sinusoidal position signal with series of amplitudes and position response of the circuit, (c)desired square position signal with series of frequencies and position response of the circuit, (d) desired square position signal with series of amplitudes and position response of the circuit, (e) desired trapezoidal position signal with series of frequencies and position response of the circuit,(f) desired trapezoidal position signal with series of amplitudes and position response of the circuit.

6.9. Summary

The experimental evaluations showed that the proposed circuit is highly efficient as compared to a valve control circuit using a pressure compensated pump. The degree of efficiency was shown to be dependent on pattern and frequency of the motion.

Smoother and slower motions (lower frequency) perform at higher efficiencies. This study of the value of average position error showed that for frequencies higher than 0.4 Hz, the proposed circuit did not respond properly. The weight of rotating parts of the electromotor and the pump as well as the latency of the VFD limited the bandwidth of responses. Using a variable displacement piston pump, with a better servo drive, improved the performance of the circuit in higher frequencies. The speed of the end effector was limited by the maximum speed of the prime mover and by the displacement of the pump. Experimental results also showed that the mean position error of the end effector was more sensitive to the frequency of motion than to the amplitude. Furthermore, the tests with trapezoidal and sinusoidal pattern of motion showed that the position tracking in higher amplitudes is better.

CHAPTER 7

CONCLUSIONS

7.1. Contributions of this thesis

The focus of this thesis has been to identify the drawbacks of existing single pump pump-controlled designs for single rod-cylinders and to introduce a new design that satisfies all possible load conditions. Simulations and experimental evaluations showed the proposed circuit is simple to implement, easy to control and highly energy efficient. The challenges of controlling a single-rod cylinder as an asymmetric hydraulic element with a pump as a symmetric hydraulic machine—in which the pump controls the pressure at only one side of the cylinder at a time while the other side is always connected to the low pressure of the hydraulic circuit—first were identified. Then the new circuit design was proposed to overcome these challenges in existing designs.

The proposed design used two counterbalance valves simultaneously to control pressure at both sides of the cylinder at the same time, thereby making the cylinder easy to control. To further facilitate differential flows to both sides of the cylinder in this proposed design, an on/off solenoid valve is used to redirect the differential fluid

of the cylinder to the tank. To protect the pump from cavitation, the pump was submerged in oil, and two check valves at the pump ports served to redirect differential fluid from the tank to the pump.

Simulation studies were conducted that showed existing circuits for single-rod cylinders are uncontrollable in some load conditions. The simulation responses of the proposed circuit approximated the simulation results of the circuit with a double-rod cylinder that is well-known and widely used in industry. Simulation studies also showed that by increasing the pressure setting of counterbalance valves, the controllability of the proposed circuit improved, and at the same time, it made the circuit less efficient. By choosing counterbalance valves with higher pilot ratios, the energy efficiency of the circuit improved, and at the same time, the control of the cylinder was more difficult.

A test rig was initially designed and manufactured to experimentally validate the performance of the proposed circuit under different loads. It was constructed using off-the-shelf industrial elements. Two load setups were also constructed to experimentally test the proposed circuit under non-switching and switching loading conditions.

An experimental evaluation of the proposed circuit was conducted. Using a simple proportional controller, it was shown that the steady state tracking error of the proposed circuit was 0.058 mm for the experiments conducted (when the stroke of the cylinder was 40 cm). The tracking performance was not sensitive to the size of the load. Furthermore, the quality of tracking performance and energy consumption was shown to be dependent on the shape and frequency of the end-effector motion. The system's efficiency was increased by reducing the frequency of motion. As well, smoother patterns of motion were shown to demand less power. The maximum

frequency for a good tracking response with the new design was 0.4 Hz. The weight of rotating parts of the pump-electromotor and response delay of the servo drive limited the test rig to lower frequencies. By using a fixed speed prime mover and variable displacement piston pump the responses of the proposed circuit could be much faster. The delivered hydraulic power in the proposed circuit was up to 75% more efficient as compared to a valve controlled circuit. For the proposed circuit, the delivered hydraulic power of the pump to the ports of the cylinder was calculated by integration of multiplication of the reading pressures at the pump ports to the flow rate of the pump. Although the flow rate of pump was calculated by multiplication of the recorded speed of the rod end of cylinder to the effective area of the acting chamber of the cylinder. The energy consumption of a valve controlled circuit using a pressure compensated pump was calculated by numerical integration of multiplication of the pump pressure to the pump flow rate. To perform the same task, the flow rate of the pressure compensated pump was assumed to be the same as the flow rate of the pump in the proposed circuit. Also it was assumed the pressure compensated pump creates the maximum required pressure for the heaviest load by the cylinder. In the case of the proposed circuit the pump creates required pressure to perform the task at each moment. The use of counterbalance valves prevented the circuit from recycling potential energy in the case of assistive loads.

In conclusion, the experimental evaluation showed that the proposed circuit is simple to implement, low in cost, easy to control, and efficient. Therefore, this circuit is a suitable candidate for general industrial applications like tote dumpers, press breaks, and mineral drilling machines.

7.2. Future work

Future work will focus on testing the proposed circuit with a fast response variable displacement piston pump and experimenting with loads that have different dynamics such as a full size excavator machine. The design of a fast changing switching and controllable load would also be required to study the performance of the proposed circuit under sudden changing loads. Energy consumption and performance of the proposed circuit need to be compared with a conventional valve controlled circuit in industrial applications, in which industrial operators perform the tasks. This would allow the researcher to collect data for statistical evaluations of the proposed circuit. Also some study needs to be done to find a solution to the limitation of this proposed design: its inability to regenerate energy.

BIBLIOGRAPHY

[1] Q. Zhongyi, Q. Long and Z. Jinman, "Review of energy efficient direct pump controlled cylinder electro-hydraulictechnology," *Renewable and Sustainable Energy Reviews,* vol. 35, pp. 336-346, 2014.

[2] J. D. Zemmerman, M. Pelos, C. A. Williamson, and M. Ivantysynova, "Energy Consumption of an LS Excavator Hydraulic System," in *Proc. ASME International Mechanical Engineering Congress and Exposition (IMECE), PP. 117-126*, Seattle, Washington, USA, 2007.

[3] M. Ivantysynova, "The swash plate machine for displacement control unit with great development potentiality," in *First International Fluid Technology Colloqium (IFK)*, Aachen, Germany, 1998.

[4] S. Habibi., "Design of a new high-performance electrohydraulic actuator," *IEEE/ASME Transactions on Mechatronics,* vol. 5 (2), pp. 158-164, 2000.

[5] K. Kang, M. Pachteri, and C.H. Houpis, "Modeling and control of an electro-hydrostatic actuator," in *Aerspace and Electronics Conference,*, Dayton,OH,USA, 1995.

[6] I. 22072, "https://www.iso.org/obp/ui/#iso:std:iso:22072:ed-2:v1:en," 2011. [Online]. Available: https://www.iso.org. [Accessed 27 01 2015].

[7] R. Rahmfeld and M. Ivantysynova, "Developing and control of of energy saving hydraulic servo drives," in *Proc. First FPNI-PhD Symposium, pp. 167-180*, Hamburg, Germany, 2000.

[8] J. Li, Y. Fu, Z. Wang, and G. Zhang, "Research on fast response and high accuracy control of an airborne electro hydrostatic actuation system," in *2004 international conference on intelligence, mechatronics and automotion*, Changdu, China, 2004.

[9] J. Huang, H. Zhao, L. Quan, and X. Zhang, "Development of an asymmetric axial piston pump for displacement-controlled system," *Proc. Institution of Mechanical Engineers, Part C: J. Mech. Eng. Sci.,* vol. 228(8), pp. 1418-1430, 2014.

[10] Z. Quan, L. Quan, and J. Zhang, "Development of a dual-acting axial piston pump for displacement-controlled system," *Proc. Institution of Mechanical Engineers, Part B: J. Eng. Manuf.,* vol. 228 (4), pp. 606-616, 2014.

[11] J. Johnson, "www.http;//www.hydraulicspnumatics.com," 10 June 2011. [Online]. Available: www.http;//www.hydraulicspnumatics.com/Classes/Article/ArticleDraw_p.aspx. [Accessed 15 Oct. 2011].

[12] A. J. Hewett, "Hydraulic Circuit Flow Control". US Patent 5 329 767, 19 July 1994.

[13] J. Grabbel and M. Ivantysynova, "Model adaptation for robust control design of hydraulic joint servo actuators," in *Proc. 4th International Symposium on Fluid Power Transmission and Control (ICFP 2003), pp. 16-24*, Wuhan,China, 2003.

[14] G. R. Wendel, "Hydraulic systems configurations for improved efficiency," in *Proc. SAE 18th international off highway congress, SAE Paper Number: 2002-01-1433*, LasVegas, Nevada, 2002.

[15] C. Williamson and M. Ivantysynova, "Pump mode prediction for four quadrant velocity

control of valve hydraulic actuators," *Proc. 7th JFPS Intrnational symposium on fluid power,* pp. 323-328, 2008.

[16] G. R. Wendel, "Regenerative hydraustatic systems for increased efficiency," in *National conference on fluid power*, Chicago, IL, 2000.

[17] L. Wang, W. J. Book, J. D. Huggins, "A hydraulic circuit for single rod cylinder," *Journal of Dynamic Systems, Measurement, and Control, ASME,* vol. 134(1), pp. 011019-1-16, 2012.

[18] C. Williamson and M. Ivantysynova, "Pump Mode Prediction for Fourquadrant Velocity Control of Valveless Hydraulic Actuators," in *7th JFPS International Symposium on Fluid Power*, Toyama, Japan, 2008.

[19] R. Navarro, "Performance of an electro-hydrostatic actuator on the F-18 systems research aircraft," Edwards, California, 1997.

[20] Li Jun, F. Yongling, Z. Guiying, G. Bo, and M. Jiming "Research on fast response and high accuracy control of an airborne electro hydrostatic actuation system," *Proceeding of the 2004 international conference on intelligence mechtronics and automation,* pp. 428-432, August 2004.

[21] C. R. Cornell, "Dynamic simulation of ahydrostatically propelled vehicle," *SAE Proceddings,* no. 811253, 1981.

[22] K. Ceasby and A. R. Plummer, "A novel high efficiency electro-hydrostatic flight motion system," *University of Bath Opus online store,* 2008.

[23] G. R. Wendel, "Hydraulic systems configurations for improved efficiency," in *SAE 18th international off-highway congress co-located with CONEXPO-CON/AGG*, LasVegas, Nevada, 2002.

[24] S. V.Vladimirov and S. Forde, "Demonstartion program to design, manufacture and test an autonomus electrio-hydrostatic actuator togimbal large booster-class engines," in *42nd AIAA/ASME/SAE/ASEE Joint propulsion & exhibit*, SAcramento, California, July9-12,2006.

[25] S. Smith and J. Irving, "Electro hydrostatic actuators for control of undersea vehicles," in *Joint undersea warfare technology fall confrence US Naval Submarine Base New London*, Groton, Connecticut, 2006.

[26] J. L. Brinkman and P. Gupta, "Hybrid hydraulic system and work machine using same". USA/IL Patent US 7234298 B2, 26 05 2007.

[27] G. R. Wendel, "Regenerative hydraustatic systems for increased efficiency," in *Proceedings of national conference on fluid power*, Chicago, Illinois, 2000.

[28] A. M. F.Sallam and A. I. Abdel-Aziz, "Dynamic Behavior of a Hyraulic Motor Controlled by a poppet type directional control valve," in *13th International Confrence on Aerospace science and aviation technology, ASAT*, 26-28 May,2009.

[29] M. I. C. Williamson, "Pump mode prediction for four-quadrant velocity control of valveles hydraulic actuators," in *Prodeedings of the 7th JFPS International symposium on fluid power* , Toyama, 2008.

[30] J. Johnson, "http://fpweb.com/Clases/Article?ArticleDraw_P.aspx," [Online].

[31] K. S. Bryan Nelson, "Rotary flow control valve with energy recovery". IL, USA Patent US8186154B, 29 May 2012.

[32] J. Lodewyks, "Differential cylinder in a closed hydrostatic transmission," Doctor

dissertation, RWTH Aachen, Germany, 1994.

[33] R. E. Khalil, "Bidirectional Hydraulic Transformer". US Patent 7 775 040, 17 Aug. 2010.

[34] G. Vael, P. Achten and Z. FU, "The Innas Hydraulic Transformer The Key to the Hydrostatic Common Pressure Rail," Society of Automation Engineers Inc. SAE Technical Paper 2000-01-2561, 2000.

[35] I. Corp., " http://www.innas.com," INNAS, [Online]. Available: http://www.innas.com/IHT.html. [Accessed 15 12 2014].

[36] T. Lin, Q. Wang, W. Gong, "Research on the energy regeneration systems for hybrid hydraulic excavators," *Elsevier, Automation in construction,* vol. 19, pp. 1016-1026, 2010.

[37] A. J. Hewett, "Hydraulic Circuit Flow Control". Vancouver, BC, Canada Patent 5329767, 21 January 1993.

[38] P. D. Lawrence , E. Salcudean, N. Sepehri, D. Chan, S. Bachmann, N. parker, M. Zhu and R. Frenette , "Coordinated and Force-Feedback Control of Excavators," in *4th International Symposium on Experimental Robotics, ISER '95*, Stanford, California, USA, 1995.

[39] R. Rhamfeld, "Developing and control of energy saving hydraulic servo drives," in *Proceeding of first FPN1-Phd symposium* , Hamburg, 2000.

[40] K. S. Gunther Munchong.Patent US6543223B2, 8 April 2003.

[41] Parker, "http://www.parker.com," 1 11 2014. [Online]. Available: http://www.parker.com/Literature/Oildyne/Oildyne%20-%20PDF%20Files/Compact-EHA-Catalog-HY22-3101E-7-13.pdf. [Accessed 24 06 2015].

[42] E. Jalayeri, A.Imam, N. Sepehri, "A throttle-less single rod hydraulic cylinder positioning system for switching loads," *Case studies in mechanical system and signal processing,* vol. 1, no. doi.org/10.1016/j.csmssp.2015.06.001, pp. 27-31, 2015.

[43] B. Rexroth, "http://apps.boschrexroth.com," Bosch Rexroth, [Online]. Available: http://apps.boschrexroth.com/products/compact-hydraulics/pib-catalogs/pdf/counterbalance.pdf.. [Accessed 22 12 2014].

[44] MatWorks, "www.mathworks.com," [Online]. Available: http://www.mathworks.com/help/physmod/hydro/ref/counterbalancevalve.html. [Accessed 17 November 2014].

[45] G. F. Ritelli; A. Vacca, "Energetic and dynamic impact of counterbalance valves in fluid power," *Energy conversion and managment, ELSEVIER,* vol. 76, pp. 701-711, 2013.

[46] G. F. Ritelli; A. Vacca, "Energetic and dynamic impact of counterbalance valves in fluid power machines," *Energy Conversion and Management,* vol. 76, p. 701–711, 2013.

[47] "http://apps.boschrexroth.com," Bosch Rexroth oil Control S.P.A., [Online]. Available: http://apps.boschrexroth.com/products/compact-hydraulics/pib-catalogs/pdf/counterbalance.pdf. [Accessed 22 Dec. 2014].

[48] P. A. Nordhammer, M. K. Bak,M. R. Hansen, "A Method for Reliable Motion Control of Pressure Compensated Hydraulic Actuation with Counterbalance Valves," in *International Conference on Control, Automation and Systems*, Jeju Island, Korea, 2012.

[49] E. Jalayeri, A.Imam, Z. Tomas, N. Sepehri, "A throttle-less single-rod hydraulic cylinder positioning system: Design and experimental evaluation," *Advances in Mechanical*

Engineering, vol. 7(5), no. DOI: 10.1177/1687814015583249, pp. 1-14, 2015.

[50] K. G. Cleasby and A. R. Plummer, "A novel high efficiency electrohydrostatic flight simulator motion sysytem," *Fluid Power and Motion Control (FPMC 2008),* no. Available: http://opus.bath.ac.uk/14740/ [Dec. 15, 2014], pp. 437-449, 2008.

[51] P. Mariani, G. Ansaloni, R. Paluzzi, "Load Sensing With Active Regeneration System," in *7th JFPS International Symposium on Fluid Power*, Toyama, 2008.

[52] L. Wang, W. J. Book, J. D. Huggins, "A hydraulic circuit for single rod cylinder," *Journal of Dynamic Systems Measurement, and Control, ASME,* vol. 134(1), pp. 011019-1-16, 2012.

APPENDIX A – GOVERNING EQUATIONS OF SIMHYDRAULIC BOLCKS [43]

This appendix presents governing formulas of Simhydraulic blocks that were used for simulations.

A-1. Hydraulic machine

In Hydraulic machine Simhydraulic block showed in Figure A- 1 A and B are two hydraulic ports presenting inlet and outlet of the machine.
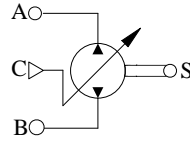
Figure A- 1. Simhydraulic hydraulic machine block.

S is the rotational conserving port and C is the physical signal port that controls the machine displacement.

The hydraulic machine is represented by following equations [43];

$$q = D.\omega - k_m.q_L \tag{A-1}$$

$$T = D.P + k_m.T_{fr} \tag{A-2}$$

$$D = \begin{cases} \frac{D_{max}}{x_{max}}.x \\ D(x) \end{cases} \tag{A-3}$$

$$P = P_A - P_B \tag{A-4}$$

where q is machine flow rate. P, P_A and P_B represent pressure across the machine and gauge pressures at the block terminals, respectively. Machine instantaneous and maximum displacements are denoted by D and D_{max}. Also, x and x_{max} are control member displacement and control member maximum stroke, respectively. Torque at the machine shaft

represents by T. ω is machine shaft angular velocity. Leakage flow is denoted by q_L. T_{fr} is the friction torque.

The Machine efficiency can be defined by machine leakage and friction on the shaft. Matlab specified these parameters on the experimental based process as follows;

$$q_L = D.\omega.k_{L1}(\frac{P}{P_{nom}})^{k_{LP}}(\frac{PD}{D_{max}})^{k_{LD}}(\frac{\omega}{\omega_{nom}})^{k_{L\omega}} \tag{A-5}$$

$$T_{fr} = D.P.k_{F1}(\frac{P}{P_{nom}})^{k_{FP}}(\frac{PD}{D_{max}})^{k_{FD}}(\frac{\omega}{\omega_{nom}})^{k_{F\omega}} \tag{A-6}$$

where P_{nom} and ω_{nom} represent machine nominal pressure and velocity, k_{L1} and k_{F1} are leakage and friction proportional coefficients and $k_{LP}, k_{LD}, k_{L\omega} k_{FP}, k_{FD}. k_{F\omega}$ are approximating coefficients. Approximation coefficients are defiened from approximation plots of the machine are provided by manufacturer . If the leakage is known the machine volumetric coefficients can be calculated as follows when the machine works in pumping mode,

$$\eta_{vp} = \frac{D.\omega - q_L}{D.\omega} = 1 - k_{L1}(\frac{P}{P_{nom}})^{k_{LP}}(\frac{PD}{D_{max}})^{k_{LD}}(\frac{\omega}{\omega_{nom}})^{k_{L\omega}} \tag{A-7}$$

And if the machine works in motoring mode the volumetric coefficient will be,

$$\eta_{vm} = \frac{D.\omega}{D.\omega + q_L} = \frac{1}{1 + k_{L1}(\frac{P}{P_{nom}})^{k_{LP}}(\frac{PD}{D_{max}})^{k_{LD}}(\frac{\omega}{\omega_{nom}})^{k_{L\omega}}} \tag{A-8}$$

Mechanical efficiency is related to the known friction torque. In pumping mode it will be,

$$\eta_{mp} = \frac{D.P}{D.P + T_{fr}} = \frac{1}{1 + k_{F1}(\frac{P}{P_{nom}})^{k_{FP}}(\frac{PD}{D_{max}})^{k_{FD}}(\frac{\omega}{\omega_{nom}})^{k_{F\omega}}} \tag{A-9}$$

In motoring mode the mechanical efficiency ,

$$\eta_{mm} = \frac{D.P - T_{fr}}{D.P} = 1 - k_{F1}(\frac{P}{P_{nom}})^{k_{FP}}(\frac{PD}{D_{max}})^{k_{FD}}(\frac{\omega}{\omega_{nom}})^{k_{F\omega}} \tag{A-10}$$

It is assumed, the hydraulic fluid is not compressible, machine's shaft inertia is negligible and the block works in room temperature.

131

A-2. Double acting cylinder

In double acting cylinder Simhydraulic block C and R represent the physical mechanical connections. C is the connection of the cylinder body to structure and R is the end-effector port that connects to load. A and B are hydraulic ports of the cylinder.
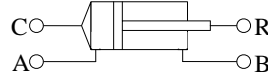
Figure A- 2. Simhydraulic cylinder block

The model is governed by following equations;

$$F = A_A.P_A - A_B.P_B - F_c \qquad \text{(A-11)}$$

$$q_A = A_A.v \qquad \text{(A-12)}$$

$$q_B = A_B.v \qquad \text{(A-13)}$$

$$v = \frac{dx}{dt}$$

$$v = v_R - v_C \qquad \text{(A-14)}$$

$$F_c = \begin{cases} (x - x_E).K_p.v & \text{when } x > x_E, v > 0 \\ (x - x_R).K_p.v & \text{when } x < x_R, v < 0 \\ 0 \end{cases} \qquad \text{(A-15)}$$

$$x_E = S - x_0 \qquad \text{(A-16)}$$

$$x_R = -x_0 \qquad \text{(A-17)}$$

where F represents the force devoted by cylinder and V represents the end-effector velocity. Absolute velocities of cylinder rod and cylinder case are denoted respectively by v_R and v_C. A_A and A_B are piston areas at port A side and port B side of cylinder. Pressures at the cylinder ports A and B are represented by P_A and P_B. Flow rates through port A and B into the cylinder ports are denoted respectively by q_A and q_B. Piston position is denoted by x and x_0 represents initial distance between piston and cap A. F_c, K_p and S are hard stop force,

penetration coefficient and piston stroke. Distance the piston can travel to fully extend and travel to fully retract from initial position are denoted by x_E and x_R. Assumptions and limitations of this block are,

- The cylinder is frictionless,
- Inertia is negligible,
- Hydraulic fluid is not compressible,
- Leakages are negligible,
- Hard stops of the cylinder are inelastic.

A-3. Check valve

In check valve Simhydraulic block A and B are hydraulic ports of a check valve. The pressure behavior of a check valve is presented by Figure A- 4, where $P = P_A - P_B$.
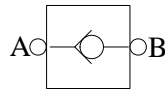

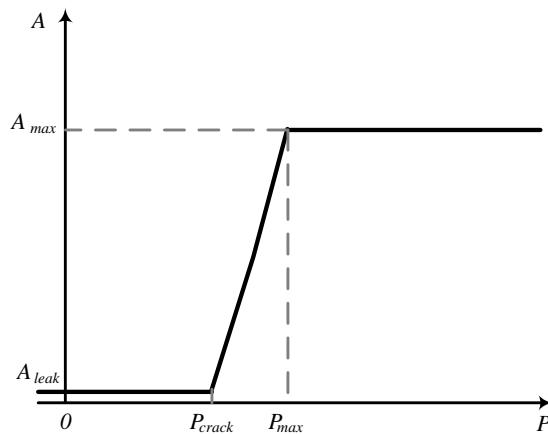Figure A- 3. Simhydraulic pilot check valve block.

Figure A- 4. Pressure graph of check valve.

Valve is closed for pressures less than cracking pressure and it will be remain fully open for pressures higher than maximum pressure. Governing equations of a check valve block are as follows,

$$q = C_D . A(P) \sqrt{\frac{2}{\rho}} . \frac{P}{(P^2 + P_{cr}{}^2)^{1/4}} \tag{A-18}$$

$$A(P) = \begin{cases} A_{leak} & , when \ P \leq P_{crack} \\ A_{leak} + k.(P - P_{crack}) & , when \ P_{crack} < P < P_{max} \\ A_{max} & , when \ P \geq P_{max} \end{cases} \tag{A-19}$$

$$k = \frac{A_{max} + A_{leak}}{P_{max} + P_{crack}} \tag{A-20}$$

$$P = P_A - P_B \tag{A-21}$$

$$P_{cr} = \frac{\rho}{2(\frac{Re_{cr}.v}{C_D.D_H})^2} \tag{A-22}$$

$$D_H = \sqrt{\frac{4A(\rho)}{\pi}} \tag{A-23}$$

where q represents the flow rate of hydraulic fluid and pressure differential (Block positive direction is from port A to port B), pressures at the block ports A and B are denoted by, P, P_A and P_B. $A(P)$, A_{max} and A_{leak} are instantaneous orifice passage area, fully open valve passage area and closed valve leakage areas. Valve cracking pressure, pressure needed to fully open the valve and minimum pressure for turbulent flow are represented by, P_{crack}, P_{max} and P_{cr}. Critical Reynolds number and fluid density are showed by Re_{cr} and ρ, C_D and v are flow discharge coefficient and fluid kinematic viscosity and D_H denoted instantaneous orifice hydraulic diameter. It is assumed the opening of valve is linear and inertia of the poppet of the valve is negligible.

A3. Pilot check valve

In pilot check valve Simhydraulic block showed in Figure A- 5, A and B are hydraulic ports of the valve and X is presenting pilot port of the valve. Plot of pressure versus passage area of the valve is showed in Figure A- 6. Pilot check valve can be opened by pilot port pressure P_x or inlet pressure P_A.
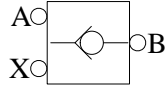

Figure A- 5. Simhydraulic pilot check valve block.

Force equation of the poppet is,

$$F = P_A . A_A + P_x . A_x - P_B . A_B \qquad \text{(A-24)}$$

or the equation can be modified as follows,

$$P_e = P_A + P_x . k_p - P_B, \quad k_p = \frac{A_x}{A_A} \qquad \text{(A-25)}$$

where P_A, P_B, P_x and P_e are pressures at the valve ports ,pressure at pilot port and equivalent pressure differential across the poppet respectively. A_A, A_B and A_x are area of the poppet in the A piston, area of the poppet in the B piston and area of the pilot piston. Pilot ratio is showed by k_p.

Flow rate of the valve is governed by following equations.

$$q = C_D . A(P) \sqrt{\frac{2}{\rho}} . \frac{P}{(P^2 + P_{cr}{}^2)^{1/4}} \qquad \text{(A-26)}$$

$$P_e = P_A + P_x . k_p - P_B \qquad \text{(A-27)}$$

$$A(P) = \begin{cases} A_{leak} & , when\ P_e \leq P_{crack} \\ A_{leak} + k.(P_e - P_{crack}) & , when\ P_{crack} < P_e < P_{max} \\ A_{max} & , when\ P_e \geq P_{max} \end{cases} \qquad \text{(A-28)}$$

$$k = \frac{A_{max} - A_{leak}}{P_{max} - P_{crack}} \qquad (A-29)$$

$$P = P_A - P_B \qquad (A-30)$$

$$P_{cr} = \frac{\rho}{2(\frac{Re_{cr}.v}{C_D.D_H})^2} \qquad (A-31)$$

$$D_H = \sqrt{\frac{4A(\rho)}{\pi}} \qquad (A-32)$$

where $P, P_A, P_B, P_x, P_{crack}, P_{max}$, and P_{cr} are pressure differential (Block positive direction is from port A to port B), pressures at the block ports, pressure at pilot port, valve cracking pressure, pressure needed to fully open the valve and minimum pressure. Instantaneous orifice passage area, fully open valve passage area and closed valve leakage area are denoted by $A(P), A_{max}$ and A_{leak}. Valve gain coefficient and valve pilot ratio (A_x/A_A) are showed by k and k_p, flow discharge coefficient is presented by C_D. Re_{cr}, q, D_H, ρ and v denote critical Reynolds number, flow rate, instantaneous orifice hydraulic diameter, fluid density and Fluid kinematic viscosity. It is assumed the fluid is not compressible, opening area of the poppet is linearly related to the differential pressure of the valve and the valve is not loaded with spring. Also the valve is not consuming fluid.
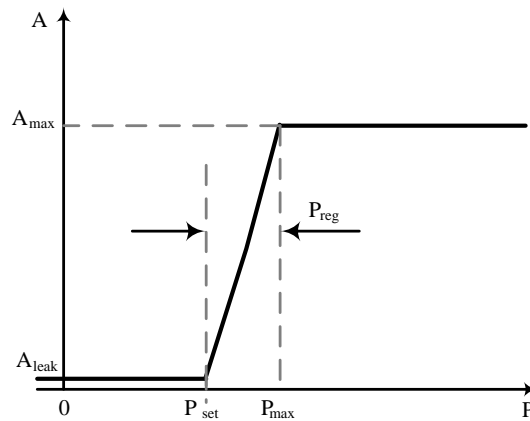

Figure A- 6. Differential pressure behavior versus passage area of a pressure relief valve.

136

A-4. Counterbalance valve

In counterbalance valve block of Simhydraulic showed in B is the pressure port of the valve, L presents load port of the valve and P is the pilot port.
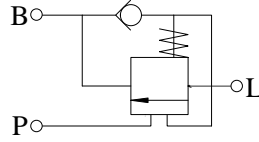

Figure A- 7. Simhydraulic counterbalance valve block.

Force equation of the valve poppet is presented by;

$$F_0 + c.x = P_{pilot}.A_{pilot} + P_{load}.A_{load} - P_{back}.A_{back} \tag{A-33}$$

the valve can be classified as internally piloted and externally piloted. All of simulation and experiments are performed for externally piloted counterbalance valves. After some minor rearrangement the force equation can be like:

$$P_{set} + c_p.x = P_{pilot}.k_{pilot} + P_{load} - P_{back}.k_{back} \tag{A-34}$$

$$P_{set} = \frac{F_0}{A_{load}} \tag{A-35}$$

$$c_P = \frac{c}{A_{load}} \tag{A-36}$$

$$k_{pilot} = \frac{A_{pilot}}{A_{load}} \tag{A-37}$$

$$k_{back} = \frac{A_{back}}{A_{load}} \tag{A-36}$$

The poppet displacement is presented by:

$$x = \frac{(P_{set} - (P_{pilot}.k_{pilot} + P_{load} - P_{back}.k_{back}))}{c_p} \quad , 0 \le x \le x_{max} \tag{A-37}$$

where $P_{pilot}, P_{load}, P_{back}$ and P_{set} are pilot pressure (pressure at port P), load pressure (pressure at port L), backpressure (pressure at return port B) and valve pressure setting respectively. Valve effective area at pilot port P, valve effective area at load port L and valve effective area at return port B are represented by A_{pilot}, A_{load} and A_{back}. Flow rate, valve opening, and spring pressure stiffness are denoted by c, x and c_p. k_{pilot} and k_{back} denote pilot ratio and backpressure ratio.

A-5. Pressure relief valve

In pressure relief valve Simhydraulic block A and B are hydraulic ports (see Figure A- 8)
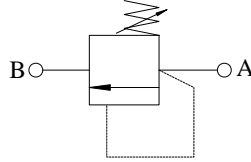
Figure A- 8. Simhydraulic pilot check valve block.

As long as the differential pressure of the valve is less than P_{set} the poppet of the valve stay closed. By raising pressure at port A the poppet opens and for differential higher than P_{max} the valve remains fully open.

The flow rate of the valve is presented by following equations.

$$q = C_D. A(P)\sqrt{\frac{2}{\rho}} \cdot \frac{P}{(P^2 + P_{cr}^2)^{1/4}} \tag{A-36}$$

$$P = P_A - P_B \tag{A-37}$$

$$P_{cr} = \frac{\rho}{2\left(\frac{Re_{cr}.v}{C_D.D_H}\right)^2} \tag{A-38}$$

$$A(P) = \begin{cases} A_{leak} & , when \ P \leq P_{set} \\ A_{leak} + k.(P - P_{set}) & , when \ P_{set} < P < P_{max} \\ A_{max} & , when \ P \geq P_{max} \end{cases} \qquad (A\text{-}39)$$

$$k = \frac{A_{max} - A_{leak}}{P_{reg}} \qquad (A\text{-}40)$$

$$D_H = \sqrt{\frac{4A(\rho)}{\pi}} \qquad (A\text{-}41)$$

where $P, P_A, P_B, P_{reg}, P_{set}, P_{max}$ and P_{cr} are pressure differential (Block positive direction is from port A to port B), pressures at the block ports, pressure regulation range, valve preset pressure, pressure needed to fully open the valve and minimum pressure for turbulent flow respectively. Instantaneous orifice passage area, Fully open valve passage area and closed valve leakage area are represented by $A(P), A_{max}$ and A_{leak}. Flow rate, instantaneous orifice hydraulic diameter, valve gain coefficient, flow discharge coefficient, critical Reynolds number, fluid density and fluid kinematic viscosity are denoted by c, $D_H, k, C_D, Re_{cr}, \rho$ and v. The block positive direction is Port A to port B. It is assumed the valve opening is linearly is related to the differential pressure across the valve.

A-6. Gas-charged accumulator

The gas-charged accumulator block is the Simhydraulic model of a gas-charged accumulator tank. The accumulator represents any type of bladder or piston accumulator (see Figure A- 9).

Figure A- 9. Simhydraulic gas-charged accumulator block

When the fluid pressure is higher than the charge pressure the fluid fills up the tank and when the fluid pressure is less than gas pressure fluid return back to hydraulic circuit. Normally the pressure of the accumulator chamber and hydraulic circuit are the same. The structural compliance of the accumulator is set to almost zero but not zero. The accumulator block is described by following equations.

$$q = \frac{dV_F}{dt} \tag{A-38}$$

$$V_F = \begin{cases} K_S \cdot (P + P_a) & , when\ P \leq P_{pr} \\ V_{pr}\left(\frac{P_{pr}+P_a}{P+P_a}\right)^{1/k} + V_a\left(1 - \left(\frac{P_{pr}+P_a}{P+P_a}\right)^{1/k}\right) & , when\ P > P_{pr} \end{cases} \tag{A-39}$$

$$V_{pr} = K_S\left(P_{pr} + P_a\right) \tag{A-40}$$

where V_F, V_A and V_{pr} are volume of fluid in the accumulator, accumulator capacity and volume of fluid at preload pressure. Volumetric flow rate, inlet gauge pressure, preload pressure and atmospheric pressure are presented by q, P, P_{pr} and P_a. K_s, k and t denote structural compliance of the accumulator inlet port structure, specific heat ratio and time respectively. The gas is assumed an ideal thermodynamically gas. The process is assumed to be polytrophic and fluid is not compressible.

A-7. Constant head tank

This Simhydraulic block presents a pressurized hydraulic tank that its fluid level remains constant all the time. In Figure A- 10, T shows the hydraulic port of the tank and V shows the physical inlet of the block.
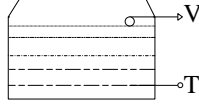

Figure A- 10. Simhydraulic constant head tank block.

Governing equations of the tank are as follows. Critical Reynolds number is set to 15.

$$q = \sqrt{\frac{1}{K}} . A_p \sqrt{\frac{2}{p}} . \frac{P_{loss}}{\left(P_{loss}^2 + P_{cr}^2\right)^{1/4}} \tag{A-41}$$

$$P_{cr} = \frac{p}{2\left(\frac{Re_{cr}.v}{\sqrt{\frac{1}{K}}.d}\right)^2} \tag{A-42}$$

$$P = P_{elev} - P_{loss} + P_{pr} \tag{A-43}$$

$$P_{elev} = \rho.g.H \tag{A-44}$$

$$A_P = \frac{\pi.d^2}{4} \tag{A-45}$$

where $P, P_{elev}, P_{loss}, P_{pr}, K$ and P_{cr} are pressure at the tank inlet, pressure due to fluid level, pressure loss in the connecting pipe, pressurization, pressure loss coefficient and minimum pressure for turbulent flow. Fluid density, acceleration of gravity and fluid level with respect to the bottom of the tank are presented by ρ, g and H. Connecting pipe area, connecting pipe diameter and flow rate are denoted by A_p, d and q.

A-8. Ideal angular velocity source

C is the physical reference node of the ideal angular velocity source Simhydraulic block and R is the mechanical output port of it. S is the control signal port of the block. Angular velocity of port the block at port R is linearly controlled by a physical control signal on port S. The block positive direction of the block is from port C to R. The port presents an ideal prime mover.
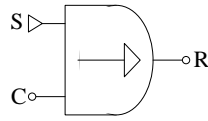

Figure A- 11. Simhydraulic ideal angular velocity source block.

A-9. Ideal mechanical force source

Ideal mechanical force source presets an ideal force source that was used as an ideal load against rod end-effector of cylinders. C and R are mechanical ports and S is the control signal port of the block (see Figure A- 12).
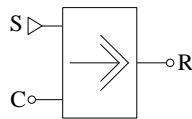

Figure A- 12. Simhydraulic ideal force source block.

A-10. Inertia

The Block shown in Figure A- 13 represents mechanical rotational inertia and it is described by following equation,

$$T = J\frac{d\omega}{dt} \tag{A-46}$$

where T, J, ω and t are inertia torque, inertia, angular velocity and time respectively.

Figure A- 13. Simhydraulic inertia block.

A-11. Rotational damper

The block shown in Figure A- 14 represents an ideal viscous damper in a mechanical rotational system and governs by following equations.

$$T = D.\omega \tag{A-47}$$

$$\omega = \omega_R - \omega_C \tag{A-48}$$

where T, D, ω_R, ω_C and ω are torque transmitted through the damper, damping (viscous friction) coefficient, absolute angular velocities of terminals R, C and relative angular velocity respectively.
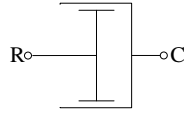

Figure A- 14. Simhydraulic rotational damper block.

A-12. Rotational spring

The symbol represents an ideal rotational spring block shown in Figure A- 15 described by following equations. R and C are mechanical ports of the block.

$$T = K.\varphi \tag{A-49}$$

$$\varphi = \varphi_{init} + \varphi_R - \varphi_C \tag{A-50}$$

$$\omega = \frac{d\omega}{dt} \tag{A-51}$$

where $\varphi, \varphi_R, \varphi_C$ and φ_{int} are relative displacement angle (spring deformation), absolute angular displacements of terminals R, C and spring preliminary winding (spring offset) respectively. Torque transmitted through the spring, spring rate, relative angular velocity and time are denoted by T, K, ω and t.
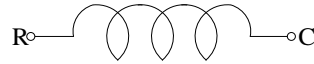

Figure A- 15. Simhydraulic rotational spring block.

A-13. Translational spring

The translational spring Simhydraulic block shown in Figure A- 16 represents an ideal mechanical spring governed by following equations.

$$F = K.x \tag{A-52}$$

$$x = x_{init} + x_R - x_C \tag{A-53}$$

$$v = \frac{dx}{dt} \tag{A-54}$$

where x, x_R, x_C and x_{init} are relative displacement (spring deformation), absolute displacements of terminals R and C and spring initial displacement (initial deformation); the spring can be initially compressed $(x_{init} > 0)$ or stretched $(x_{init} < 0)$ respectively. Force transmitted through the spring, spring rate, and relative velocity and time are presented by F, K, v and time.

Figure A- 16. Simhydraulic translational spring block.

A-14. Translational damper

The translational damper block present an ideal translational viscous damper described by following equations;

$$F = Dv \tag{A-55}$$

$$v = v_R - v_C \tag{A-56}$$

where F , D , v_R, v_C and v are force transmitted through the damper, damping (viscous friction) coefficient, absolute velocities of terminals R, C and relative velocity respectively.
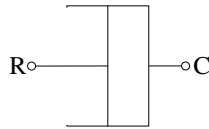

Figure A- 17. Simhydraulic translational damper block.